SMITHSONIAN CONTRIBUTIONS TO PALEOBIOLOGY • NUMBER 77

Ontogenetic Morphometrics of Some Late Cretaceous Trochospiral Planktonic Foraminifera from the Austral Realm

Brian T. Huber

SMITHSONIAN INSTITUTION PRESS
Washington, D.C.
1994

ABSTRACT

Huber, Brian T. Ontogenetic Morphometrics of Some Late Cretaceous Trochospiral Planktonic Foraminifera from the Austral Realm. *Smithsonian Contributions to Paleobiology,* number 77, 85 pages, 37 figures, 10 plates, 15 tables, 1994.—Biometric analysis of ontogenetic changes in test morphology is employed to determine the taxonomic status of several trochospiral planktonic foraminiferal species from southern high latitude Upper Cretaceous sediments. Ontogenetic morphometric data obtained from specimens of *Hedbergella sliteri* Huber, *Archaeoglobigerina australis* Huber (both micromorph and normal-sized populations), and *Archaeoglobigerina mateola* Huber are compared with topotype populations of *Hedbergella holmdelensis* Olsson, *H. monmouthensis* (Olsson), *Costellagerina pilula* (Belford), and *Rugoglobigerina rugosa* (Plummer). Southern South Atlantic specimens of *Archaeoglobigerina bosquensis* Pessagno and *Archaeoglobigerina cretacea* (d'Orbigny) are also analyzed for comparison. Numerous biometric data, measured from exterior observations of whole tests, contact microradiographs, and Scanning Electron Microscope (SEM) micrograph images of serially dissected foraminifera, are used to characterize developmental changes in morphology of the planktonic foraminiferal species. The most useful variables for discriminating taxonomic differences are discussed for each method.

Results indicate that the ontogenetic morphometric approach to study of planktonic foraminifera can be effectively used to resolve problems in taxonomic classification, particularly for species that appear homeomorphic in exterior view. This approach was particularly useful for demonstrating that the ontogenetic morphologies of *A. australis, C. pilula,* and *R. rugosa* are very different and, therefore, previous assignment of *A. australis* morphotypes to various species of *Rugoglobigerina* and *Costellagerina* were incorrect. This study also demonstrates that the growth morphology of the new high latitude species *H. sliteri* significantly differs from *H. holmdelensis* and *H. monmouthensis,* thus confirming recognition of *H. sliteri* as a valid taxon. However, taxonomic uncertainty persists for some high latitude morphotypes that have external characteristics similar to *R. rugosa* (e.g., faint umbilical apertures, faint costellae that are meridionally aligned, presence of tegilla), but ontogenetic morphologies more similar to *A. australis.*

Morphologic changes during ontogeny, including changes in (1) shell pore characteristics (pore diameter, pore density, and porosity), (2) rates of increase in cross-sectional chamber area, (3) apertural position, (4) chamber surface ornamentation, and (5) umbilical diameter, were used to recognize ontogenetic stages in the foraminiferal shells. These include the prolocular, juvenile, neanic, and adult stages. The growth patterns of *H. holmdelensis, H. monmouthensis, H. sliteri,* and *C. pilula* are very uniform and do not show discernable transitions from the juvenile to neanic and adult stages. All four ontogenetic stages were recognized in *A. australis, A. bosquensis, A. mateola, A. cretacea,* and *R. rugosa,* although the abruptness of the transitions and the chamber number where these transitions occur are variable within and between species. Recognition of these growth stages enables taxonomic identification of pre-adult morphologies that occur in smaller size fractions. This is particularly useful since these smaller forms have dominated in unstable environments such as the highly seasonal circum-antarctic oceans.

OFFICIAL PUBLICATION DATE is handstamped in a limited number of initial copies and is recorded in the Institution's annual report, *Smithsonian Year.* SERIES COVER DESIGN: The trilobite *Phacops rana* Green.

Library of Congress Cataloging-in-Publication Data
Huber, Brian T.
Ontogenetic morphometrics of some Late Cretaceous trochospiral planktonic foraminifera from the austral realm / Brian T. Huber.
p. cm. — (Smithsonian contributions to paleobiology ; no. 77)
Includes bibliographical references.
1. Foraminifera, Fossil. 2. Paleontology—Cretaceous. 3. Foraminifera—Morphology. I. Title. II. Series.
QE701.S56 no. 77 [QE772] 560 s-dc20 [563'.12] 93-27089

♾ The paper used in this publication meets the minimum requirements of the American National Standard for Permanence of Paper for Printed Library Materials Z39.48—1984.

Contents

Ontogenetic Morphometrics of Some Late Cretaceous Trochospiral Planktonic Foraminifera from the Austral Realm

Brian T. Huber

Introduction

A stable taxonomic framework is of paramount importance in all faunal analyses for biostratigraphic, paleoclimatic, and paleoceanographic reconstructions. Therefore, the first and most important stage in any paleontological study should be to accurately identify fossil species using as many morphologic criteria as preservation will allow. Identification depends, however, on an adequate knowledge of the species in question, including its range of morphologic variability in space and time, which is lacking for most fossil groups. Although limitations of the fossil record prevent complete attainment of this information, the continuing refinement of stratigraphic knowledge on a global scale affords a considerably improved basis for correlation and a more detailed knowledge of species distributions.

Nearly all taxonomic schemes used in the classification of foraminifera are based on the external morphology of the adult shell, and have thus overlooked considerable ontogenetic information preserved in the early growth stages. Small sized (<150 μm) planktonic foraminifera are often ignored in biostratigraphic studies because of the difficulty in relating the simpler morphologies of juvenile specimens with the more complex adult morphotypes of the same species. Because early growth stages are often obscured by the addition of chambers and shell thickening during the development of involute taxa, the ontogenetic morphology of whole specimens cannot be characterized using standard methods of light microscope or scanning electron microscope (SEM) observation of the test exterior.

Some specialists have used internal and external shape characteristics of thin-sectioned planktonic foraminifera as a basis for species identification (see Sliter, 1989, and references therein). This approach is particularly useful for biostratigraphic correlation of indurated carbonate sequences that will not yield isolated specimens using conventional disaggregation methods. Among the criteria used to identify species in thin-section are the ontogenetic changes in chamber size and shape and wall microstructural characteristics as determined from axial views. Taxonomic accuracy is diminished using this approach, however, because of limitations of using a two-dimensional rather than three-dimensional view.

Although the general pattern of developmental change in planktonic foraminiferal morphology was recorded for both fossil and modern populations by several authors (e.g., Rhumbler, 1911; Parker, 1962; Banner and Blow, 1967; Olsson, 1972; Blow, 1979), few detailed ontogenetic studies were pursued until recently. A significant advance was made by Huang (1981) who used a test dissection and SEM observation method to portray the ontogenetic morphology of several Recent and Neogene species. Sverdlove and Bé (1985) subsequently described a method for obtaining ontogenetic morphometric information from light microscopic analysis of planktonic foraminifera embedded in plastic. Their approach is limited to Recent or exceptionally well preserved fossil specimens which are optically transluscent. In a study of the planktonic foraminiferal species *Globigerinoides sacculifer* (Brady) and *G. ruber* (d'Orbigny) recovered from surface plankton tows, Brummer et al. (1986, 1987) identified five developmental stages, designated as the prolocular (= embryonic), juvenile, neanic, adult, and terminal (= reproductive) stages. These were defined on the basis of significant quantitative and qualitative changes in test morphology (e.g., test size, chamber inflation, apertural position, etc.), as well as changes in vital behavior observed in laboratory cultures. All of the above authors convincingly demonstrated the importance of ontogenetic analyses in improving taxonomic classification

Brian T. Huber, Department of Paleobiology, National Museum of Natural History, Smithsonian Institution, Washington, D.C. 20560.

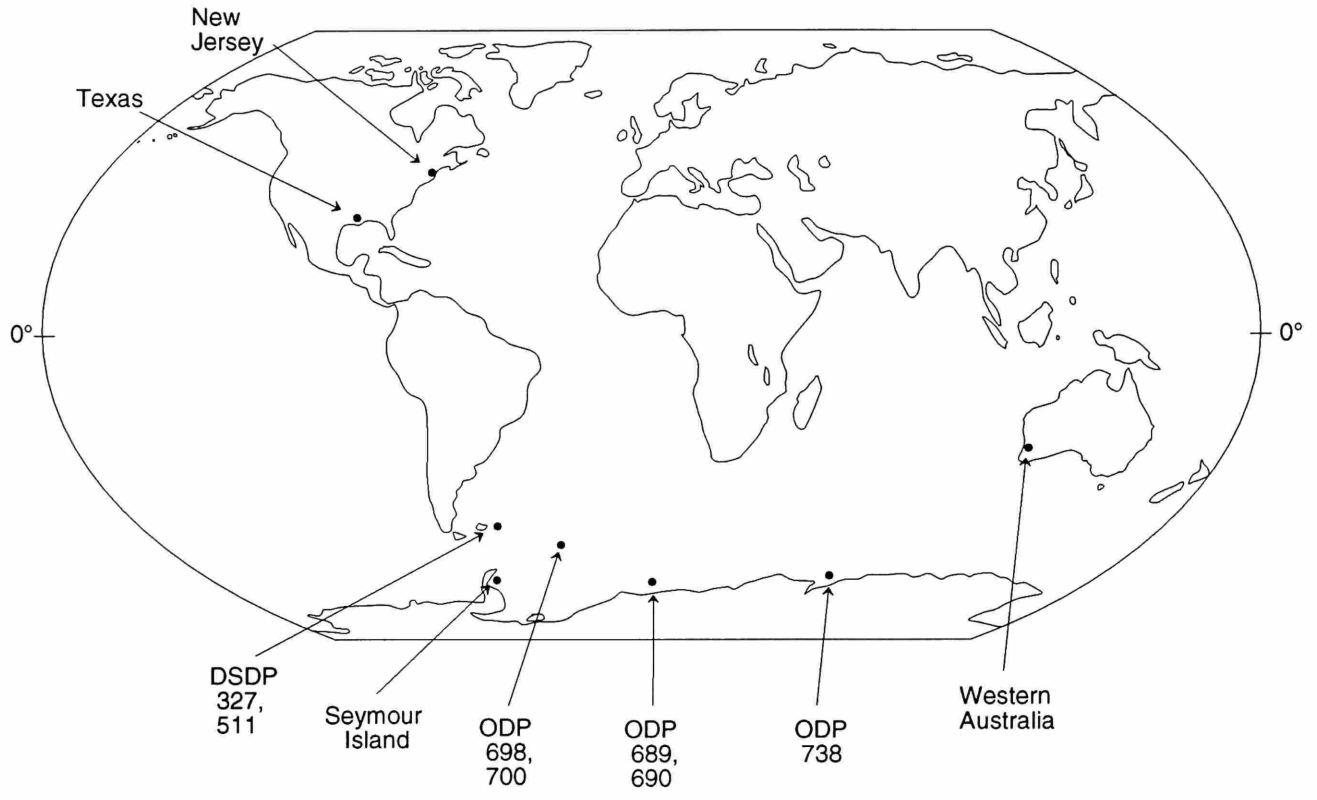

FIGURE 1.—Localities of land-based and deep-sea foraminiferal samples discussed in this study.

schemes. They further emphasized potential applications of ontogenetic information in phylogenetic reconstructions, testing of evolutionary models, as well as improving biostratigraphic resolution, particularly within paleoenvironmentally stressed habitats.

A need for extensive revision of taxonomic concepts for several southern high latitude planktonic foraminiferal groups was recognized by Huber (1987, 1988a) in a study of upper Campanian-Maastrichtian assemblages from Seymour Island in the northern Antarctic Peninsula (Figure 1). Species identified by Sliter (1977) as *Hedbergella monmouthensis* (Olsson), *Rugoglobigerina pilula* Belford, and *Ruglobigerina rotundata* Brönnimann from Falkland Plateau Deep Sea Drilling Project (DSDP) Site 327 were found among the shallow marine Antarctic foraminiferal assemblages. However, comparison with type specimens of these species revealed significant morphologic differences. Moreover, comparison of published SEM micrographs from the Cretaceous southern high latitude studies of Sliter (1977), Krasheninnikov and Basov (1983), and Webb (1973) revealed little agreement in species concepts for non-keeled globigerine taxa. Illustrations of the problematic high latitude morphotypes are reproduced in Plate 1. The taxonomic uncertainties were not resolved in the Huber (1988a) Antarctic foraminiferal study, as the problematic forms were morphologically diverse. Small (<200 μm) normalform specimens with umbilical-extraumbilical apertures (Figure 2*a–d*), kummerform specimens with umbilical to slightly extraumbilical apertures (Figures 2*e–h*), and large normalform specimens with umbilical apertures (Figures 2*i–l*) were tentatively assigned to *Rugoglobigerina*? sp. 1. and *Rugoglobigerina*? sp. 2.

Analysis of Cretaceous planktonic foraminifera from a number of Ocean Drilling Program (ODP) Sites recently drilled in the circum-Antarctic region (Figure 1) revealed abundant specimens identical to the problematic taxa described from the Falkland Plateau and Antarctic Peninsula with a similar range of morphologic variability. These were formally described as *Archaeoglobigerina australis, A. mateola*, and *Hedbergella sliteri* by Huber (1990) and are considered to have been endemic to the Austral Biogeographic Realm during late Campanian–Maastrichtian time (Huber, 1990, 1991a, 1992a; Quilty, 1992). The ontogenetic morphometric approaches described in this study are utilized with several goals in mind. First, the study will verify that the newly described Austral Realm species are not ecophenotypic variants of species previously described from lower latitude regions. The second goal is to establish the range of phenotypic variability of these austral taxa. The morphologies of small forms (referred to as neanic forms or micromorphs) are compared to the interior, pre-adult morphologies of large (gerontic) adults to establish

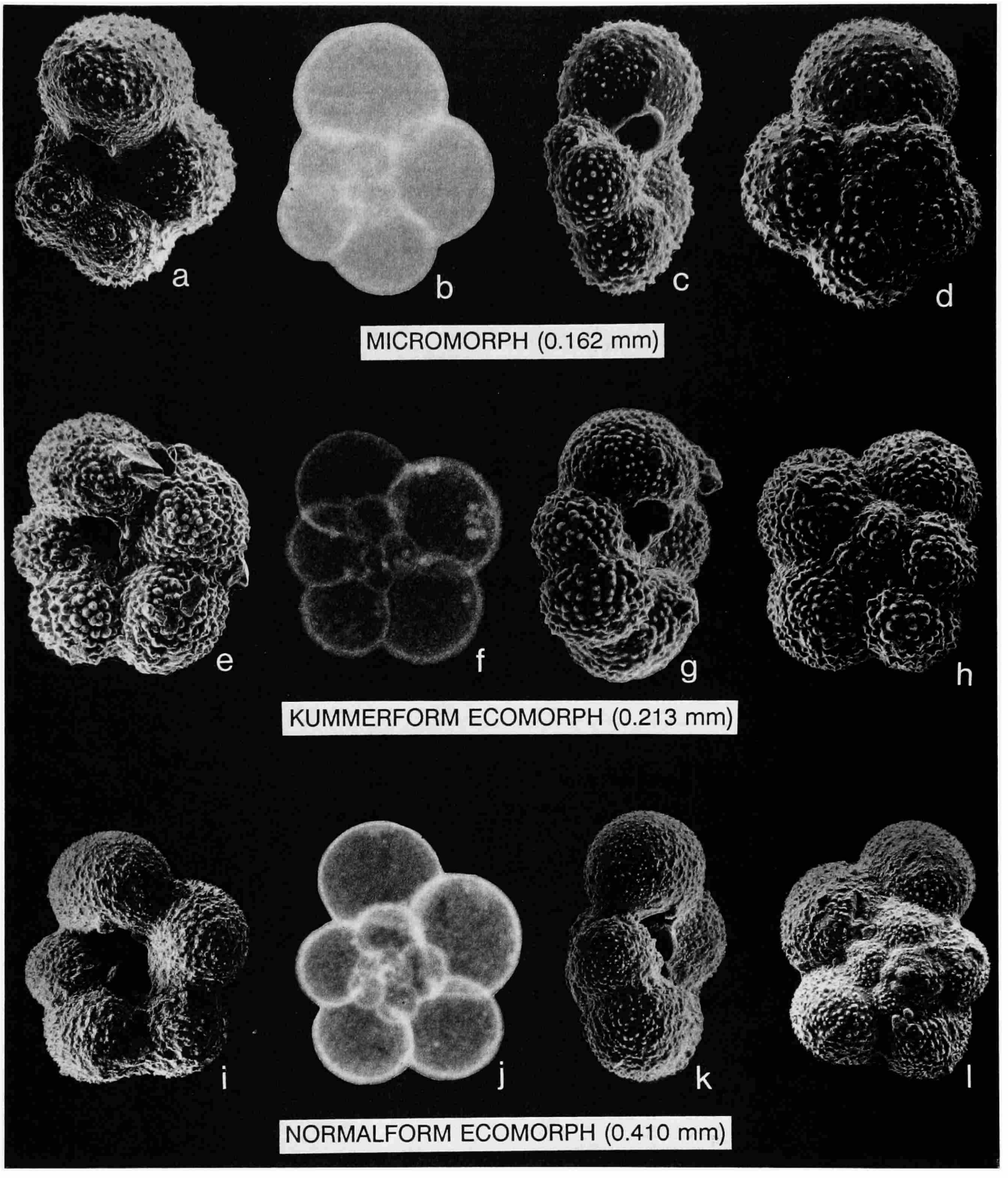

FIGURE 2.—Micromorph, kummerform adult, and normalform adult planktonic foraminifera from Seymour Island (northern Antarctic Peninsula) previously designated by Huber (1988a:207, figs. 29.1–29.14, 30.5–30.10) as *Rugoglobigerina*? sp. 1, but presently identified as *Archaeoglobigerina australis* Huber. Microradiographs of each specimen (*b,f,j*) show the chamber arrangement in the penultimate and earlier whorls. *a–d:* micromorph from sample SI-165; *e–h:* kummerform ecomorph from sample SI-165; *i–l:* normalform ecomorph from sample SI-415. Maximum test diameters in parentheses.

that they are conspecific. Finally, topotypes of two Late Cretaceous species that have meridionally costellate ornamentation will be compared with high-latitude forms that bear faintly similar surface architecture to determine whether their ontogenetic morphologies are similar. Results from this study will lead to a better understanding of the phylogenetic relationships among trochospiral Austral Realm taxa.

ACKOWLEDGMENTS.—Part of this study was undertaken while I was a Ph.D. candidate at The Ohio State University. I am very grateful to Peter -N. Webb, William I. Ausich, Stig M. Bergström, and Larry Krissek (all at OSU) for their comments on an early draft of this manuscript, and to Kou-Yen Wei (Yale University) and Bill Sliter (USGS) for their careful reviews and helpful sugggestions on a later draft. I would also like to thank Peter-N. Webb for providing the resources to conduct my biometric research and Larry Krissek for making his x-ray machine available for my usage. Sample material was kindly sent to me by George C. Chapronière (Bureau of Mineral Resources, Australia), Richard K. Olsson (Rutgers University), and the staff at the Deep Sea Drilling Project East Coast Core Repository (Lamont-Doherty Earth Observatory). Many thanks to Liz Valiulis and Chris Hamilton (U.S. National Museum) for their help with preparation of the illustrations and Mary Parrish (U.S. National Museum) for drawing the foraminifera shown in Tables 2 and 3. Financial support from the Friends of Orton Hall Geology Fund (The Ohio State University) and the Geological Society of America is also gratefully acknowledged.

Materials

A total of 473 specimens of nine different planktonic foraminiferal species were analysed in this study. The sample localities are shown in Figure 1 and include material from: (1) lower to middle Maastrichtian Samples 113-689B-28X-3, 83–87 cm, 113-18X-2, 119–123 cm, 113-690C-19X-3, 119–123 cm, and 113-690C-20X-4, 96–98 cm all from ODP Leg 113 Sites 689 and 690, drilled on Maud Rise, Weddell Sea (64°–65°S, 1°–3°E, 2084–2920 m water depth; see Huber, 1990); (2) lower Maastrichtian Sample 71-511-24-5, 69–71 cm, DSDP Site 511, recovered from Falkland Plateau, southern South Atlantic (51°S, 47°E, 2,589 m depth; see Krasheninnikov and Basov, 1983); (3) lower to middle Maastrichtian Sample 36-327A-10-3, 22–24 cm from DSDP Site 327, from Falkland Plateau, southern South Atlantic (52°S, 46°W, 2410 m depth; see Sliter, 1977); (4) samples 165 and 415 from the lower Maastrichtian of the Lopez de Bertodano Formation on Seymour Island, Antarctic Peninsula (64°S, 57°W; see Huber, 1988a); (5) Maastrichtian samples from the Kemp Clay, Austin County, Texas, (New Zealand Geological Survey samples F101166 and F101167 provided by Dr. P.-N. Webb); (6) lower Maastrichtian Navesink Formation (sample NJK-126), and middle Maastrichtian Redbank Formation, (sample NJK-3) from New Jersey (provided by R.K. Olsson, Rutgers University); and (7) Santonian Toolonga Calcilutite, sample #71640043, Pillawara Hill, Western Australia (provided by Dr. G. Chapronière, Bureau of Mineral Resources, Australia).

Approach to Study

Sample Preparation

Sediment samples were dissaggregated in water by gentle stirring over a warm hotplate for five to ten minutes, then ultrasonically cleaned for several seconds to two minutes, stirred again and wet-sieved through a 63 μm screen. The sieved residues were ultrasonically cleaned again for a few seconds, then dried and picked.

External Morphology

Conventional classification schemes and phylogenetic reconstructions of planktonic foraminifera are primarily based on observation of the external morphology of the test (Tables 1–3). Therefore, all foraminiferal groups in this study are illustrated with SEM micrographs showing the standard umbilical, edge, and spiral views and enlarged views of important external structures. Measurements of apertural height/width ratios (A_h/A_w) on specimens with extraumbilical apertures and test breadth/diameter ratios (B/D) (Figure 3, Table 4) were taken using a stereomicroscope with a camera lucida attachment, a mouse driver, and a digitizing tablet linked to a personal computer. Bioquant™ and Optimas™ biometrics software were used to collect measurements from the digitized images.

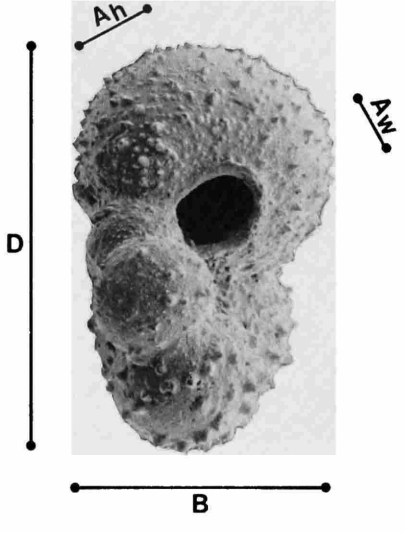

FIGURE 3.—Biometric variables measured from external views of planktonic foraminifera. Apertural height/width ratios measured only on specimens showing extraumbilical apertures. Variables include: A_h = apertural height; A_w = apertural width; B = test breadth; D = test diameter.

TABLE 1.—Contrasting hierarchical schemes used to taxonomically subdivide the Rotaliporacea and Globotruncanacea (sensu Loeblich and Tappan, 1988).

Taxonomic units	Brönnimann and Brown, 1956	Bolli, Loeblich, and Tappan, 1957	Banner and Blow, 1959	Pessagno, 1967	Masters, 1977	Banner, 1982	Loeblich and Tappan, 1988
Superfamily	Not stated.	Not stated.	Not stated.	Not stated.	Not stated.	Not stated.	Apertural position. Presence/absence of tegilla.
Family	Presence/absence of costellae, and/or imperforate peripheral band and/or presence/absence of accessory aperatures.	Wall composition and structure. Apertural position. Chamber arrangement.	Presence/absence of lips, portici, or tegilla.	Presence/absence of lips, portici, or tegilla. Position of aperture. Type of chamber arrangement.	Type of coiling. Characteristics of equatorial periphery. Presence/absence of lips, portici, or tegilla.	Presence/absence of lips, portici, or tegilla. Presence/absence of supplementary apertures. Position of primary aperture.	Presence/absence of supplementary apertures. Presence/absence of lips, portici, or tegilla. Surface ornamentation.
Subfamily	Presence/absence of accessory apertures.	Presence/absence of lips, portici, or tegilla. Modifications in chamber arrangement.	Shape and position of primary aperture.	Presence/absence of accessory, relict, or sutural supplementary apertures. Position of primary aperture.	Presence/absence of peripheral band and/or keel(s). Apertural position.	Presence/absence of peripheral band and/or keel(s).	Presence/absence of accessory apertures, peripheral band, and/or keel(s).
Genus	Modifications of aperture (lips, portici, tegilla). Modifications of chamber shape.	Shape and character of adult aperture. Presence/absence of chamber modifications. General form and development of test.	Presence/absence of supplementary or relict apertures. Modifications of chamber shape. Presence/absence of imperforate peripheral keels.	Presence/absence of keels, imperforate peripheral bands, pseudocarinae. Structure of keels. Shape of chambers. Presence of unique ornamentation (eg., meridional costellae).	Presence/absence of accessory apertures. Modifications of chamber shape.	Surface ornamentation. Size of umbilicus. Modifications in chamber shape. Relative size proportions of test.	Presence/absence of peripheral band and/or keel(s). Modifications of test and chamber shape. Surface ornamentation. Relative size proportions of test.
Species	Chamber morphology and arrangement. Size, shape, and surface ornament of test.	Size; relative proportions of test, chambers, aperture, etc. Surface ornament.	Not stated.	Relative size proportions of test. Shape of primary aperture. Surface ornamentation. Character of early growth stages.	Size of umbilicus. Surface ornamentation. Relative size proportions of test.	Not stated.	Not stated.

TABLE 2.—Classification scheme used by Loeblich and Tappan (1988) to distinguish genera included in the Rotaliporacea.

	Rotaliporacea													
	Hedbergellidae								Favusel.	Rotaliporidae				
	Asterohedbergella	*Costellagerina*	*Hedbergella*	*Whiteinella*	*Falsotruncana*	*Praeglobotruncana*	*Concavotruncana*	*Helvetoglobotruncana*	*Favusella*	*Biticinella*	*Clavihedbergella*	*Ticinella*	*Anaticinella*	*Rotalipora*
Primary aperture	umb.-extumb.	umb.-extumb.	umb.-extumb.	umb.-extumb.	umb.-extumb.	umb.-extumb.	umb.-extumb.	umb.-extumb.	umb.-extumb.	umb.-equator.	umb.-extumb.	umb.-extumb.	umb.-extumb.	umb.-extumb.
Supplement. apertures	no	no	no	no	no	no	no	no	no	yes	yes	yes	yes	yes
Apertural projection	narrow lip	narrow lip	narrow lip or flap	flap or porticus	narrow lip	lip or flap	coalescing portici	flap or porticus	narrow lip	lip	lip	lip	lip or flap	lip
Equatorial periphery	angular, tubulo-spinate	rounded	rounded	rounded	two keels	one keel	two keels	one keel	rounded	rounded	rounded, clavate	rounded	weak keel	one keel
Surface ornament	smooth-finely hispid	meridional costellae	smooth to finely hispid	pustulose	pustulose	pustulose	pustulose	pustulose	cancellate	smooth	smooth	smooth	smooth to hispid	smooth to pustulose
Cameral sutures	depressed	depressed	depressed	depressed	depressed	depressed	depressed	depressed	depressed	depressed	depressed	depressed	depressed	raised
Represent-ative illustration (edge view)														
Type species	*Hedbergella (Astero-hedbergella) asterospinosa* Hamaoui, 1964	*Rugoglobigerina bulbosa* Belford, 1960	*Anomalina lorneiana* d'Orbigny var. *trochoidea* Gandolfi, 1942	*Whiteinella archaeocretacea* Pessagno, 1967	*Falsotruncana maslakovae* Caron, 1981	*Globorotalia delrioensis* Plummer, 1931	*Rotalia concavata* Brotzen, 19 34	*Globotruncana helvetica* Bolli, 1945	*Globigerina washitensis* Carsey, 1926	*Anomalina bregglensis* Gandolfi, 1942	*Hastigerinella subcretacea* Tappan, 1943	*Anomalina roberti* Gandolfi, 1942	*Globorotalia? multiloculata* Morrow, 1934	*Globorotalia cushmani* Morrow, 1934

TABLE 3.—Classification scheme used by Loeblich and Tappan (1988) to distinguish genera included in the Globotruncanacea.

	GLOBOTRUNCANACEA																			
	Globotruncanidae												Rugoglobigerinidae							
	Contusotruncana	*Ganserina*	*Globotruncana*	*Globotruncanita*	*Kassabiana*	*Marginotruncana*	*Radotruncana*	*Rugotruncana*	*Sigalitruncana*	*Globotruncanella*	*Abathomphalus*	*Archaeoglobigerina*	*Buchelina*	*Kuglerina*	*Plummerita*	*Rugoglobigerina*	*Trinitella*			
Primary aperture	umb.	umb.	umb.	umb.-slightly ext.-umb.	umb.	umb.-extumb.	umb.	umb.	umb.-extumb.	umb.-extumb.	umb.-extumb.	umb.	umb.	umb.	umb.	umb.	umb.			
Supplement. apertures	no	no	no	no	no	no	no	no	no	no	no	no	no	no	no	no	no			
Apertural projection	coalescing portici	portici & tegilla	coalescing portici	coalescing portici	coalescing portici	portici & tegilla	coalescing portici	portici & tegilla	coalescing portici	portici & tegilla	portici & tegilla	tegilla	tegilla	tegilla	tegilla	tegilla	tegilla			
Equatorial periphery	two keels	one or two keels	two keels	one keel	one keel sometimes tubulospinate	two keels	one keel tubulospinate	band or two keels	one or two keels	band or one keel	one or two keels	band or two wk. keels	one faint keel	rounded	rounded to compressed, tubospinate	rounded	rounded to truncate, faint carinal band			
Surface ornament	smooth-pustulose	pustulose	smooth-pustulose	smooth	smooth-pustulose	smooth-pustulose	smooth-pustulose	pustulose to meridionally rugose	smooth	pustulose	pustulose to costellate	pustulose to costellate	papillose-hispid	pustules & rugosities	rugosities & meridional costellae	meridional costellae	meridional costellae			
Cameral sutures	depressed	depressed to raised	depressed to raised	depressed to raised	raised	depressed to raised	depressed to raised	depressed	depressed to raised	depressed	depressed	depressed	depressed	depressed	depressed	depressed	depressed			
Represent-ative illustration (edge view)																				
Type species	*Pulvinulina arca* var. *contusa* Cushman, 1926	*Globotruncana ganseri* Bolli, 1951	*Pulvinulina arca* Cushman, 1927	*Rosalina stuarti* de Lapparent, 1918	*Globotruncana falsocalcarata* Kerdany & Abdelsalam, 1969	*Rosalina marginata* Reuss, 1846	*Globotruncana calcarata* Cushman, 1927	*Rugotruncana tilevi* Brönnimann & Brown, 1956	*Globotruncana sigali* Reichel, 1950	*Globotruncana havanensis* Voorwijk, 1937	*Globotruncana mayaroensis* Bolli, 1951	*Archaeoglobigerina blowi* Pessagno, 1967	*Buchelina sandidgei* Brönnimann & Brown, 1956	*Rugoglobigerina rugosa rotundata* Brönnimann, 1952	*Rugoglobigerina* (*Plummerella*) *hantkenoides hantkenoides* Brönnimann, 1952	*Globigerina rugosa* Plummer, 1927	*Trinitella scotti* Brönnimann, 1952			

TABLE 4.—Biometric data obtained from external observations and microradiographs of species discussed in this study.

SPECIES	*Hedbergella holmdelensis*	*Hedbergella monmouthensis*	*Hedbergella sliteri*	*Costellagerina pilula*	*Archaeoglob. australis* (neanic)	*Archaeoglob. australis* (adult)	*Archaeoglob. bosquensis*	*Archaeoglob. mateola*	*Archaeoglob. cretacea*	*Rugoglobigerina rugosa*
LOCALITY	New Jersey Navesink Fm.	New Jersey Red Bank Fm.	DSDP 327A, 10-3, 22-24	W. Australia Toolonga Calcil.	DSDP 511, 23-4, 67-69	DSDP 511, 23-4, 67-69	DSDP 511, 47-5, 27-29	ODP 690C, 20-4, 96-98	DSDP 511, 34-4, 1-3	Texas Kemp Clay
AGE	early Maastrichtian[1]	late Maastrichtian[1]	early Maastricht.[2]	Santonian[3]	early Maastricht.[2]	early Maastricht.[2]	Santonian[5]	middle Maastrichtian[6]	early Campanian[5]	Maastrichtian[7]
OBSERVATIONS	11	13	52	67	46	94	47	41	60	42
ULTIMATE WHORL CHAMBER NUMBER*	5.21 (0.49) 4.50-5.75	5.48 (0.50) 4.75-6.25	5.35 (0.20) 5.00-6.00	4.88 (0.37) 4.00-5.75	4.61 (0.33) 3.75-5.75	4.59 (0.32) 3.75-4.75	4.23 (0.53) 3.00-5.50	4.23 (0.53) 3.00-5.50	5.16 (0.39) 4.50-5.75	4.43 (0.36) 3.75-5.25
PENULTIMATE WHORL CHAMBER NUMBER*	6.25 (0.21) 6.00-6.50	5.88 (0.24) 5.50-6.25	5.15 (0.28) 4.50-6.00	5.57 (0.54) 4.50-6.25	4.96 (0.29) 4.25-5.50	4.66 (0.28) 4.00-5.50	4.64 (0.34) 4.00-5.50	4.43 (0.59) 3.75-5.75	5.00 (0.37) 4.50-5.75	5.31 (0.47) 4.50-6.00
PERCENT DEXTRAL	67%	39%	52%	46%	87%	76%	86%	78%	97%	98%
PERCENT KUMMERFORM	0%	23%	8%	10%	66%	36%	55%	80%	30%	0%
APERTURAL HEIGHT/WIDTH RATIO*	0.55 (0.10) 0.44-0.63	0.48 (0.12) 0.41-0.62	0.37 (0.12) 0.17-0.68	---	0.94 (0.13) 0.72-115	---	---	---	---	---
UMBILICUS/TEST DIAMETER RATIO*	0.19 (0.03) 0.17-0.23	0.21 (0.01) 0.20-0.21	0.28 (0.02) 0.21-0.34	0.30 (0.05) 0.18-0.45	0.25 (0.05) 0.14-0.34	0.28 (0.06) 0.15-0.50	0.19 (0.04) 0.13-0.30	0.19 (0.04) 0.13-0.30	0.29 (0.04) 0.20-0.36	0.21 (0.06) 0.09-0.34
AVG. DIAM (μm)	163	165	274	279	192	280	285	270	356	256
MAX. DIAM. (μm)	218	230	340	421	---	400	340	415	468	410
BREADTH/DIAMETER RATIO OF TEST*	0.49 (0.04) 0.45-0.54	0.49 (0.03) 0.47-0.52	0.45 (0.03) 0.39-0.51	0.60 (0.08) 0.46-0.93	0.62 (0.06) 0.44-0.78	0.55 (0.06) 0.29-0.85	0.68 (0.08) 0.52-0.85	0.69 (0.09) 0.55-0.95	0.47 (0.06) 0.31-0.63	0.64 (0.09) 0.27-0.79
PENULT./ANTEPEN. CHAMBER RATIO*	1.25 (0.10) 1.09-1.43	1.19 (0.09) 1.05-1.30	1.18 (0.06) 1.08-1.30	1.16 (0.15) 0.90-1.67	1.31 (0.25) 0.80-1.89	1.16 (0.16) 0.72-1.56	1.03 (0.21) 0.74-1.47	0.99 (0.12) 0.77-1.23	1.11 (0.12) 0.92-1.28	1.29 (0.12) 0.03-1.52
PORTICI	present	present	common	rare	common	common	rare	common	common	none
TEGILLA	none	none	none	none	none	rare	none	none	none	common

*Values include the population mean, standard deviation (in parentheses), and minimum to maximum range.
[1]Olsson, 1964; [2]Huber, 1991a; [3]Belford, 1960; [4]Huber, 1988a; [5]Krasheninnikov and Basov, 1983; [6]Huber, 1990; [7]Pessagno, 1967.

Measurement precision using external views of specimens under the light microscope is considerably less than with the methods described below, particularly for specimens smaller than 200 μm. Although variation about the mean for 20 μm bar scale measurements is ±8 μm at ×50 magnification, greater uncertainty (up to ±15 μm) occurs with measurement of three-dimensional images with reflective surfaces, such as foraminiferal shells.

Contact Microradiography

Methods.—Foraminiferal microradiographs were obtained by adapting the methods described by Arnold (1982). A 2 × 5 inch cardboard sheet with a grid of 30 holes was backed with tracing paper and used to hold the foraminiferal specimens during the x-ray exposure. The tracing paper was coated with gum tragacanth so that the mounted specimens could be oriented to obtain a full axial image. The image was recorded on 2 × 5 inch sheets of High Resolution KODAK Film #SO-343, with the emulsion side placed in contact with the bottom of the cardboard sheets. The film and mounted specimens were placed on the middle shelf of a Hewlitt-Packard Faxitron x-ray unit and exposed at 40 KVP for 40 minutes. The developed film was cut, labelled, mounted on glass slides, and photographed through a Leitz Orthoplan microscope. The best images were obtained from low trochospiral specimens free of adhering matrix and without infilled chambers.

Biometric data were collected from the microradiographs by measuring the x-ray images on a video screen using a video camera mounted on a Leitz Orthoplan microscope, a digitizing tablet linked to a personal computer, and biometrics software. Because vertical portions of the chamber walls are opaque to x-rays, the cross-sectional outline of the axial periphery, chamber sutures, and whorl sutures appear as unexposed curves on the microradiographs (e.g., see Figure 4). Individual distances, size ratios, and area measurements can be rapidly and accurately obtained from the microradiographs using the biometrics software and hardware. Precision in measuring the x-ray images was determined to be within ±2 μm at ×160 magnification.

Biometric Variables.—Biometric data collected from x-ray images measurements are portrayed in Figure 4 and listed in Table 4. The number of chambers in the ultimate whorl (U) are calculated by adding the number of whole chambers to the ratio of the distance between the exterior sutural contacts of the first chamber in the ultimate whorl (c_1) and the total of $c_1 + c_2$, the length of the first ultimate whorl chamber overlapped by the final chamber. The same method is used to determine the number of chambers in the penultimate whorl (P). The presence of kummerform (reduced) final chambers was determined based on the ratio of the ultimate chamber width (Uw_1) and the penultimate chamber width (Uw_2); values of less than one were recorded as kummerform. The ratios of the size of the penultimate (Uw_2) and antepenultimate (Uw_3) chambers are also recorded using this method. The ratio of the umbilical/test diameter is determined by measuring the ratio of the distance from the coiling axis to the umbilical edge of the penultimate chamber (g_1) to the total to $g_1 + g_2$, the width between umbilical edge of the penultimate chamber and the chamber's peripheral edge (Figure 4).

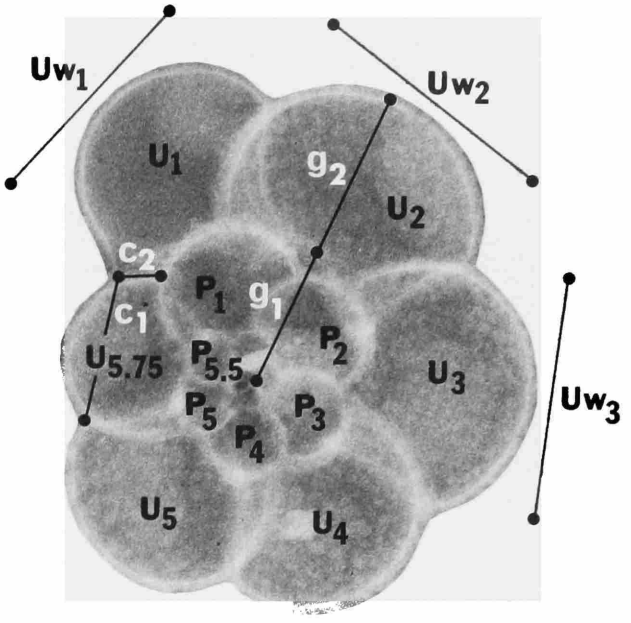

Figure 4.—Biometric variables measured from x-ray images. Initial whorl dimensions were only obtained from the most evolutely coiled specimens. Variables include: $c_1/(c_2 + g_2)$ = n^{th} chamber proportion; $g_1/(g_2 + g_2)$ = umbilicus/test diameter ratio; P = penultimate whorl chambers; U = ultimate whorl chambers; Uw_1/Uw_2 = ultimate/penultimate chamber ratio; Uw_2/Uw_3 = penultimate/antepenultimate chamber ratio.

Utility and Limitations.—The main advantage to the x-ray method for biometric analysis of foraminifera is the ease and rapidity with which large data sets can be generated. Statistical differences in the number of chambers within the penultimate whorl, chamber size parameters, and position of the generating curve can readily be determined for different species populations of several hundreds to thousands of specimens. The x-radiographs also show accurate detail of ontogenetic changes in chamber and whorl suture morphology particularly among the more evolute coiled taxa. An additional benefit is that the internal morphology of sufficiently preserved holotype or paratype specimens can be observed without recourse to test dissection or thin sectioning. Furthermore, the cost of obtaining the microradiographs is generally limited to the price of the film used, as the necessary equipment is available at most research institutions.

This method could not be applied to specimens with coarsely ornamented, heavily encrusted, or infilled tests, as these are opaque to x-rays and thus the chamber sutures cannot be

differentiated. In addition, several biometric characters are difficult to measure in high-spired specimens because of the weak images produced by strongly overlapping chambers. Chamber overlap prevents accurate total chamber number counts and measurement of morphocharacters within the initial whorl in all but the most evolutely coiled taxa. Attempts at measuring ontogenetic changes in cross-sectional chamber area from the x-ray images were abandoned for all species except the evolutely coiled *H. sliteri* because of obscured chamber sutures and uncertainty of where in the ontogeny the measurable chambers were positioned.

The number of specimen measurements needed to sufficiently characterize planktonic foraminiferal populations depends on the morphologic variability of each species group. For example, the mean value for the number of ultimate whorl chambers was determined as 5.28 for the first 20 measurements of *Hedbergella sliteri* Huber, a morphologically conservative species, and 5.34 for the total population of 52 specimens (Table 4), a difference of less than 2%. On the other hand, the mean value of the first 20 measurements of *Archaeoglobigerina australis* Huber, which shows considerable morphologic variability, differed by 6% from mean values obtained for 52 specimens. The mean values for 42 more specimens of *A. australis*, changed only by 1% from the values obtained for 20 specimens.

Serial Dissections

Specimen Preparation.—The procedures for preparing specimens for serial dissection and SEM analysis were modified from methods described by Huang (1981). A small amount of xylol-free Canada balsam is evenly sprinkled on the surface of an SEM stub that is placed on a small lead block and heated on a hotplate at 140°C. When the balsam begins to melt, several drops of xylene are added until the mounting medium homogenizes into a smooth coating about 0.5 mm thick. The stub is removed from the heat after about two minutes. Once cooled, the consistency of the balsam is tested in several areas by the pressure of a needle. The stub must be reheated if the cooled balsam is still soft; otherwise mounted specimens will move while being dissected. About 25 specimens are aligned in several rows with their spiral sides down on the hardened balsam. The stub is then reheated to 150°C while viewed with a microscope. At this temperature, the balsam is too viscous to penetrate the walls of porous specimens, but soft enough to partially emplace the specimens in the medium by lightly pressing with a fine needle. If the specimens sink too far in the embedding medium or become infilled with balsam, they can be reheated, removed with a needle, and cleaned in a small vial of acetone. The stub is removed from the hotplate after all specimens are embedded to their equatorial periphery and adjusted so that their coiling axes are perpendicular to the stub surface.

Specimen dissection was made easier by using a device that acts as a universal stage. For this study, a Leitz mechanical micromanipulator was used with a modified attachment for holding an SEM stub. Use of this device allows tilting and rotation of the mounted specimens in any orientation, which is particularly crucial during dissection of moderately to high-spired specimens.

Tests are dissected with a fine needle that is sharpened to a wedge about 10 μm in width. The needle is mounted on the end of a micromanipulator, which affords precise three-dimensional movement, enabling dissection of chambers as small as 10 μm in diameter. Foraminiferal tests are dissected under a light microscope with the wedged needle oriented parallel to the plane of the axial periphery. After each whorl is dissected, the specimens are cleaned in a ultrasonic bath and prepared for SEM study. High-spired specimens are the most difficult to dissect as the walls of the adult chambers obscure the view of the test interior. Care must be taken to avoid cutting chambers in the initial whorls beyond their maximum diameter so that accurate measurements can be obtained.

The most tedious aspect of this dissection method arises with repeated serial dissection and SEM study of each whorl down to the prolocular chamber. In order to characterize their complete morphology, the umbilical, spiral, and edge views of external morphology are recorded by SEM, before the specimens are mounted in balsam. Specimens chosen for dissection were previously x-rayed to confirm that the test chambers were not infilled. The specimen is photographed on the SEM after each whorl is removed until complete dissection is achieved. If the specimen is damaged during any stage of this process, the goal of illustrating the complete ontogeny of individual specimens cannot be attained. Therefore, several specimens of the same species were serially dissected to improve the odds for complete success.

Biometric information from the initial whorl was most rapidly obtained by completely dissecting up to 25 specimens on a single SEM stub immediately after being embedded, without the repeated SEM photography subsequent to each whorl removal. The most cost- and time-efficient way to record the information from the dissected populations is by photographing with a 35 mm camera mounted on the SEM. Biometric variables can then be easily measured from proof sheets of the SEM images with the light microscope and the biometrics equipment described above.

Biometric Variables.—*Qualitative Observations:* Serial dissection of ventral chamber walls facilitates identification of pre-adult growth stages inside the foraminiferal tests. The exterior of the early formed chambers provides several important criteria that can be used for supraspecific assignment. These include the (1) degree of chamber compression, (2) angularity of chamber sutures, (3) changes in apertural position, and (4) surface ornament of the outer walls of interior chambers.

Brummer et al. (1987) cautioned that secondary calcification of earlier formed chambers may obscure their primary surface structure, producing a smoothened surface ornament on the outer wall of interior chambers. The presence of spines and pustules on early formed chambers, however, is considered a primary feature as these are not added after initial chamber calcification (Bé et al., 1979).

Quantitative Observations: Biometric data obtained from the initial whorl of planktonic specimens in this study include the diameter of the proloculus (earliest formed chamber), initial whorl diameter, and number of chambers in the initial whorl (Figure 5). Microradiographs of involute taxa do not show this information because of the strong chamber overlap, resulting in blurred images of the initial whorl sutures. Only microradiographs of *Hedbergella sliteri*, a nearly evolute species, recorded accurate detail of the initial whorl chamber sutures. Therefore, the number of measurements for this species (51) far exceeds those for serially dissected specimens, which generally number less than 20 (Table 5).

Serial dissections also enable an accurate count of the maximum number of chambers for each species. This information may be obscured in some trochospiral taxa due to secondary calcification on the external surface of earlier formed chambers.

A measure of the increase in cross-sectional chamber area per successive chamber is proposed in this study as a means for characterizing the rate of chamber size increase throughout ontogeny. This two-dimensional approach accounts for changes in chamber size and shape, whereas the measure of developmental changes in test diameter used by Brummer et al. (1987) only recognizes growth increase in the direction of coiling.

The chamber-by-chamber changes in test porosity were also measured from the serial dissections. The inner shell surfaces provide the best estimation of shell porosity since secondary calcification of chamber walls can greatly reduce or obliterate pore openings on the outer chamber surface (Bé, 1968). Diagenetic overgrowths and recrystallization of inner wall surfaces will also reduce the pore number and pore areas, resulting in an underestimation of shell porosity. Thus, care must be taken to use the best preserved specimens available.

Although the pore shapes vary between species (Figures 6, 7), all are cylindrical (e.g., Figure 6*d*) and most have a funnel-shaped opening (e.g., Figure 6*a*). Average diameters of the cylindrical section of the pores were taken for five pores per chamber through the coiling shells of five specimens per species. All pore diameters were measured from the SEM screen at high magnification (×8,000) and converted to pore areas (P_A). Based on the perforation diameters, two major wall types are recognized (after Steinick and Fleisher, 1978; Blow, 1979; Li Qianyu and Radford, 1991): microperforate (<1 μm) and medioperforate (1–4 μm). Macroperforate (>4 μm) walls were not encountered among the species analyzed in this study.

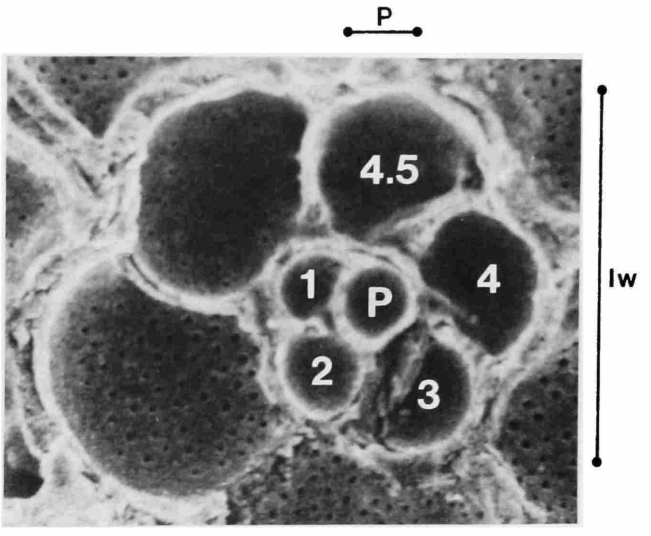

FIGURE 5.—Biometric variables measured from the initial whorl exposed after complete test dissection. The initial whorl chamber number is determined from the sequential count of chambers following the proloculus (P) to the point of overlap with the proloculus–deuteroconch (= first chamber) suture, recorded as 0.25 increments.

Pore concentration (P_C) values were determined for five specimens of each species by counting the number of pores per cross-sectional chamber area for the first seven to nine chambers. In the subsequent chambers, pores were counted within a measured area in the central part of the chambers to avoid distortion caused by curvature of the chamber walls. These values were then normalized to an area of 625 μm^2 so that the measurements could be compared with the pore concentrations determined by Bé (1968) for several modern planktonic species. Shell porosity (S_P), expressed in percent, is determined by the equation $S_P = [(P_A * P_C)/625] * 100$ for the ontogenetic series of all measured specimens (Tables 6–15).

UTILITY AND LIMITATIONS.—Serial dissection of ventral chamber surfaces coupled with SEM analysis of test interiors is the best method for characterizing morphologic changes that occur during the ontogeny of trochospirially coiled fossil planktonic foraminifera. Attributes of the pre-adult morphology exposed during test dissection provide a whole new suite of morphocharacters that can be used to supplement observations of the test exterior. The value of this information for improved taxonomic classification is demonstrated in this study, as is the potential for improved phylogenetic and paleoenvironmental reconstructions.

The disadvantage of this method is that it is a slow, laborious process requiring equipment not available at many institutions. Careful dissections of the small, interior chambers of numerous specimens could not have been made without the micromanipulator, a specialized and expensive tool. In addition, the amount of SEM work needed to complete each species analysis adds to the time and expense of this technique. This dissection method

TABLE 5.—Biometric and observational data obtained from planktonic foraminiferal serial dissections.

SPECIES	*Hedbergella holmdelensis*	*Hedbergella monmouthensis*	*Hedbergella sliteri*	*Costellagerina pilula*	*Archaeoglob. australis* (neanic)	*Archaeoglob. australis* (adult)	*Archaeoglob. bosquensis*	*Archaeoglob. mateola*	*Archaeoglob. cretacea*	*Rugoglobigerina rugosa*
LOCALITY	New Jersey Navesink Fm.	New Jersey Red Bank Fm.	DSDP 327A, 10-3, 22-24	W. Australia Toolonga Calcil.	DSDP 511, 23-4, 67-69	DSDP 511, 23-4, 67-69	DSDP 511, 47-5, 27-29	ODP 690C, 20-4,96-98	DSDP 511, 34-4, 1-3	Texas Kemp Clay
AGE	early Maastrichtian[1]	late Maastrichtian[1]	early Maastricht.[2]	Santonian[3]	early Maastricht.[2]	early Maastricht.[2]	Santonian[5]	middle Maastricht.[4]	early Campanian[5]	Maastricht.[6]
OBSERVATIONS	2	2	51	18	18	34	23	16	16	19
PROLOCULUS DIAMETER* (μm)	10.49 (1.48) 9.44-11.53	10.86 (1.01) 10.14-11.57	16.9 (1.8) 13.6-20	14.5 (1.1) 12.6-17.1	13.9 (2.8) 10.4-22.0	15.1 (1.8) 12.6-18.7	15.3 (2.0) 12.3-19.4	17.4 (4.5) 12.7-27.8	19.8 (2.3) 16.2-23.4	15.3 (1.9) 10.9-18.5
INITIAL WHORL DIAMETER* (μm)	42.15 (8.18) 36.36-47.93	40.66 (3.15) 38.43-42.89	74.3 (11.2) 53.6-99.7	67.6 (6.0) 57.4-78.2	61.1 (13.8) 41.2-91.3	71.8 (7.9) 61.8-93.2	74.9 (12.2) 50.4-95.8	74.1 (18.8) 51.6-117.0	92.2 (9.3) 77.1-115.2	62.7 (7.8) 57.4-78.2
INITIAL WHORL CHAMBER NUMBER*	6.00 (0.00) 6.00-6.00	5.13 (0.18) 5.00-5.25	5.03 (0.16) 4.75-5.25	5.42 (0.33) 4.75-6.00	4.69 (0.33) 4.00-5.25	4.38 (0.27) 3.75-5.00	4.36 (0.22) 4.00-4.75	4.48 (0.25) 4.00-5.00	4.57 (0.28) 4.00-5.00	4.75 (0.23) 4.50-5.00
INIT. WHORL APERT. POSITION	extraumbilical	extraumbilical	extraumbilical	extraumbilical	extraumbilical	extraumbilical	extraumbilical	extraumbilical	extraumbilical	extraumbilical
PENULT. WHORL APERT. POSITION	extraumbilical	extraumbilical	extraumbilical	extraumbilical	umbilical-extraumbilical	umbilical-extraumbilical	umbilical-extraumbilical	umbilical-extraumbilical	umbilical-extraumbilical	umbilical-extraumbilical
INITIAL WHORL CHAMB. ORNAMENT.	smooth	smooth	smooth	smooth	smth. to fn. pustules	smth. to fn. pustules	smth. to fn. pustules	fine pustules	smth. to fn. pustules	fine pustules
PENULT. WHORL CHAMB. ORNAMENT.	smth. to fn. pustules	smth. to fn. pustules	smth. to fn. pustules	smth. to fn. pustules	fine pustules	fine pustules	fine pustules	fn. to med. pustules	fine pustules	fn. to med. pustules
EXTERN. WHORL SURF. ORNAMENT.	smth. to fn. pustules	smth. to fn. pustules	smth. to fn. pustules	meridional costellae	fine pustules	coarse pustules	coarse pustules	coarse pustule large spines	med. pustule fine keeled	meridional costellae
MAXIMUM SHELL POROSITY	0.56%	1.33%	0.97%	4.37%	1.43%	3.72%	6.61%	2.75%	8.14%	23.25%
MAX. CHAMBER NUMBER	15	15	16	19	11	16	14	16	17	16

*Values include the population mean, standard deviation (in parentheses), and minimum to maximum range.
[1]Olsson, 1964; [2]Huber, 1991a; [3]Belford, 1960; [4]Huber, 1990; [5]Krasheninnikov and Basov, 1983; [6]Pessagno, 1967.

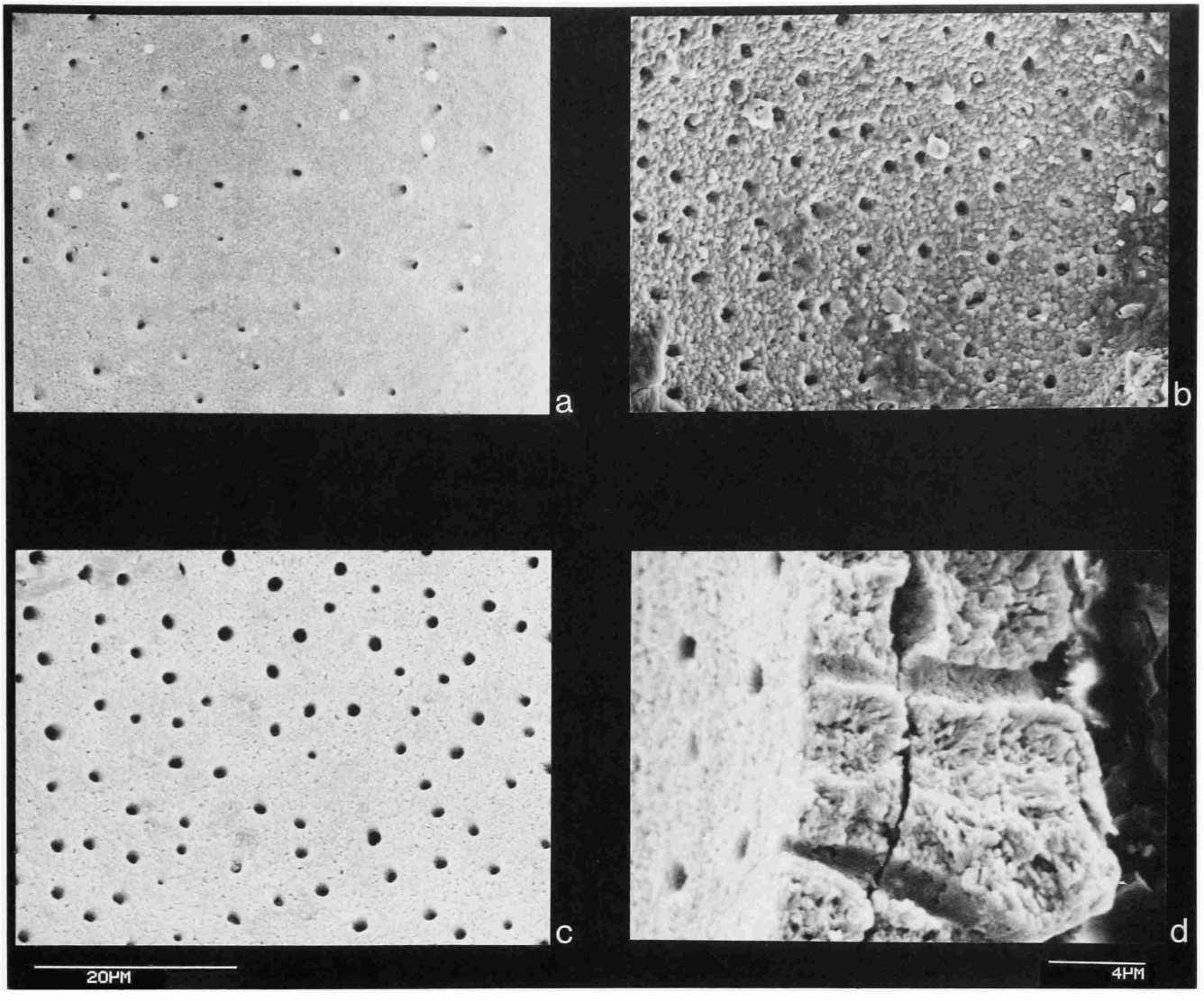

FIGURE 6.—Interior views of ventral chamber surfaces showing pore distributions in the twelfth chamber wall of *a, Hedbergella sliteri*; *b, Costellagerina pilula*; and *c, Archaeoglobigerina bosquensis*. A cross-sectional view of wall pores in the twelfth chamber of *A. bosquensis* is shown in Figure 6*d*. (Scale bar is 20 μm for Figures 6*a–c*, 4 μm for Figure 6*d*.)

can be applied to specimens that are permeated by unconsolidated sediment, which can be removed in an ultrasonic bath, but it cannot be used on specimens infilled with lithified materials.

As with the x-radiographic method, the number of specimens needed to adequately characterize planktonic foraminiferal populations using biometric characters derived from serial dissections depends on the degree of variablity within each species group. One species, *Archaeoglobigerina mateola* Huber, shows a bimodal distribution of proloculus and initial whorl diameters (see below), but this was only recognized after measurement of the first nine dissected specimens. Addition of the two "megalospheric" specimens to the data set of 11 microspheric proloculus diameters changed the population mean by 9.2%. This total is considered insufficient for an accurate representation of whole population variability. On the other hand, the proloculus diameter means of a less variable species, *Costellagerina pilula* (Belford) changed by less than 2% after eight specimen measurements were added to the first ten. Data sets of less than 20 specimens presented in this study can be used for preliminary interpretation, but more specimens should be measured to provide a more statistically reliable base for comparison.

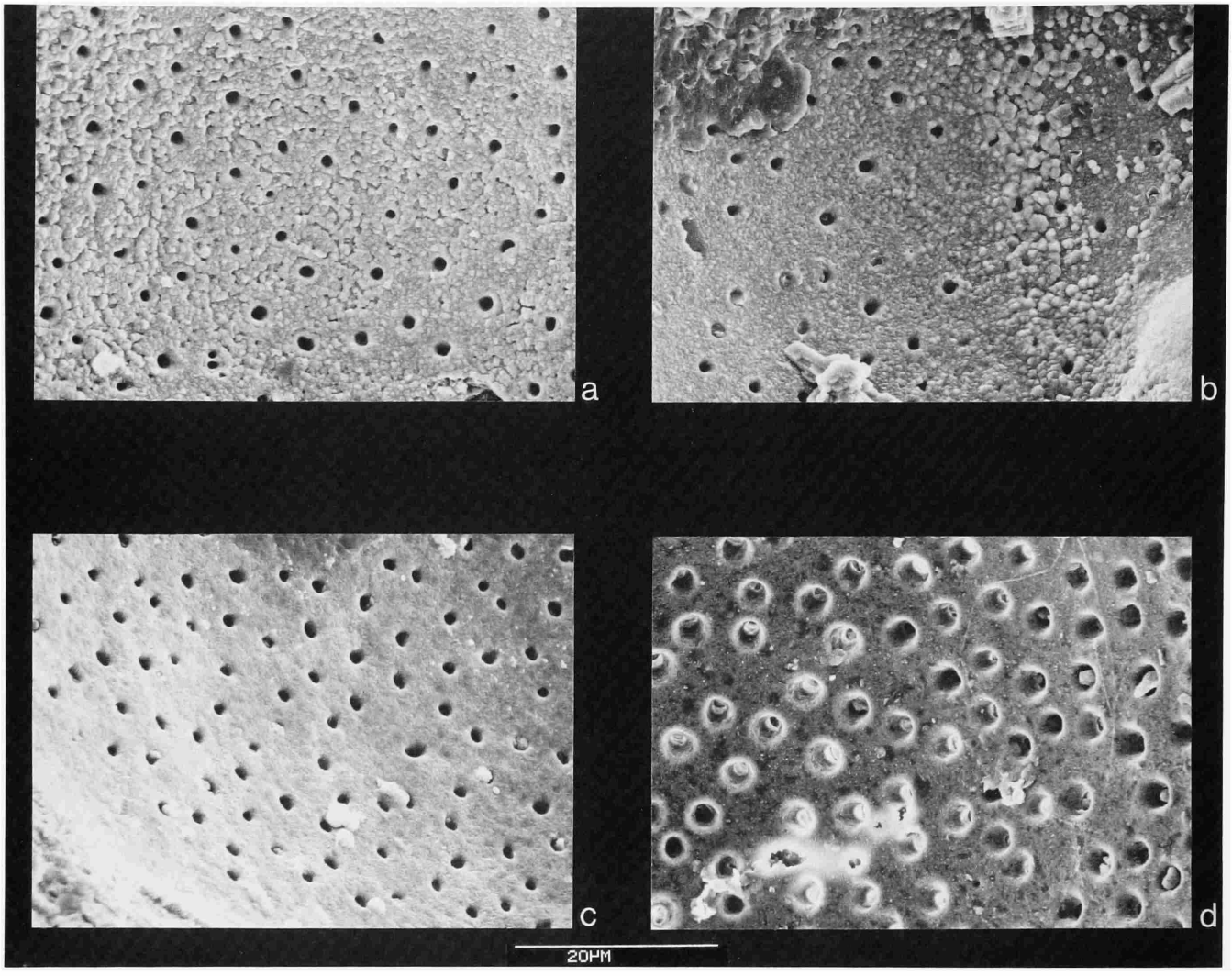

FIGURE 7.—Interior views of ventral chamber surfaces showing pore distributions in the twelfth chamber wall of *a, Archaeoglobigerina australis*; *b, Archaeoglobigerina mateola*; *c, Archaeoglobigerina cretacea*; and *d, Rugoglobigerina rugosa*. (Scale bar is 20 µm for all photographs.)

Criteria for Taxonomic Classification

CONVENTIONAL CLASSIFICATION SCHEMES

The standard approach to taxonomic classification of Cretaceous planktonic foraminifera has been based primarily on observations of external features of the foraminiferal shell. Opinions have varied, however, on the hierarchical order of morphological characters that should be used to identify different taxonomic levels (Table 1). Unlike their Cenozoic descendants, Cretaceous planktonic foraminifera with trochospirally coiled tests cannot be subdivided into spinose versus non-spinose groups; the earliest known species with true spines probably did not evolve until the early Danian (Olsson et al., 1992). The presence or absence of surface costellae has been proposed as a primary criterion for taxonomic subdivision (Brönnimann and Brown, 1956), but subsequent studies (e.g., Belford, 1983; Petters et al., 1983) have shown that this structural feature appears several times during the Late Cretaceous among distantly related clades, such as *Costellagerina, Rugoglobigerina*, and *Rugotruncana* (see Tables 2, 3).

Bolli et al. (1957) considered the position of the primary aperture as the most important morphocharacter for family level classification, whereas Banner and Blow (1959) attached greater significance to the external structural modifications of the aperture (i.e., presence or absence of lips, portici, or tegilla). Since the publication of Loeblich and Tappan's volume of the Treatise (1964), most authors agree that the presence of an extraumbilical primary aperture and sutural supplementary apertures, and absence of a tegillum are the most important

bases for distinguishing the Rotaliporidae from the Globotruncanidae. More recently, Loeblich and Tappan (1988) have raised these two families to superfamily rank, using the position of the primary aperture and presence or absence of tegilla as the key discriminating features (Table 1).

There is no single morphologic criterion by which all genera of the Rotaliporacea and Globotruncanacea can be distinguished. Although the Globotruncanacea has been defined as having an umbilical primary aperture (Loeblich and Tappan, 1988:467), five genera included in this superfamily (*Globotruncanita, Marginotruncana, Sigalitruncana, Globotruncanella*, and *Abathomphalus*) are characterized by having apertures that extend outside the umbilical region (Table 3).

The Globotruncanacea are also stated to have "tegilla of successive chambers covering the umbilical area" (Loeblich and Tappan, 1988:467). However, the genera *Contusotruncana* (= *Rosita* defined in Robaszynski et al., 1984), *Globotruncanita, Kassabiana, Radotruncana*, and *Sigalitruncana* are distinguished from other globotruncanids by having either free or coalescing portici rather than true tegilla. Unfortunately, consistent recognition of the type of umbilical structure present is not as simple as many taxonomic studies imply. Several factors account for this: (1) portici and tegilla are delicate chamber extensions that may suffer taphonomic damage; (2) post-depositional infilling of the umbilicus may obscure identification of umbilical structures; (3) the distinction between coalescing portici and true tegilla is vague; and (4) the expression of lips, portici, or tegilla may change with ontogenetic development. Because of the variability in the preservation or expression of umbilical structures, Weidich (1987) has suggested lessening their relative importance in classification schemes for Cretaceous planktonic foraminifera and abandoning the genera *Contusotruncana* (= *Rosita*), *Gansserina*, and *Globotruncanita*. Although this view may be considered extreme by some taxonomists, it does correctly point out problems with studies that overemphasize the taxonomic significance of umbilical cover plates.

Koutsoukos et al. (1989) determined that ontogenetic polymorphism and ecophenotypic variability has caused much taxonomic confusion within the mid Cretaceous taxon *Favusella*. These authors found that a morphologic continuum exists between shallow neritic specimens that are small, variable in chamber shape, and bearing surface textures with discontinuous costae or pustules and deeper neritic specimens that are larger, less variable in chamber shape, and with a more coarsely ornamented reticulate surface texture. Determination that the different morphotypes belong to a single broadly defined species was based primarily on comparison of test size, chamber arrangements in spiral view, and relative abundance within various paleobathymetric settings. However, a biometric study of ontogeny within this group was not included in this investigation.

Morphologic features that are currently used to characterize planktonic foraminifera appear relatively late in the ontogeny, usually after the beginning of the penultimate whorl. In fact, Brummer et al. (1986, 1987) found that small (<150 μm), pre-adult forms that dominate highly variable and cold surface water environments in the modern ocean bear little resemblance to their adult counterparts. These authors further noted that application of the existing taxonomy to pre-adult ontogenetic stages would result in assignment of the same species to different genera. This also holds true for Cretaceous populations. Thus, it is highly desirable to establish an approach to classification that incorporates morphologic changes that occur throughout foraminiferal ontogeny.

Ontogenetic Morphology

Pessagno (1967:250) stated that "Any study made of Upper Cretaceous planktonic Foraminifera based on external characteristics alone is hazardous [because] homeomorphy or near homeomorphy is common among many species." As the SEM was unavailable during preparation of Pessagno's monograph, and because stereomicroscopes have inadequate optical resolution for detailed morphologic study, Pessagno relied on thin sectioning techniques to characterize differences in species' growth morphologies. This approach has not been widely adopted in taxonomic studies, however, due to the tedium of thin-sectioning foraminifera and limitations of distinguishing growth morphologies based on two-dimensional, rather than three-dimensional views.

Few subsequent studies have realized the potential wealth of information revealed by biometric study of planktonic foraminiferal ontogenies. Olsson (1971, 1972, 1974) was one of the first to quantify changes in the pattern of chamber growth in the developmental history of planktonic foraminifera. Within the ontogeny of several subspecies of *Globorotalia fohsi*, Olsson (1972) identified two phases of geometric growth that are separated by a sudden change in growth allometry based on measurements of chamber widths plotted against shell radius. Single growth phases were observed by Olsson (1971, 1974) in *Globorotalia mayeri* and *Neogloboquadrina pachyderma* and as many as four growth phases were observed in forms identified by Olsson (1974) as *Globorotalia pseudopachyderma*. Population statistics were not available in any of these studies, however, as too few specimens were measured.

Huang (1981) was the first to systematically employ a method of serial dissection and SEM examination to reveal morphologic differences among planktonic foraminifera. Huang's method involved the use of a hand-held dissecting needle to crush and remove ventral chamber surfaces and photograph a succession of the newly exposed pre-adult chambers throughout the ontogeny of an individual specimen. This elegant study demonstrated significant differences in the coiling patterns, chamber morphology and ornamentation, proloculus dimensions, and chamber number at successive growth stages within the tests of some modern and late Neogene planktonic foraminifera. Observations from this study

led Huang (1981) to propose new criteria for supraspecific classification of late Neogene planktonic foraminifera.

Following Huang's (1981) approach, Brummer et al. (1986, 1987) combined information from test dissections of adult specimens with study of pre-adult forms that were recovered from plankton tows. Based on their observations, these authors identified five developmental phases in the ontogeny of modern planktonic foraminifera. These were defined as the prolocular, juvenile, neanic, adult, and terminal stages. Recognition of these stages was based on sudden shifts in the chamber-by-chamber pattern of (1) test size increase, (2) apertural position, (3) chamber shape, (4) chamber arrangement, (5) surface ornament (e.g., presence/absence of pore pits, pore distribution, or spine bases), and (6) vital behavior. Pre-adult forms of the same species in plankton tow samples were recognized by back-tracking the morphologic changes that occur within the shells of dissected adult specimens. Abrupt changes in ontogenetic morphology were attributed to changes in trophic behavior (Brummer et al., 1987) and changing physiology of the increasing volume of cell cytoplasm (Brummer, 1988). Brummer et al. (1987) noted that transition from one ontogenetic stage to another depends more on test size than chamber number; shells with large proloculi and initial whorl chambers may reach the adult stage with fewer chambers than a conspecific form with smaller proloculi and initial whorl chambers.

Recognition of ontogenetic growth stages among specimens analyzed in this study is based largely on the criteria outlined by Brummer et al. (1986, 1987), with some modifications that are discussed in a later section. Below is a summary of the most important morphological and biological characteristics that distinguish ontogenetic growth stages in planktonic foraminifera.

PROLOCULAR STAGE.—The prolocular stage consists of the first chamber formed in the ontogenetic series. The morphology of the proloculi of all species is spherical, except for occasional specimens that show flattening of the wall shared with the deuteroconch. This flattening does not appear to have any taxonomic value, as it occurs in at least one specimen of all species studied. As has been observed previously for modern species (Huang, 1981; Sverdlove and Bé, 1985; Brummer et al., 1986, 1987; Brummer, 1988), proloculi are invariably larger than the deuteroconch, and wall pores do not appear until the second or subsequent chambers (Figure 8*a*).

The size of the proloculus plays an important role in the ontogeny of planktonic foraminifera because it strongly influences the size development and chamber arrangement of the total shell. Generally, the larger the proloculus, the smaller number of chambers needed to reach a certain test size in the initial whorl (Sverdlove and Bé, 1985). This holds true for most of the Cretaceous species examined in this study. For example, the species with the smallest mean proloculus diameter, *C. pilula*, has the greatest number of chambers in a relatively small initial whorl (Table 5). On the other hand, *A. cretacea*, which has the largest mean proloculus diameter, has fewer initial whorl chambers but a considerably larger initial whorl size. Pores are absent from the proloculi of all species examined in this study, as has been observed in modern and Neogene globigerine taxa (Huang, 1981; Brummer et al., 1986, 1987; Brummer, 1988).

According to some authors, differences in the shape and size of prolocular chambers may be used as criteria for distinguishing supraspecific groups of planktonic foraminifera. Huang (1981) suggested that *Globigerina* and *Globigerinella* are unique among late Neogene genera by possessing spherical rather than oval-shaped proloculi. However, Brummer et al. (1987) observed that all globigerinid species have some degree of flattening of the wall between the proloculus and deuteroconch. They concluded that proloculus shape is variable both intra- and interspecifically and, thus, does not have any taxonomic value.

In a comparative study of 24 species of planktonic foraminifera collected from plankton tows, Sverdlove and Bé (1985) detected significant size differences between spinose and and non-spinose taxa. They found that with the exception of *Globigerina bulloides*, all spinose species have a mean proloculus diameter of 15.7 μm, whereas the average proloculi of non-spinose species is greater. A subsequent analysis by Hemleben et al. (1988), on the other hand, revealed much greater overlap in proloculus sizes between modern spinose and non-spinose groups due to wide intraspecific variability. For example, Sverdlove and Bé (1985) estimated the mean proloculus diameter of left coiling *Neogloboquadrina pachyderma* at 20.2 μm with a standard deviation of about 4 μm, whereas Hemleben et al. (1988) obtained a mean value of 29 μm and a standard deviation of 10 μm for left coiling forms of the same species. These contrasting results could suggest that the surface water environment may strongly influence proloculus and initial whorl dimensions. On the other hand, this variability could be a function of the size distribution among the measured populations; wide variation of sizes will likely yield prolocular measurements that show a high degree of variability.

JUVENILE STAGE.—The deuteroconch denotes the onset of the juvenile stage. According to Brummer et al. (1987), this stage includes a variable, but species-specific, number of chambers coiled in about 1.5 whorls around the proloculus. These chambers show uniform morphologies and a steady rate of size increase.

Initial whorl morphologies of all species analyzed in the present study are very similar (Figure 8*c,d*); apertures are extraumbilical in position, the umbilical region is relatively broad, the test surface is smooth to finely hispid, and pores are initally rare and initially restricted to the spiral suture. As few as seven or as many as eleven chambers may occur in the juvenile stage, depending on the species.

NEANIC STAGE.—Transition from the juvenile to neanic

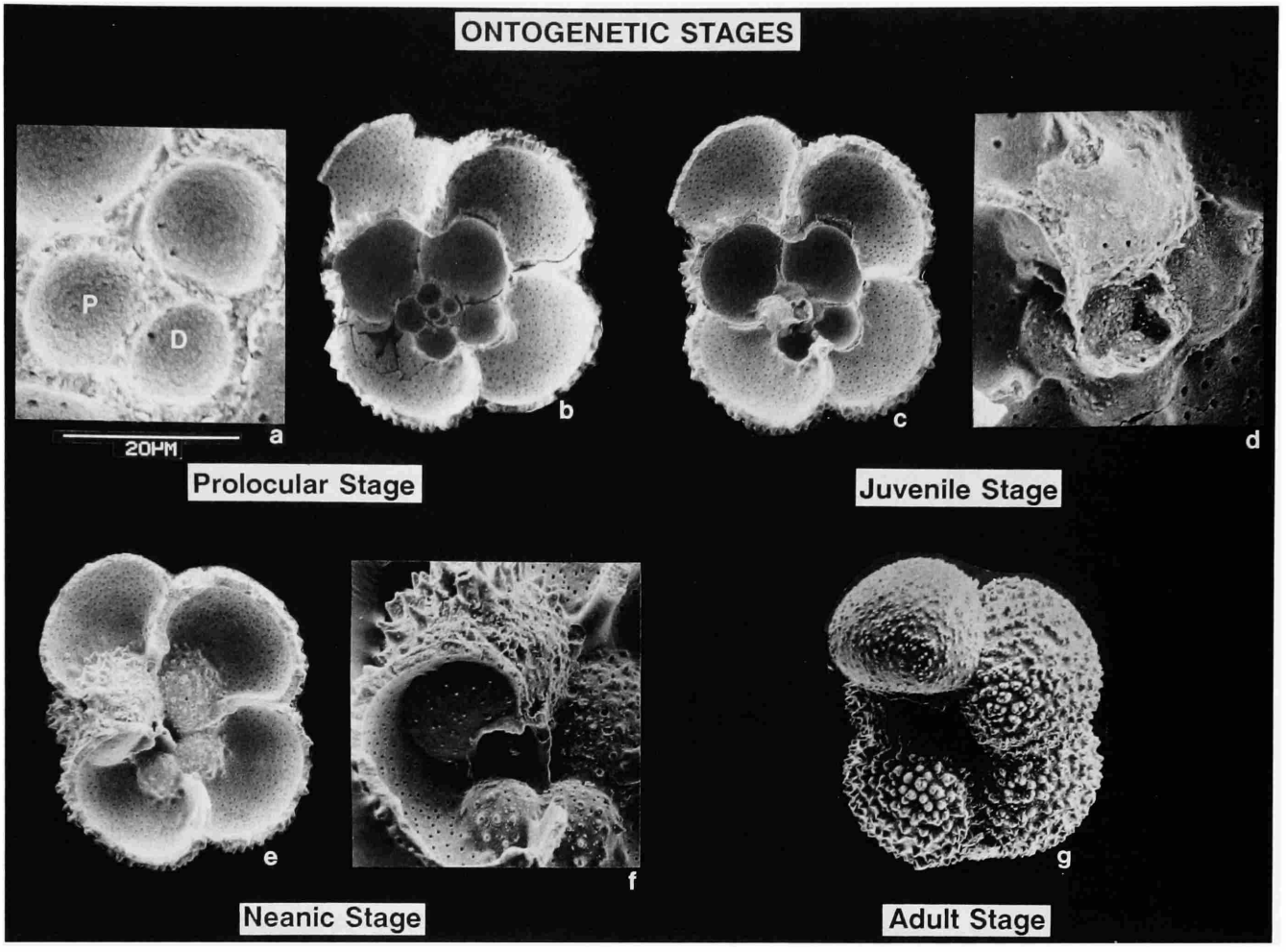

FIGURE 8.—Magnified view of the first chambers of the initial whorl in *Archaeoglobigerina bosquensis* (*a*) and complete serial dissection of the same specimen of *A. bosquensis* (*b–g*) revealing morphologic changes associated with transitions from the prolocular, juvenile, neanic, to adult stages. Prolocular stage: note the absence of pores on the wall of the proloculus (P) but presence of pores on the deuteroconch (D) and subsequent chambers (*a*). Also note that the deuteroconch is always smaller than the proloculus (*a,b*). Juvenile stage: this includes from chamber 2 up to about chamber 7; note nearly equatorial position of the aperture, presence of narrow lip bordering the aperture, axial compression and smooth surface texture of the chambers, slow rate of chamber size increase, and wide, shallow umbilicus (*c,d*). Neanic stage: this includes from about chamber 8 through chamber 10; note the umbilical-extraumbilical position of the aperture, widening of the lip bordering the aperture into a narrow flap, appearance of fine, randomly distributed pustules on the chamber surfaces, increase rate of chamber size increase, and narrowing of the umbilicus (*e,f*). Adult stage: this includes the the final three chambers; note the umbilical position of the aperture, increased number and coarsening of surface pustules, further narrowing of the umbilicus, and diminished rate of chamber size increase (*g*). Presence of a kummerform final chamber may indicate that the terminal stage was reached in this specimen, although this cannot be verified in extinct taxa.

stage in modern spinose species typically occurs in test diameters between 65 μm and 95 μm (Brummer et al., 1987). Other developmental changes in this stage that these authors have observed include: (1) an inflection in the logarithmic growth curve followed by increased growth rates in several following chambers; (2) the step-wise appearance of about 0.5 to 1.0 whorl of more globular, loosely coiled chambers; (3) occurrence of an increasingly lobate equatorial outline; (4) migration of the aperture from an extraumbilical to an umbilical-extraumbilical position in some species; (5) change in the number of chambers per whorl to approximately the same as in the final whorl of adult specimens; and (6) an increase in the density of surface texture approaching that of adult specimens.

Most species in the present study do exhibit some or all of the above features by the eighth to ninth chamber (Figure 8*e,f*), along with an abrupt increase in shell porosity. However, a neanic stage is not recognized in some species that have uniformly changing morphologies throughout ontogeny. Test size at the onset of the neanic stage generally ranges from 70 to 120 μm among specimens of *Costellagerina, Archaeoglobigerina,* and *Rugoglobigerina.* Pores in most neanic chambers are evenly scattered around the shell wall, from the spiral suture outward toward the axial periphery.

Brummer et al. (1987) suggested that morphologic changes occurring in the neanic stage are at least partly related to an increase in trophic activity. This in turn results from a larger cytoplasmic volume and shell size, enabling a greater capability of prey capture.

ADULT STAGE.—The onset of the adult stage occurs at a test diameter between 160 μm and 200 μm in modern globigerine species (Brummer et al., 1987). It is also characterized by the final positioning of the primary aperture and the maturation of the wall texture, surface ornamental features, and chamber shape. From one to several chambers are added in the adult stage before initiation of the terminal stage.

Most species analysed in this study attain maximum porosity and show a diminishing rate of chamber size increase by the adult stage (Figure 8*g*). Adult specimens of *H. sliteri, Costellagerina, Archaeoglobigerina,* and *Rugoglobigerina* have diameters that are generally larger than 200 μm, whereas the adult stage in *H. holmdelensis* and *H. monmouthensis* is reached in tests of about 150 μm.

TERMINAL STAGE.—According to Brummer et al. (1987), the terminal stage occurs at the onset of reproduction, and is characterized by addition of a kummerform, sac-like, or normalform chamber. There is no way to prove that the presence of kummerform or bullate chambers in Cretaceous species necessarily indicates that reproduction has occurred. Because of this, no attempt is made in the present study to identify the terminal stage.

Systematic Descriptions and Biometric Data

Qualitative observations and biometric data were obtained from test exterior views, microradiographs, and SEM micrographs of serially dissected tests of *H. holmdelensis, H. monmouthensis, H. sliteri, C. pilula, A. australis, A. bosquensis, A. mateola, A. cretacea,* and *R. rugosa.* The following section includes a brief synonomy list for each species followed by discussion of the principle features that can be used for species identification and a summary of the biometric data. Based on these results, the phylogenetic relationships of the studied taxa are discussed.

Genus *Hedbergella* Brönnimann and Brown, 1958

TYPE SPECIES.—*Anomalina lorneiana* var. *trochoidea* Gandolfi, 1942.

DESCRIPTION.—*Hedbergella* is characterized by having a low trochospiral test that is lobate and subcircular in outline, with globular chambers that increase gradually in size throughout ontogeny, a low-arched aperture that is umbilical-extraumbilical in position and bordered by a narrow lip or porticus. The wall is finely perforate and the surface texture is smooth to hispid.

REMARKS.—Although Loeblich and Tappan (1988:462) have stated that species included in this genus do not have a poreless margin, topotype specimens of *H. holmdelensis* and *H. monmouthensis* clearly do have an imperforate equatorial periphery throughout ontogeny (see below). This does not warrant placement of these species in the genus *Globotruncanella,* however, as imperforate carinal bands are absent from *H. holmdelensis* and *H. monmouthensis* populations elsewere. Pore distribution within *Hedbergella* may therefore be environmentally controlled.

Hedbergella holmdelensis Olsson, 1964

PLATE 2: FIGURES 1–8

Hedbergella holmdelensis Olsson, 1964:160, pl. 12: figs. 1, 2.—Huber, 1990:503, pl. 2: figs. 2–4, pl. 6: fig. 1.

Not *Hedbergella holmdelensis* Olsson.—Sliter, 1977:542, pl. 3: figs. 1–3.

OBSERVATIONS OF THE TEST EXTERIOR.—The test is very low trochospiral, lobate and subovate in outline, and moderately compressed in the axial direction with a subrounded equatorial periphery. Maximum diameter of the holotype is 190 μm and maximum breadth is 91 μm, and topotypes with tests up to 218 μm and average 163 μm in test diameter, 80 μm breadth, and 0.49 in breadth/diameter ratio (Table 4). The umbilicus is quite small, averaging 19% of the test diameter and tests generally have a total of 14 to 15 chambers, with an average of 5.21 and range of 4.50 to 5.75 chambers occurring in the final whorl. Final whorl chamber size increase is moderate, as indicated by a penultimate/antepenultimate chamber size ratio of 1.25. No kummerform specimens were observed, and about 67% of the population is dextrally coiled. The aperture is a low, extraumbilical or umbilical-extraumbilical arch with a mean height/width ratio of 0.55, and is bordered by a narrow porticus extending from near the umbilicus to the equatorial periphery. The wall is smooth or finely pustulose, sometimes imperforate along the equatorial periphery, and microperforate elsewhere on the test.

OBSERVATIONS OF THE TEST INTERIOR.—*Initial Whorl:* The smallest size proloculi observed in this study occur in *H. holmdelensis,* with diameters averaging 10.49 μm and ranging from 9.44 to 11.53 μm (Figures 9–11, Table 5).

FIGURE 9 (facing page).—Scatter plots and least squares regression of proloculus and initial whorl diameter measurements for 10 Upper Cretaceous species of planktonic foraminifera. Most species show strong correlation between these two variables. Note the wide scatter of points shown by micromorph specimens of *Archaeoglobigerina australis* and the strongly bimodal point distribution portrayed by *Archaeoglobigerina mateola.* Least squares regression line equation, correlation coefficient (r), and number of measured specimens (n) are presented for each species.

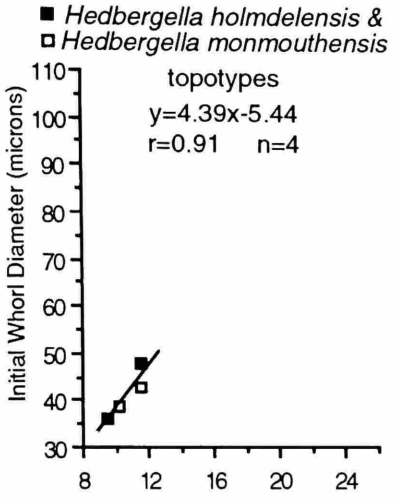
■ Hedbergella holmdelensis &
□ Hedbergella monmouthensis
topotypes
y=4.39x-5.44
r=0.91 n=4
Initial Whorl Diameter (microns)

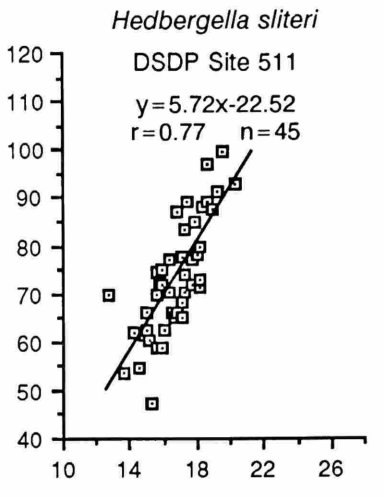
Hedbergella sliteri
DSDP Site 511
y=5.72x-22.52
r=0.77 n=45

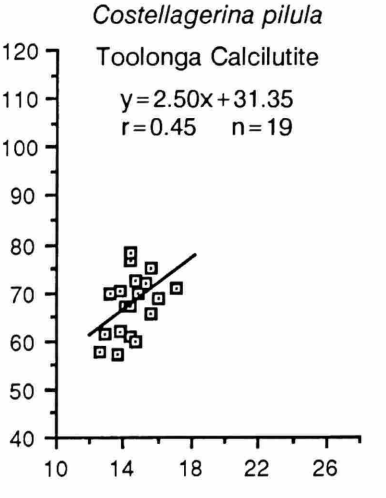
Costellagerina pilula
Toolonga Calcilutite
y=2.50x+31.35
r=0.45 n=19

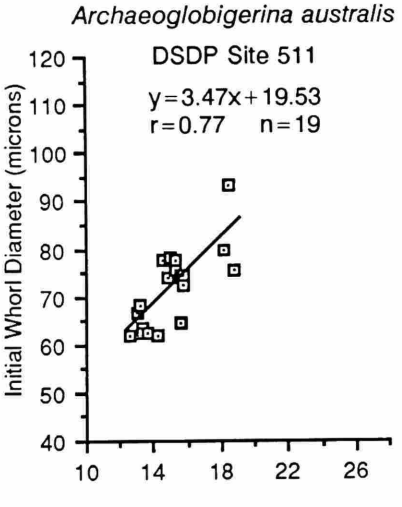
Archaeoglobigerina australis
DSDP Site 511
y=3.47x+19.53
r=0.77 n=19
Initial Whorl Diameter (microns)

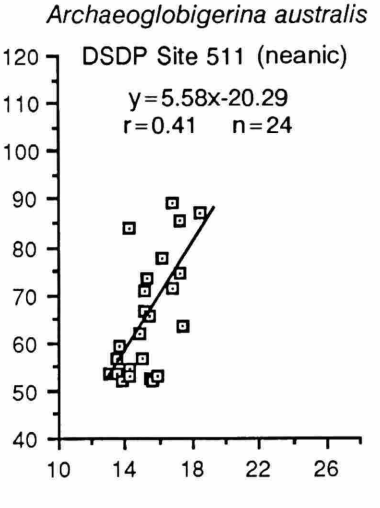
Archaeoglobigerina australis
DSDP Site 511 (neanic)
y=5.58x-20.29
r=0.41 n=24

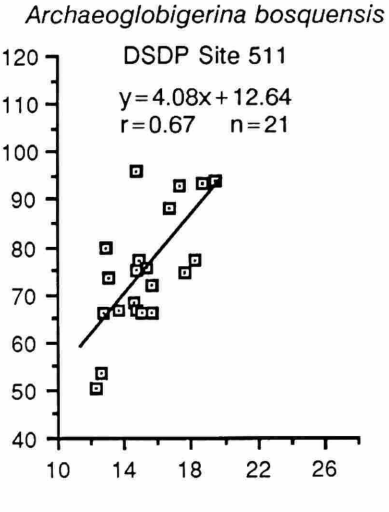
Archaeoglobigerina bosquensis
DSDP Site 511
y=4.08x+12.64
r=0.67 n=21

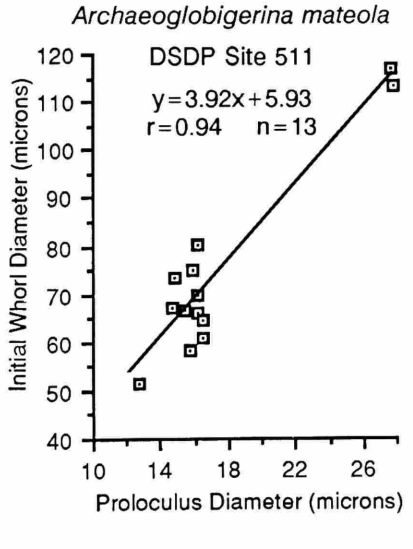
Archaeoglobigerina mateola
DSDP Site 511
y=3.92x+5.93
r=0.94 n=13
Initial Whorl Diameter (microns)
Proloculus Diameter (microns)

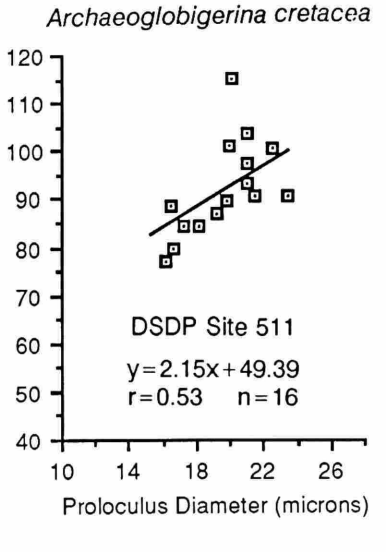
Archaeoglobigerina cretacea
DSDP Site 511
y=2.15x+49.39
r=0.53 n=16
Proloculus Diameter (microns)

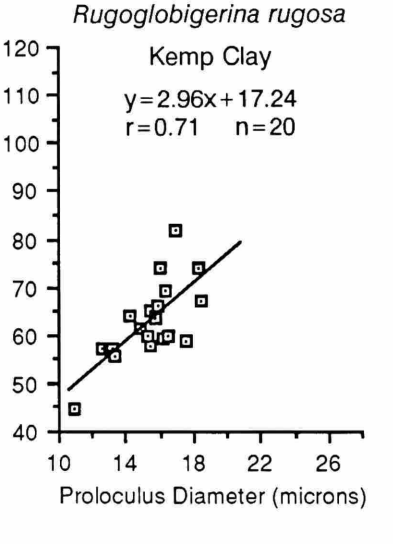
Rugoglobigerina rugosa
Kemp Clay
y=2.96x+17.24
r=0.71 n=20
Proloculus Diameter (microns)

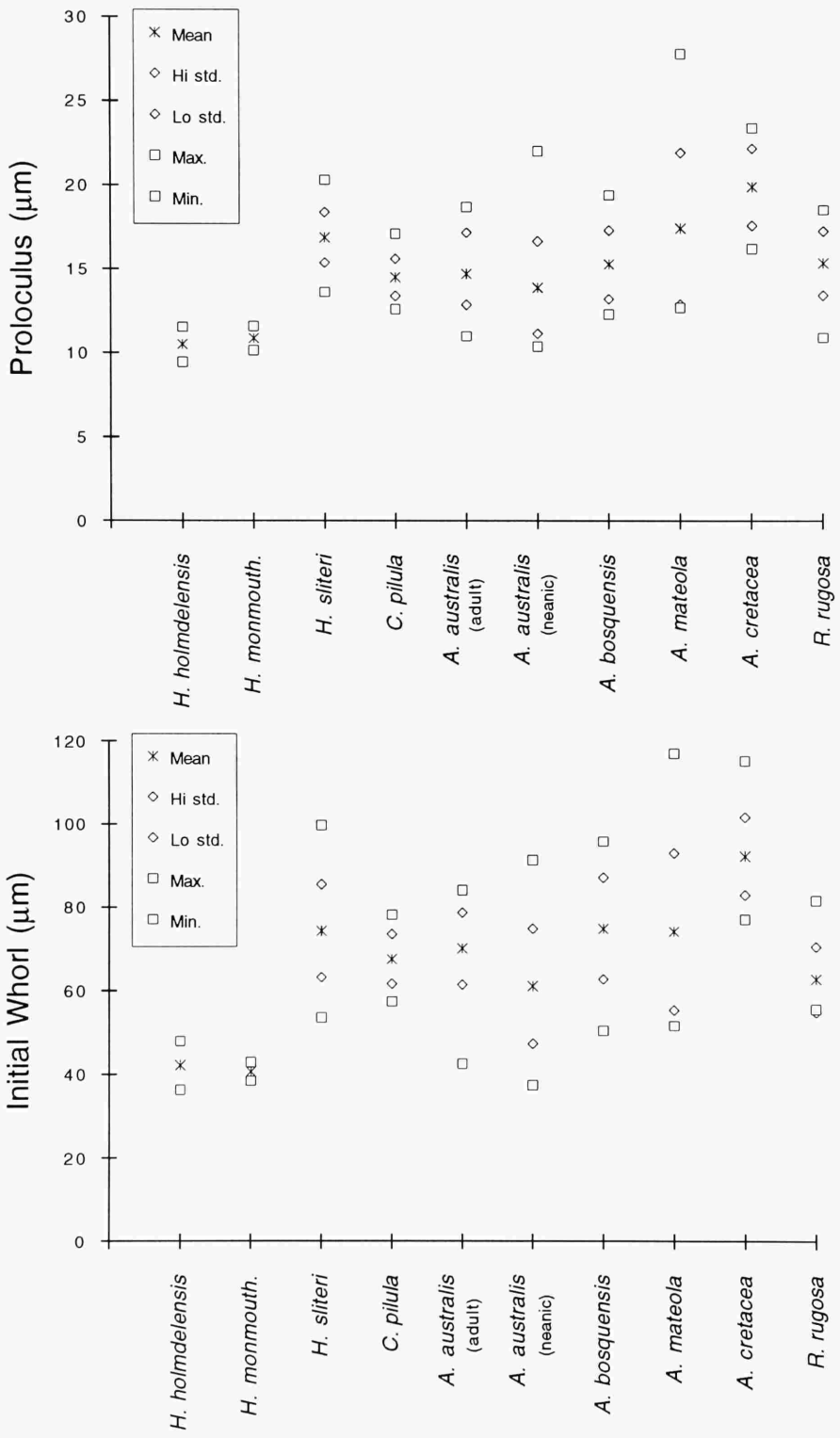

FIGURE 10.—Univariate plots of mean, one standard deviation about the mean, and total size range for proloculus and initial whorl diameters for the planktonic foraminifera analyzed in this study. See Figure 9 for the number of specimens measured for each species.

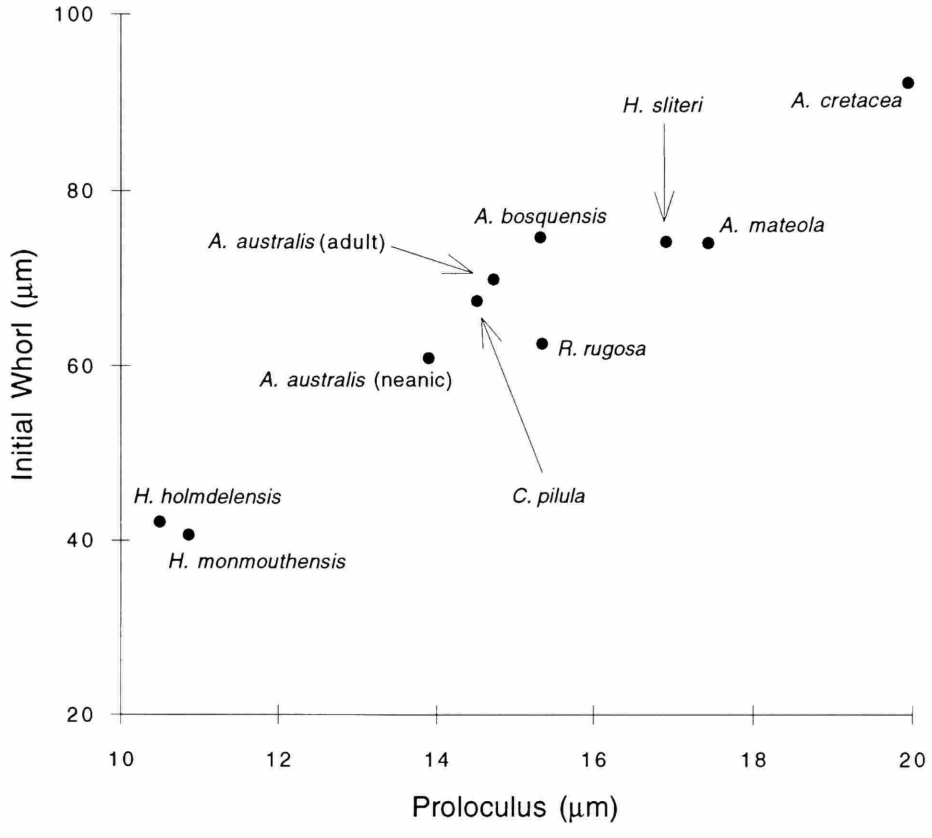

FIGURE 11.—Bivariate plot of mean proloculus and initial whorl diameters for Upper Cretaceous planktonic foraminifera analyzed in this study. *Archaeoglobigerina cretacea* (d'Orbigny) shows much larger mean values than any of the other species, whereas *H. holmdelensis* and *H. monmouthensis* are nearly the same with the smallest values. See Figure 9 for the number of specimens measured of each species. The standard deviations for proloculus and initial whorl diameters are shown in Figure 10.

The initial whorl is also comparatively small, averaging 42.15 µm, and includes an average of 6.00 chambers. Apertural position is nearly equatorial in the initial whorl, and remains extraumbilical throughout ontogeny. Chamber surfaces generally lack pustulose ornamentation in the initial whorl.

Penultimate Whorl: The highest number of chambers in the penultimate whorl occurs in this species, with an average of 6.25 chambers and a range of 6.00 to 6.50 chambers (Table 4). Fewer chambers are accomodated as coiling becomes tighter in the final whorl. Apertural position is nearly equatorial in the penultimate whorl (Plate 2: Figure 6), and surface textures are smooth to very finely pustulose.

Ontogenetic Growth Curves: The chamber expansion rate curve for *H. holmdelensis* is plotted in Figure 12 together with plots for *H. monmouthensis* and *H. sliteri*. The slope of the curve for the latter species varies much less than in *H. holmdelensis* and *H. monmouthensis* because the mean values determined for *H. sliteri* are based on measurement of many more specimens. The curves for *H. holmdelensis* and *H. monmouthensis* are nearly identical except for the larger final chamber size of *H. holmdelensis*. Chamber growth is isometric throughout the ontogeny of *H. holmdelensis*, whereas *H. sliteri* deviates from isometric growth within the adult growth stage.

Porosity: Pores are absent from all but the last chamber of the initial whorl in *H. holmdelensis* and, among the topotype populations, no pores occur in a broad band around the peripheral margin throughout ontogeny (Plate 2: Figures 2, 4, 7, 8). However, perforate equatorial margins have been observed among specimens of this species elsewhere (e.g., Huber, 1990, pl. 2: fig. 3). The pores are cylindrical with a slight funnel-shaped broadening on the interior chamber wall. Pore diameters are small, reaching a maximum of about 0.8 µm, and pore densities do not exceed 12 pores/625 μm^2 (Figure 13). Pore diameter and pore density show no significant correlation, and maximum porosity values are less than 0.6% (Table 6).

GENERAL REMARKS.—The most important features that distinguish *H. holmdelensis* from *H. monmouthensis* include compression of the peripheral margin of the final whorl chambers, resulting in an asymmetric profile of the final chamber face, and greater chamber elongation in the direction of coiling. Otherwise, these species are very similar in their

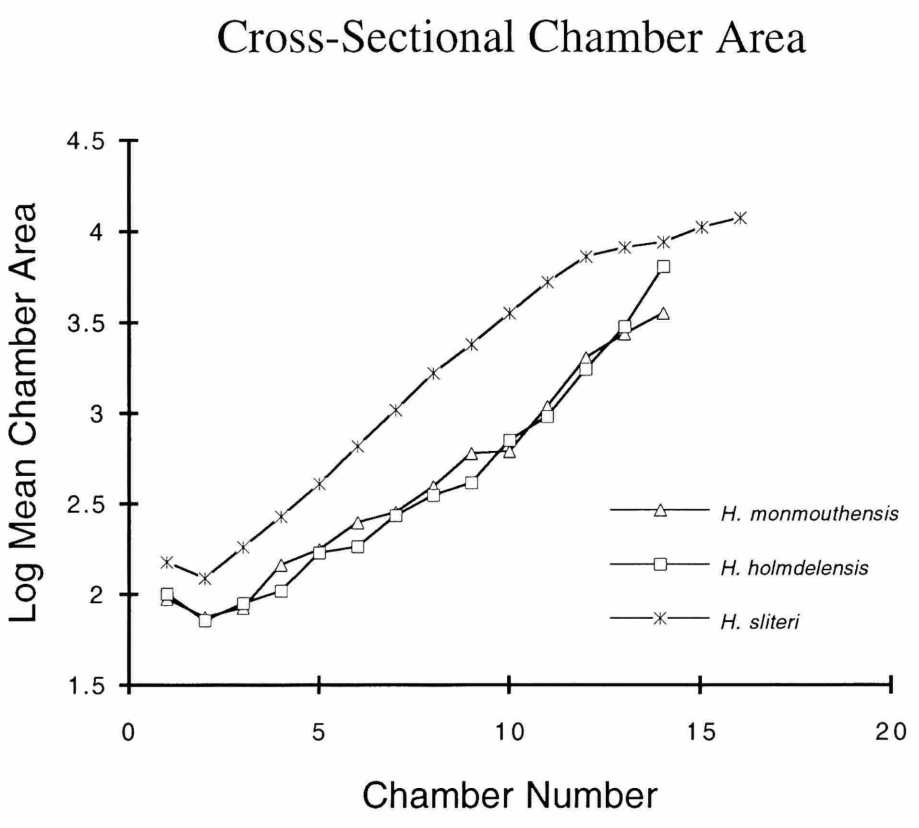

FIGURE 12.—Comparison of logarithmic plots of the mean increase in cross-sectional chamber area (in μm^2) for *Hedbergella holmdelensis*, *H. monmouthensis*, and *H. sliteri*. Note that the curves for *H. holmdelensis* and *H. monmouthensis* are very similar, differing primarily in the larger final chamber in *H. holmdelensis*. The plot for *H. sliteri* shows that its chamber sizes are considerably larger than the other two hedbergellids throughout the ontogenetic series, but the rate of chamber size increase is nearly the same until the final whorl, where the growth rate diminishes. Curves for *H. holmdelensis* and *H. monmouthensis* are based on measurement of two specimens each, whereas the *H. sliteri* plot is based on measurement of 21 specimens.

initial whorl characteristics, growth rates, shell porosity, and chamber surface textures. The growth rates of *H. holmdelensis* and *H. sliteri* are similar throughout most of the ontogenetic series, but the smaller proloculus and initial whorl sizes in *H. holmdelensis* result in a difference in mean adult test diameter of more than 100 μm (Table 4). *Hedbergella holmdelensis* is most commonly found in middle to high latitudes of both hemispheres, and is reported to range from the late Campanian (Olsson, 1964) through the earliest Danian (Olsson et al., 1992).

Hedbergella monmouthensis (Olsson, 1960)

PLATE 2: FIGURES 9–16

Globorotalia monmouthensis Olsson, 1960:47, pl. 9: figs. 22–24.

Hedbergella monmouthensis (Olsson).—Huber, 1990:503–504, pl. 2: figs. 6–8, pl. 6: fig. 2.

Not *Hedbergella monmouthensis* (Olsson).—Webb, 1973:552, pl. 3: figs. 1, 2.—Sliter, 1977:542, pl. 3: figs. 1–3.—Krasheninnikov and Basov, 1983:805–806, pl. 6: figs. 5–8.—Huber, 1988a:206, figs. 24.14–24.17.

OBSERVATIONS OF THE TEST EXTERIOR.—The test is very low trochospiral, lobate and subcircular in outline, with a rounded axial periphery. Test diameter averages 165 μm with a maximum of 230 μm, mean test breadth is 81 μm, and the mean breadth/diameter is 0.49 (Table 4). The umbilicus is narrow, comprising 21% of the mean test diameter. Adult specimens generally have a total of 14 to 15 chambers, and have an average of 5.48 and range of 4.75 to 6.25 chambers in the final whorl. Chamber size increase in the final whorl is moderate, with a mean penultimate/antepenultimate chamber ratio of 1.19. Kummerform frequency is 23%, and 39% were found to be dextrally coiled. The aperture is a low, extraumbilical or umbilical-extraumbilical arch with a height/width ratio of 0.48. It extends from near the umbilicus to the equatorial periphery and is bordered by a narrow porticus. The exterior wall surface is smooth to finely hispid, sometimes imperforate along the equatorial margin (e.g., Plate 2: Figures 10, 12), and microperforate on the spiral and umbilical sides of the chambers.

H. holmdelensis

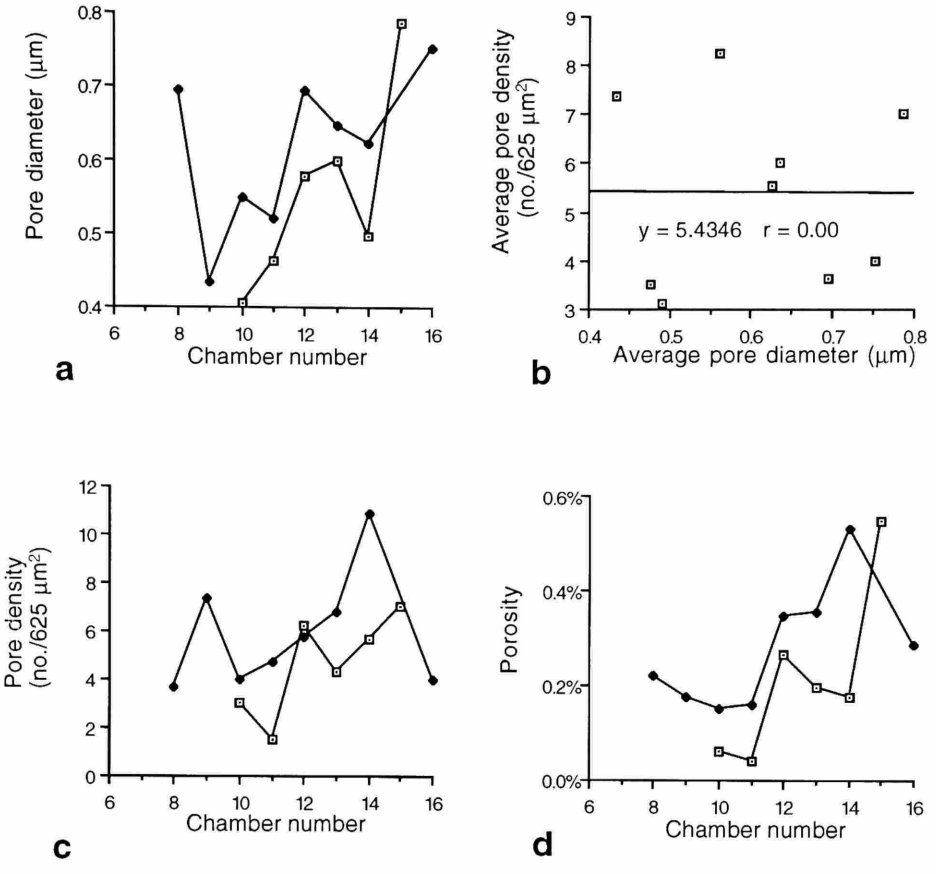

FIGURE 13.—Ontogenetic changes in *a*, pore diameter; *c*, pore density; and *d*, porosity, measured from two specimens of *Hedbergella holmdelensis*. *b*, is a linear regression curve calculated from the mean values of pore diameter and pore density of all measured chambers of *H. holmdelensis*. A least squares regression line is also shown.

TABLE 6.—Pore diameter, pore density, and porosity data, including averages, standard deviations, and maximum and minimum values, determined for each chamber within two serially dissected specimens of *Hedbergella holmdelensis*.

Ch.	DIAMETER				DENSITY				POROSITY			
No.	AVG	STD	MAX	MIN	AVG	STD	MAX	MIN	AVG	STD	MAX	MIN
1	0.00	0.00	0.00	0.00	0.00	0.00	0.00	0.00	0.00%	0.00%	0.00%	0.00%
2	0.00	0.00	0.00	0.00	0.00	0.00	0.00	0.00	0.00%	0.00%	0.00%	0.00%
3	0.00	0.00	0.00	0.00	0.00	0.00	0.00	0.00	0.00%	0.00%	0.00%	0.00%
4	0.00	0.00	0.00	0.00	0.00	0.00	0.00	0.00	0.00%	0.00%	0.00%	0.00%
5	0.00	0.00	0.00	0.00	0.00	0.00	0.00	0.00	0.00%	0.00%	0.00%	0.00%
6	0.00	0.00	0.00	0.00	0.00	0.00	0.00	0.00	0.00%	0.00%	0.00%	0.00%
7	0.00	0.00	0.00	0.00	0.00	0.00	0.00	0.00	0.00%	0.00%	0.00%	0.00%
8	0.69	0.00	0.69	0.00	3.65	0.00	3.65	0.00	0.22%	0.00%	0.22%	0.00%
9	0.43	0.00	0.43	0.00	7.39	0.00	7.39	0.00	0.17%	0.00%	0.17%	0.00%
10	0.48	6.43	0.55	0.40	3.50	0.65	3.96	3.04	0.11%	0.06%	0.15%	0.06%
11	0.49	6.04	0.52	0.46	3.13	2.27	4.73	1.52	0.10%	0.08%	0.16%	0.04%
12	0.64	8.08	0.69	0.58	6.01	0.37	6.27	5.75	0.31%	0.06%	0.35%	0.26%
13	0.62	7.49	0.64	0.60	5.55	1.75	6.78	4.31	0.28%	0.11%	0.36%	0.20%
14	0.56	7.29	0.62	0.50	8.26	3.69	10.87	5.65	0.35%	0.25%	0.53%	0.18%
15	0.79		0.79	0.79	7.03		7.03	7.03	0.55%		0.55%	0.55%
16	0.75		0.75	0.75	4.00		4.00	4.00	0.28%		0.28%	0.28%

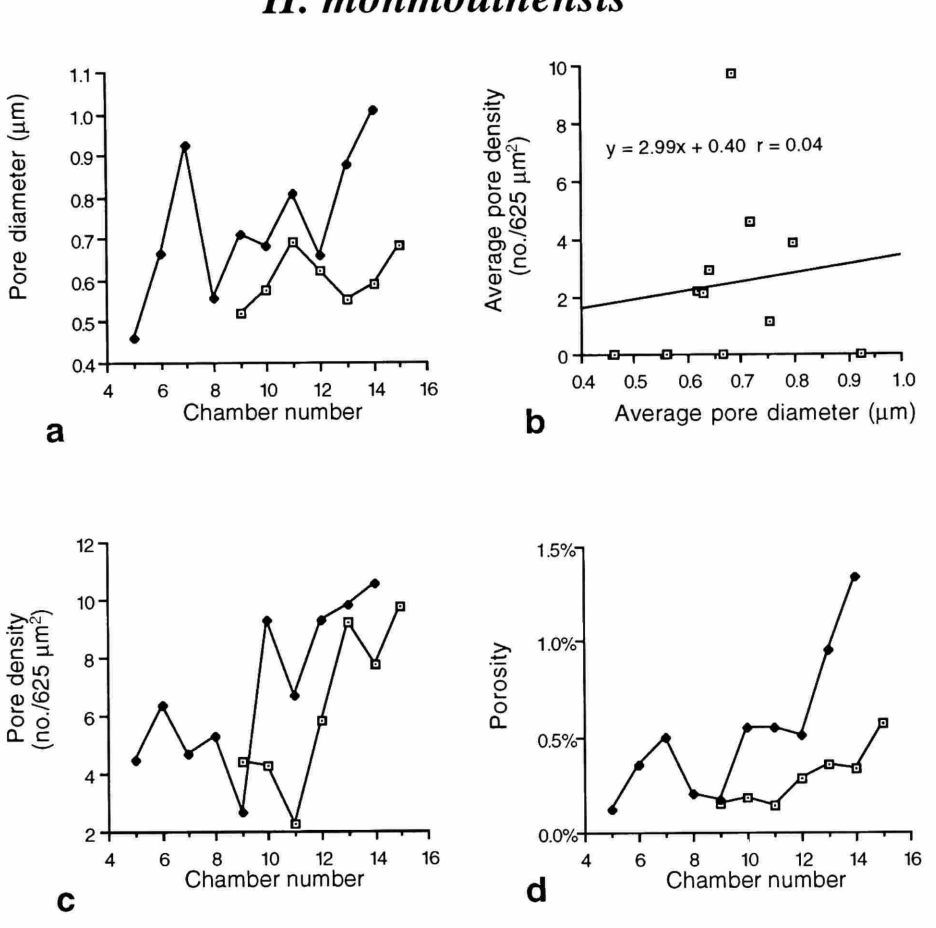

FIGURE 14.—Ontogenetic changes in *a*, pore diameter; *c*, pore density; and *d*, porosity, measured from two specimens of *Hedbergella monmouthensis*. *b*, is a linear regression curve calculated from the mean values of pore diameter and pore density of all measured chambers of *H. monmouthensis*. A least squares regression line is also shown.

TABLE 7.—Pore diameter, pore density, and porosity data, including averages, standard deviations, and maximum and minimum values, determined for each chamber within two serially dissected specimens of *Hedbergella monmouthensis*.

Ch. No.	DIAMETER AVG	STD	MAX	MIN	DENSITY AVG	STD	MAX	MIN	POROSITY AVG	STD	MAX	MIN
1	0.00	0.00	0.00	0.00	0.00	0.00	0.00	0.00	0.00%	0.00%	0.00%	0.00%
2	0.00	0.00	0.00	0.00	0.00	0.00	0.00	0.00	0.00%	0.00%	0.00%	0.00%
3	0.00	0.00	0.00	0.00	0.00	0.00	0.00	0.00	0.00%	0.00%	0.00%	0.00%
4	0.00	0.00	0.00	0.00	0.00	0.00	0.00	0.00	0.00%	0.00%	0.00%	0.00%
5	0.46	0.00	0.46	0.00	4.46	0.00	4.46	0.00	0.12%	0.00%	0.12%	0.00%
6	0.66	0.00	0.66	0.00	6.31	0.00	6.31	0.00	0.35%	0.00%	0.35%	0.00%
7	0.92	0.00	0.92	0.00	4.64	0.00	4.64	0.00	0.50%	0.00%	0.50%	0.00%
8	0.56	0.00	0.56	0.00	5.29	0.00	5.29	0.00	0.21%	0.00%	0.21%	0.00%
9	0.62	0.14	0.71	0.52	3.55	1.24	4.43	2.67	0.16%	0.01%	0.17%	0.15%
10	0.63	0.07	0.68	0.58	6.78	3.55	9.29	4.27	0.36%	0.26%	0.54%	0.18%
11	0.75	0.08	0.81	0.69	4.47	3.07	6.64	2.30	0.34%	0.29%	0.55%	0.14%
12	0.64	0.03	0.66	0.62	7.55	2.45	11.40	5.82	0.39%	0.16%	0.51%	0.28%
13	0.72	0.23	0.88	0.55	9.51	0.41	9.80	9.22	0.65%	0.42%	0.95%	0.36%
14	0.80	0.29	1.01	0.59	9.13	1.97	10.52	7.74	0.84%	0.71%	1.34%	0.34%
15	0.68		0.68	0.68	9.76		9.76	9.76	0.57%		0.57%	0.57%

OBSERVATIONS OF THE TEST INTERIOR.—*Initial Whorl:* Proloculus diameters average 10.86 μm and range from 10.14 to 11.57 μm (Table 5). The initial whorl has a mean diameter of 40.66 μm and ranges from 38.43 to 42.89 μm, and has an average of 5.13 chambers. Apertural position in the initial whorl is nearly equatorial, chamber surfaces are smooth, and chamber morphology is globose to slightly compressed.

Penultimate Whorl: An average of 5.88 chambers comprise the penultimate whorl (Table 4), chamber surfaces are smooth to finely hispid, and chamber shape is globular with slight axial compression (Plate 2: Figure 14).

Ontogenetic Growth Curves: As previously noted, the plot of mean cross-sectional chamber area for *H. monmouthensis* is nearly the same as for *H. holmdelensis* except the latter species typically has a larger final chamber (Figure 12). Although the plots for these species parallel the graph for *H. sliteri*, the chamber sizes are smaller throughout their ontogeny. As a result, adult specimens of *H. monmouthensis* are smaller than *H. sliteri* by an average diameter of more than 100 μm.

Porosity: Pore distributions in *H. monmouthensis* are similar to those observed in the *H. holmdelensis* topotype populations; pores are nearly absent from all but the last chamber of the initial whorl and the equatorial margin remains imperforate throughout ontogeny (Plate 2: Figures 10, 12, 15, 16). As with *H. holmdelensis*, not all specimens of *H. monmouthensis* retain an imperforate equatorial peripheral margin (e.g., Huber, 1990, pl. 2: fig. 7). Throughout ontogeny, the pores are cylindrical with funnel-shaped openings on the interior wall. Pore diameters typically range between 0.5 to 1.0 μm, pore densities and pore densities reach a maximum of about 10 pores/625 μm^2 in the final whorl chambers (Figure 14). Pore diameters and pore densities are poorly correlated, and porosity values generally fall between 0.50% and 1.33% (Table 7).

GENERAL REMARKS.—*Hedbergella monmouthensis* has frequently been misidentified because of its small size and often inadequate preservation (R. Olsson, pers. comm., 1986). Such is the case in the southern high latitudes; forms previously identified as *H. monmouthensis* are now included in species as different as *Archaeoglobigerina australis, H. holmdelensis*, and *H. sliteri*. Key features that distinguish *H. monmouthensis* from these other taxa include its small size, tight coiling, nearly smooth surface texture, and inflated, spherical to subspherical final whorl chambers. Although the holotype of *H. monmouthensis* has been missing for over a decade, a neotype has recently been selected and will soon be added to the USNM collections (R. Olsson, pers. comm., 1992).

Hedbergella monmouthensis was thought to have been derived from *H. holmdelensis* during the Maastrichtian (Olsson, 1964), and then survived into the earliest Danian to give rise to a new stock of Cenozoic planktonic foraminifera (Olsson et al., 1992). It is much more common in the middle to high latitudes of both hemispheres than in the low latitudes, and has been found to range back to the late Campanian in the southern South Atlantic (Huber, 1991a).

Hedbergella sliteri Huber, 1990

PLATE 1: FIGURES 1–5, PLATE 3: FIGURES 1–9

Hedbergella monmouthensis (Olsson).—Webb, 1973:552, pl. 3: figs. 1, 2.—Huber, 1988a:206, figs. 27.14–27.17.

Hedbergella holmdelensis Olsson.—Sliter, 1977:542, pl. 2: figs. 1–4.

Hedbergella sliteri Huber, 1990:504, pl. 2: figs. 5, 9, 10; pl. 6: figs. 4, 5; 1991a:292, pl. 1: figs. 4, 8; 1991b:461, pl. 1: fig. 9.

OBSERVATIONS OF THE TEST EXTERIOR.—The test is coiled in a very low trochospire and is sometimes nearly planispiral, with a maximum diameter of 340 μm, an average diameter of 274 μm, an average breadth of 123 μm, and an average breadth/diameter ratio of 0.45 (Table 4). The outline is subcircular to ovate, the equatorial periphery is strongly lobate, and the axial periphery is broadly rounded. The umbilical region is shallow and averages 28% of the maximum test diameter. Adult tests have a total of 12 to 16 chambers, while the number of chambers in the final whorl ranges from 5.00 to 6.00 with an average of 5.35. Chamber size increase in the final whorl is relatively slow, as indicated by the low size ratio of penultimate/antepenultimate chamber diameters. Nearly all specimens are normalform and about half show dextral coiling. The aperture is a low, extraumbilical, interiomarginal arch, sometimes positioned very near the equatorial periphery, bordered by a narrow porticus. Relict portici are usually present in the umbilicus. The test wall is microperforate and smooth or covered by small pustules.

OBSERVATIONS OF THE TEST INTERIOR.—*Initial Whorl:* Proloculus diameters average 16.9 μm and range from 13.6 μm to 20.3 μm. From 4.75 to 5.25 chambers comprise the initial whorl, which has an average diameter of 74.3 μm and a range of 53.6 μm to 99.7 μm. All chambers following the proloculus have an extraumbilical aperture and a globular to slightly appressed chamber morphology. The analyzed specimens show a strongly positive correlation of proloculus and initial whorl diameters (Figures 9–11).

Penultimate Whorl: The average of 5.15 chambers in the penultimate whorl is slightly less than the number of chambers in the final whorl, which average 5.35 (Table 4). Chamber shape does not change in the penultimate whorl and surface ornamentation remains smooth to very finely pustulose.

Ontogenetic Growth Curves: The chambers increase very gradually in size throughout ontogeny; logarithmic plots of the ontogenetic increase in cross-sectional chamber areas are uniformly log-linear until the final whorl chambers, although there is a greater range of chamber size variability and an average decrease in growth rates of the final whorl chambers (Figure 15).

Porosity: Pores are absent from the proloculus and deuteroconch and, if present, are largest and most concentrated near the inner spiral suture of the third and fourth chambers (Figure 16*a*). The pores generally are not evenly scattered across the chamber wall until the final whorl. In adult chambers, the cylindrical part of the pores are bordered on the interior wall by a broad, funnel-shaped opening (Figure 6*a*).

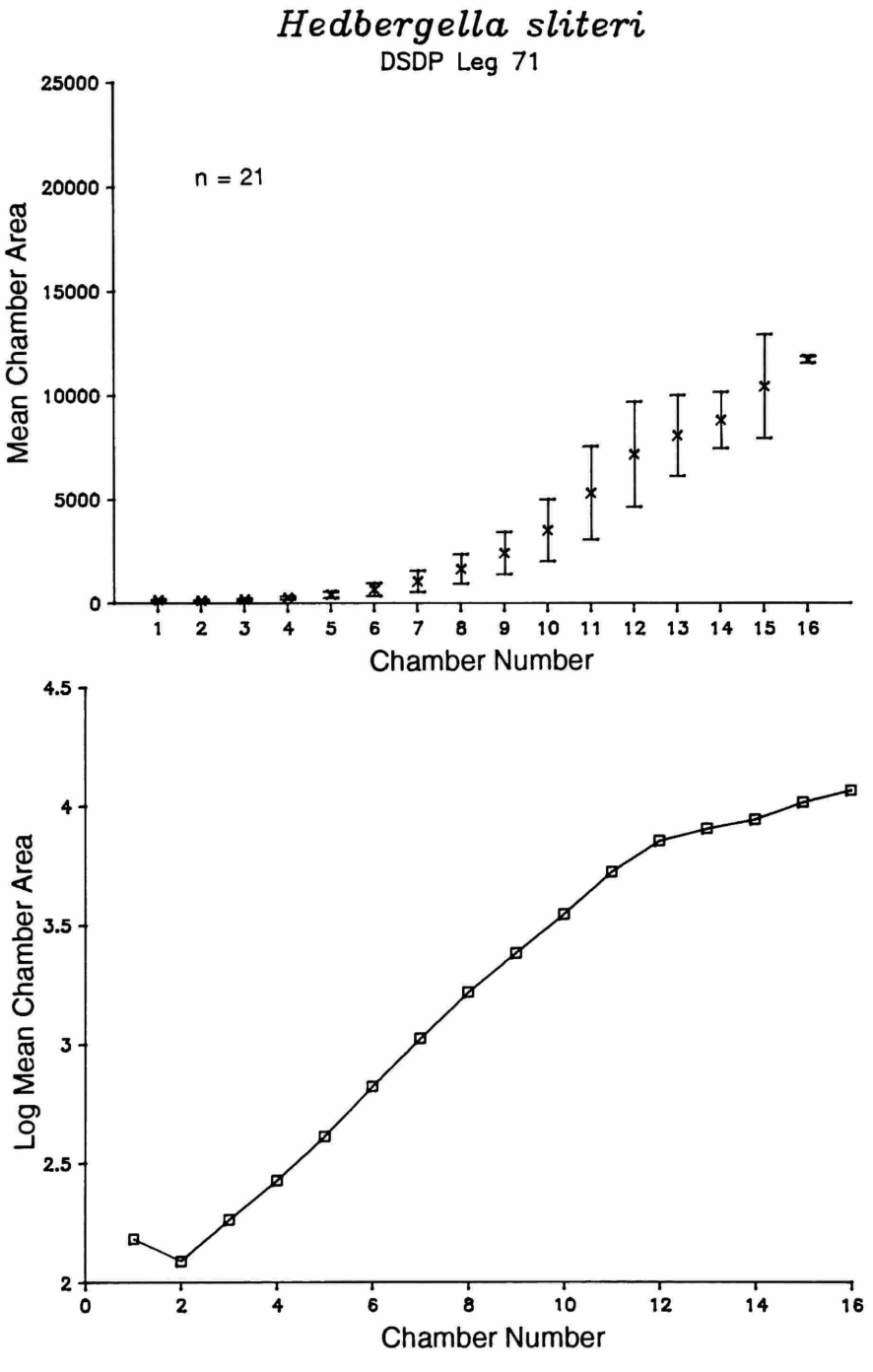

FIGURE 15.—Arithmetic and logarithmic plots of the chamber-by-chamber increase in cross-sectional chamber area (in μm^2) of *Hedbergella sliteri*. The arithmetic plots show one standard deviation about the mean and the logarithmic plots show only the mean values. The number (n) of specimens analyzed is also shown.

FIGURE 16 (facing page).—Ontogenetic patterns of pore distribution on the ventral chamber surfaces of *a, Hedbergella sliteri*; *b, Costellagerina pilula*; *c, Archaeoglobigerina australis*; *d, Archaeoglobigerina bosquensis*; *e, Archaeoglobigerina australis* (micromorph specimen); and *f, Archaeoglobigerina mateola*. Note that pores are absent from the proloculi and are initially concentrated along the spiral sutures.

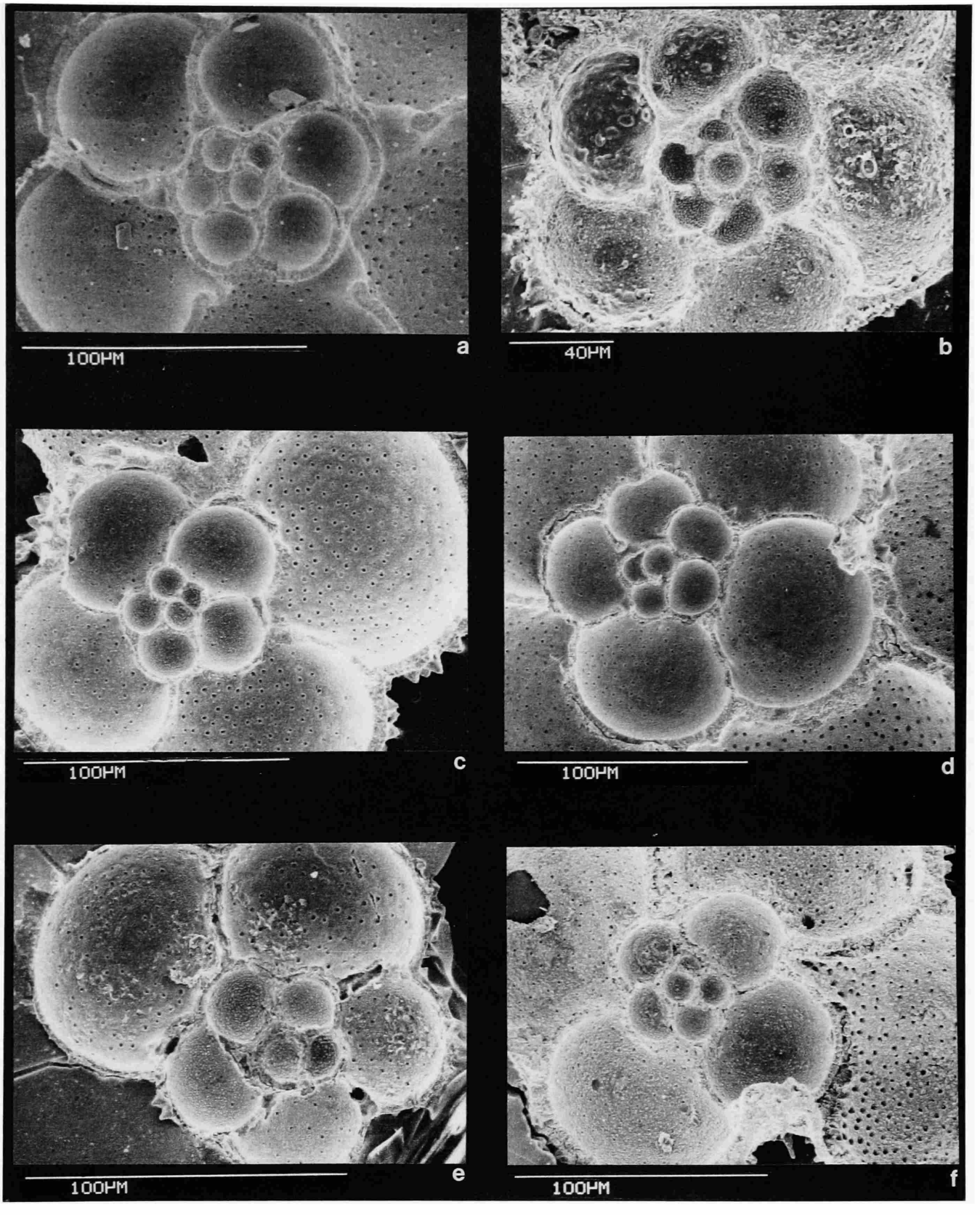
100µM
a
40µM
b
100µM
c
100µM
d
100µM
e
100µM
f

H. sliteri

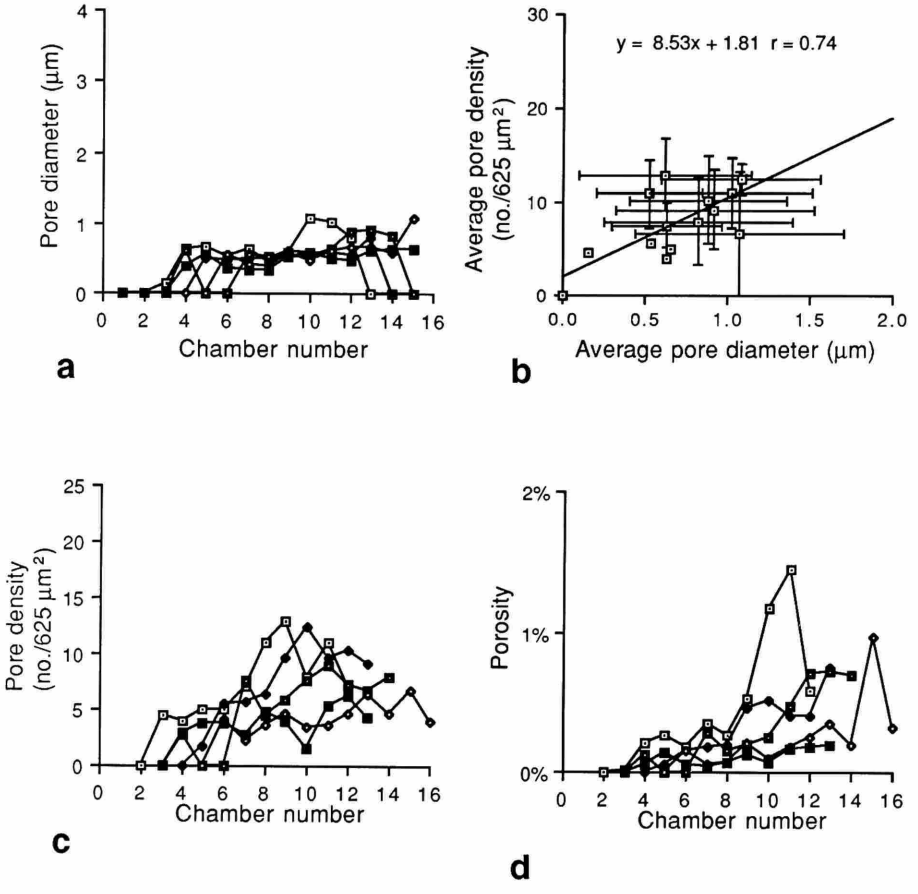

FIGURE 17.—Ontogenetic changes in *a*, pore diameter; *c*, pore density; and *d*, porosity, measured from five adult specimens of *Hedbergella sliteri*. *b*, is a linear regression curve calculated from the mean values of pore diameter and pore density of all measured chambers of *H. sliteri* with bars representing one standard deviation above and below the mean values. A least squares regression line is also shown.

TABLE 8.—Pore diameter, pore density, and porosity data, including averages, standard deviations, and maximum and minimum values, determined for each chamber within five serially dissected specimens of *Hedbergella sliteri*.

Ch. No.	DIAMETER AVG	STD	MAX	MIN	DENSITY AVG	STD	MAX	MIN	POROSITY AVG	STD	MAX	MIN
1	0.00	0.00	0.00	0.00	0.00	0.00	0.00	0.00	0.00%	0.00%	0.00%	0.00%
2	0.00	0.00	0.00	0.00	0.00	0.00	0.00	0.00	0.00%	0.00%	0.00%	0.00%
3	0.03	0.07	0.15	0.00	0.90	2.01	4.50	0.00	0.00%	0.01%	0.01%	0.00%
4	0.33	0.31	0.63	0.00	1.92	1.82	4.00	0.00	0.08%	0.09%	0.20%	0.00%
5	0.34	0.31	0.65	0.00	2.10	2.25	5.00	0.00	0.09%	0.11%	0.27%	0.00%
6	0.38	0.22	0.54	0.00	3.72	2.19	5.60	0.00	0.11%	0.07%	0.18%	0.00%
7	0.48	0.11	0.63	0.33	5.06	2.44	7.60	2.30	0.18%	0.14%	0.35%	0.04%
8	0.43	0.08	0.52	0.32	6.08	2.91	11.00	3.68	0.15%	0.08%	0.26%	0.06%
9	0.56	0.04	0.62	0.52	7.38	3.84	13.00	3.90	0.30%	0.18%	0.52%	0.13%
10	0.65	0.25	1.08	0.48	6.62	4.25	12.50	1.60	0.42%	0.46%	1.18%	0.07%
11	0.67	0.21	1.02	0.49	7.74	3.10	11.00	3.70	0.53%	0.53%	1.44%	0.16%
12	0.68	0.17	0.88	0.48	7.08	2.08	10.30	4.60	0.42%	0.22%	0.70%	0.18%
13	0.75	0.14	0.92	0.60	6.63	2.01	9.20	4.30	0.50%	0.32%	0.74%	0.20%
14	0.68	0.13	0.82	0.57	6.35	2.33	8.00	4.70	0.44%	0.30%	0.68%	0.19%
15	0.85	0.31	1.07	0.63	6.70		6.70	6.70	0.97%		0.97%	0.97%
16					4.00		4.00	4.00	0.32%		0.32%	0.32%

Pore diameters are less than one micron throughout the ontogeny of most specimens, reaching a maximum of 1.08 μm in a few adult chambers (Table 8). Pore densities show a greater increase with ontogeny, but are also very low, with maximum values of 13 pores/625 μm^2 in the adult chambers. Pore densities and pore diameters show a high positive correlation throughout the ontogenetic series (Figure 17). The microperforate character of this species is demonstrated by low porosity values, which are generally less than 1% and never more than 1.5%.

GENERAL REMARKS.—The features that distinguish *Hedbergella sliteri* from *H. holmdelensis* and *H. monmouthensis* are its larger size, wider umbilicus, and a more gradual rate of chamber size increase in the final whorl. Moreover, it has a shallower umbilicus than *H. monmouthensis* and more spherical chambers than *H. holmdelensis*. So far, *H. sliteri* has been found only within the Austral Realm (Huber, 1992a). The first occurrence of this species is within Subchron C32R in the early Maastrichtian and it ranges to just below the Cretaceous–Tertiary boundary (Huber, 1990, 1991b). Morphologic similarities and stratigraphic evidence indicate that *H. sliteri* probably evolved from *H. monmouthensis* during latest Campanian or earliest Maastrichtian time (Figure 18).

Genus *Costellagerina* Petters, El-Nakhal, and Cifelli, 1983

TYPE SPECIES.—*Rugoglobigerina bulbosa* Belford, 1960.

DESCRIPTION.—Test coiled in a low to medium trochospire, with a lobate peripheral margin, broadly rounded axial periphery, and subcircular to quadrate equatorial outline. Chambers are spherical and increase gradually in size in the early ontogeny, but more rapidly in size in the final whorl. Aperture is a low, interiomarginal arch, umbilical-extraumbilical, and bordered by a porticus, but never a tegillum. Wall surface is finely perforate and covered by pustules that often coalesce into meridionally arranged costellae.

REMARKS.—Petters et al. (1983) distinguished *Costellagerina* from *Hedbergella* and *Whiteinella* because of the presence of meridionally aligned costellae, whereas the extraumbilical position of the aperture and absence of a tegillum and imperforate peripheral band separate *Costellagerina* from *Archaeoglobigerina* and *Rugoglobigerina* (Tables 2, 3). *Costellagerina* ranges from the Cenomanian through the early Campanian.

Costellagerina pilula (Belford, 1960)

PLATE 4: FIGURES 1–13

Rugoglobigerina bulbosa Belford, 1960:94, text-fig. 7, pl. 26: figs. 1–10.

Rugoglobigerina pilula Belford, 1960:92, text-fig. 6, pl. 25: figs. 7–13.—Robaszynski et al., 1984:285, 302.

Whiteinella bulbosa (Belford).—Belford, 1983:2–3, pl. 1: figs. 1–12, pl. 2: figs. 1, 2.

Whiteinella pilula (Belford).—Belford, 1983:2–3, pl. 2: figs. 3–8, pl. 3: figs. 1–5.

Costellagerina bulbosa (Belford).—Petters et al., 1983:250, pl. I: figs. 1–14.

OBSERVATIONS OF THE TEST EXTERIOR.—The test is coiled in a moderately low trochospire, forming a quadrate to subcircular, strongly lobate outline with a rounded axial periphery. Average adult test diameter is 279 μm with a maximum diameter of 421 μm, average breadth is 167 μm, and the average breadth/diameter ratio is 0.60 (Table 4). The umbilicus is small to moderate in size, ranging from 18%–45% of the maximum test diameter with an average of 30%. Adult tests have a total of 14 to 19 chambers and, in the final whorl, have an average of 4.88 chambers and a range of 4.00 to 5.75 chambers. The relatively low penultimate/antepenultimate chamber size ratio demonstrates a moderately low rate of chamber size increase in the final whorl. As observed for *H. sliteri*, nearly half of the studied population shows dextral coiling and kummerform chambers are relatively rare. The aperture is umbilical-extraumbilical in position and bordered by a porticus. A tegillum has not been observed on any specimens. The wall is medioperforate and its surface is covered by pustules that tend to fuse into costellae that are often aligned in a meridional pattern (Plate 4: Figures 2, 7, 11).

OBSERVATIONS OF THE TEST INTERIOR.—*Initial Whorl:* Specimens of *C. pilula* have relatively small proloculi, with an average diameter of 14.5 μm and a range of 12.6 to 17.1 μm (Figures 9–11, Table 5). Because of the smaller proloculus size, the number of chambers in the initial whorl is higher, averaging 5.42 with a range of 4.75 to 6.00. The average initial whorl diameter of 67.6 μm is also relatively small. Proloculus and initial whorl diameters do not show good correlation in *C. pilula*. Throughout the early ontogeny, chamber morphology is globular and the apertural position remains extraumbilical.

Penultimate Whorl: The average of 5.57 chambers in the penultimate whorl is comparable to values obtained from the hedbergellids, and is significangly higher than the other studied taxa (Table 4). Fewer chambers occur in the final whorl because of the tendency toward a more involute (tighter) coiling mode. Apertural position is extraumbilical and chamber shape is globular in the penultimate whorl. Chamber surfaces in the penultimate whorl show an increasing density of randomly situated pustules.

Ontogenetic Growth Curves: The rate of chamber size increase is gradual and remains nearly constant until the final whorl, when the rate slightly diminishes (Figure 19). Size variability in chambers 12–16 is comparable to *H. sliteri*, but considerably less than most of the other taxa at the same ontogenetic stage.

Porosity: All of the specimens of *C. pilula* show some degree of shell recrystallization and secondary calcite overgrowth. As a result, porosity values are probably underesti-

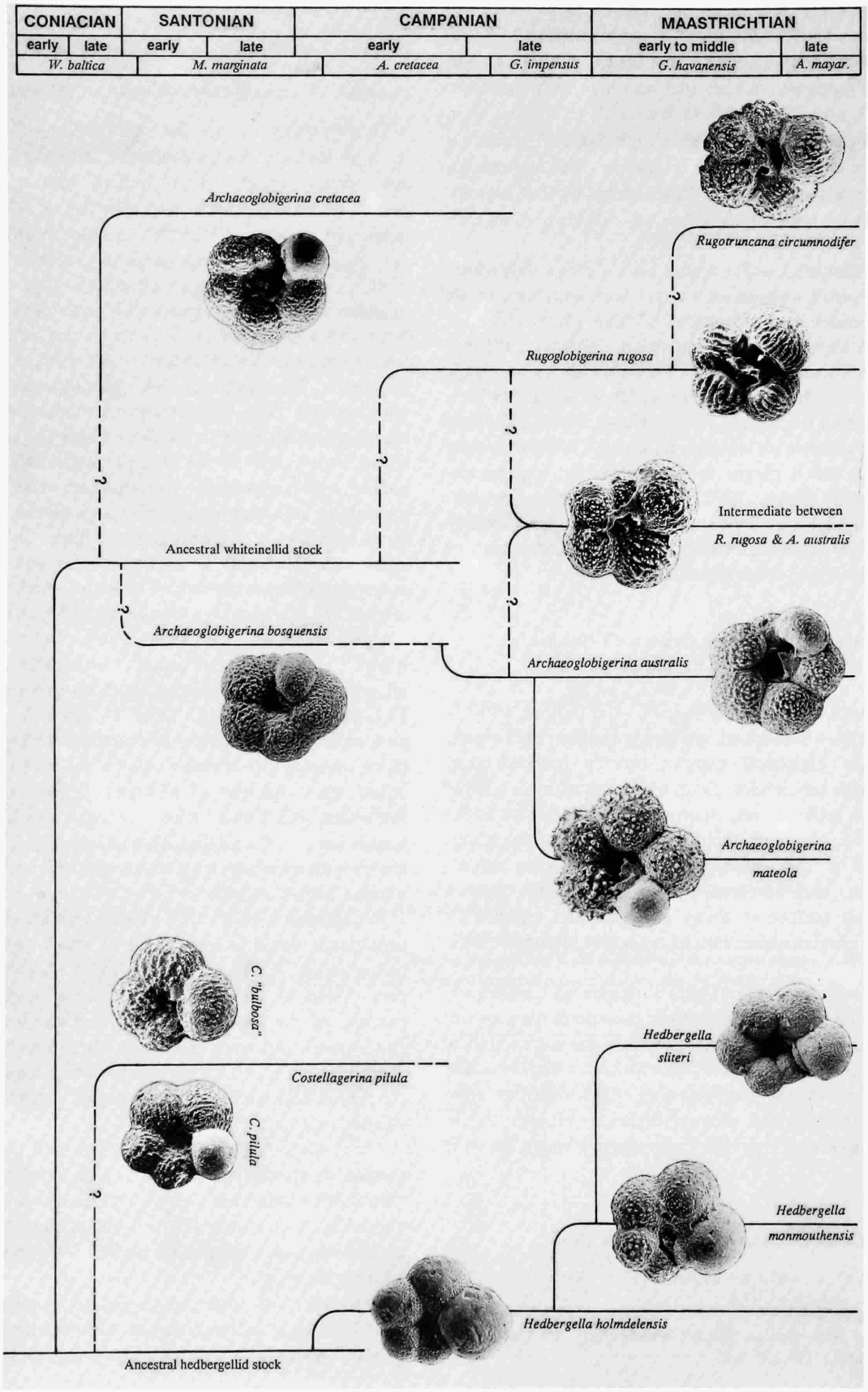
CONIACIAN
early
late
W. baltica
SANTONIAN
early
late
M. marginata
CAMPANIAN
early
late
A. cretacea
G. impensus
MAASTRICHTIAN
early to middle
late
G. havanensis
A. mayar.
Archaeoglobigerina cretacea
Rugotruncana circumnodifer
Rugoglobigerina rugosa
Intermediate between
R. rugosa & A. australis
Ancestral whiteinellid stock
Archaeoglobigerina bosquensis
Archaeoglobigerina australis
Archaeoglobigerina
mateola
C. "bulbosa"
Costellagerina pilula
C. pilula
Hedbergella
sliteri
Hedbergella
monmouthensis
Hedbergella holmdelensis
Ancestral hedbergellid stock

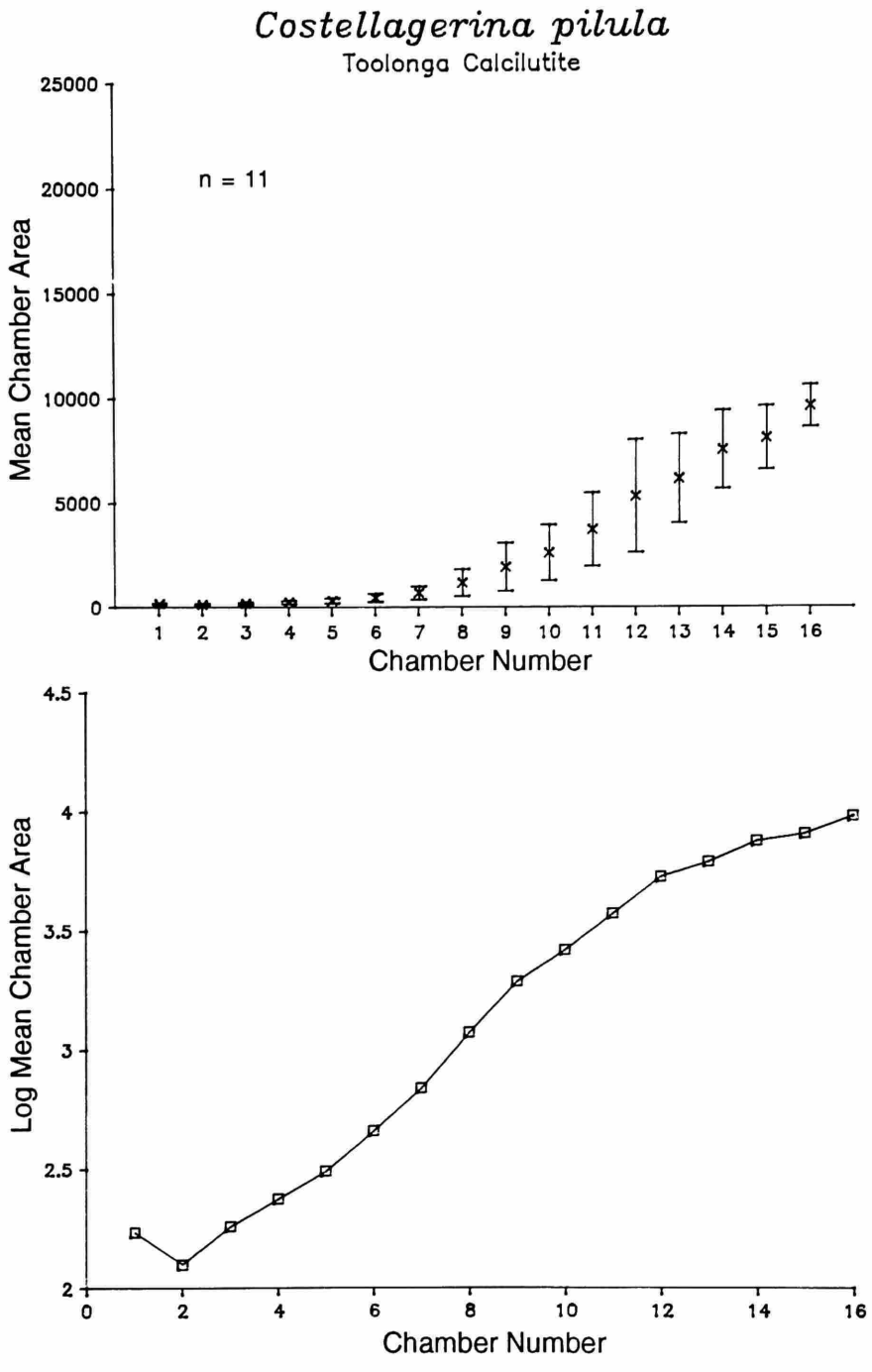

FIGURE 19.—Arithmetic and logarithmic plots of the chamber-by-chamber increase in cross-sectional chamber area (in μm^2) of *Costellagerina pilula*. The arithmetic plots show one standard deviation about the mean and the logarithmic plots show only the mean values. The number (n) of specimens analyzed is also shown.

FIGURE 18 (facing page).—Phylogenetic reconstruction inferred for Late Cretaceous planktonic foraminiferal species discussed in this study based on results of ontogenetic comparisons. *Rugotruncana circumnodifer* (Finlay) was not analyzed in this study; the phylogenetic link inferred for *Rugotruncana* and *Rugoglobigerina* is from Robaszynski et al. (1984). Ontogenetic analyses reveal that *A. australis*, *A. bosquensis*, and *A. mateola* have internal morphologies that are distinctly different from *A. cretacea*, and therefore may not belong in the same genus. Until topotypes of *A. blowi* and *A. bosquensis* are studied, no generic revision is recommended, although a separate origin from a common ancestral whiteinellid stock is postulated. Upper Cretaceous zonation from Huber (1992b).

mated particularly for the early growth stages. Pores are generally absent from the initial whorl chambers and are concentrated along the spiral suture in several following chambers, and then are more evenly scattered by the seventh to eighth chambers (Figure 16*b*). Pore diameters are less than 1.00 μm for most chambers and up to 1.21 μm in the final chamber (Table 9). Pore densities are greater than 10 pores/625 μm^2 by about the eleventh chamber and reach a maximum of 24 pores/625 μm^2 in final whorl chambers. Average pore densities and pore diameters show a highly positive correlation throughout the ontogenies (Figure 20). Maximum porosity values are between 3% and 5%.

GENERAL REMARKS.—The taxonomic classification of this species has undergone several revisions since Belford's (1960) original description of Santonian specimens from Western Australia. Because of their similar surface ornamental features, Masters (1977) placed *C. bulbosa* and *C. pilula* in the synonomy of *Rugoglobigerina rugosa*, although the latter species differs in having a wholly umbilical aperture and the presence of a tegillum. Belford (1983) noted that the meridional pattern of ornamentation, defined as a primary generic character of *Rugoglobigerina* by Brönnimann and Brown (1956), was repeated several times during the Cretaceous. Although he also considered this ornamental feature to be of generic importance, Belford (1983) proposed that the absence of tegilla and imperforate peripheral bands and the extraumbilical tendency of apertures in specimens of *R. bulbosa* and *R. pilula* warranted their removal from *Rugoglobigerina*. Belford placed these species in *Whiteinella*, but indicated that the type description of that genus made no reference to surface ornamentation of the test (Pessagno, 1967).

Petters et al. (1983) subsequently described a new genus, *Costellagerina*, to accomodate Belford's species, and they designated *C. bulbosa* as the type species. They placed *C. bulbosa* and *C. pilula* in the family Rotaliporidae and subfamily Hedbergellinae because of the extraumbilical-umbilical aperture, absence of tegilla, and presence of portici.

Robaszynski et al. (1984), apparently unaware of the work of Petters et al. (1983), placed Belford's meridionally costellate species in *Rugoglobigerina* and synonymized the four chambered morphotype (= *R. bulbosa* of Belford, 1960) under *R. pilula*. They indicated that *R. pilula* may have been the ancestral stock from which Campanian–Maastrichtian rugoglobigerinid species evolved.

Similarity in the ontogenies of the four to five chambered morphotype, originally designated as *R. bulbosa*, and the five to six chambered morphotype, originally named *R. pilula* (Plate 4: Figures 1–13), suggests that these forms are ecophenotypes of the same species. *Costellagerina pilula* is regarded as a senior synonym of the two species following the recommendation of Robaszynski et al. (1984) and Article 24 of the International Code of Zoological Nomenclature.

Differences in the ontogenetic morphology of *C. pilula* from the interior morphology of *R. rugosa* demonstrates that Petters et al. (1983) were justified in removing *C. bulbosa* and *C. pilula* from *Rugoglobigerina* and designating a new genus. Dissection of the test interior of *C. pilula* reveals that it has a greater number of chambers in adult specimens, the rate of chamber size increase is more gradual, and the aperture does not occupy a nearly umbilical position until the last several chambers of adult tests (Table 5, Plate 4). Meridionally-aligned costellae of *C. pilula* do not appear on chambers in the initial through penultimate whorls and show variability in external expression on chambers of the ultimate whorl. Although the log-linear growth curves and extraumbilical position of the aperture suggest a closer affinity to the hedbergellid lineage, *C. pilula* is probably only distantly related due to the higher shell porosity and presence of meridionally costellate wall ornamentation (Figure 18).

Genus *Archaeoglobigerina* Pessagno, 1967

TYPE SPECIES.—*Archaeoglobigerina blowi* Pessagno, 1967.

DESCRIPTION.—Tests of *Archaeoglobigerina* are low trochospiral, biconvex to slightly spiroconvex, subcircular and strongly lobate in outline, with a broadly rounded, non-carinate peripheral margin with or without an imperforate band or a weakly developed double keel. Chambers are spherical to ovate, strongly inflated, and increase moderately in size. Sutures are depressed, never raised. Aperture is umbilical and may be covered by tegilla. The wall is medioperforate, ornamented with randomly situated pustules.

REMARKS.—As formally defined, the absence of meridionally aligned pustules or costellae distinguish this genus from *Rugoglobigerina* and *Costellagerina*. The latter genus is more easily separated from *Archaeoglobigerina* because of the extraumbilical position of the primary aperture. However, discrimination from *Rugoglobigerina* can be blurred in middle to high latitude regions where the meridional alignment of pustules on rugoglobigerine taxa weakens or is completely absent (e.g., see Olsson, 1964:158; Huber, 1988b:207).

In an effort to more accurately characterize the generic concept of *Archaeoglobigerina*, biometric data were obtained from well-preserved specimens of *A. bosquensis* and *A. cretacea* from DSDP Site 511. Results discussed below indicate major differences in the ontogenetic morphology of these two species, such that retaining both in the same genus seems unjustified. Unfortunately, biometric analysis of *A. blowi*, the type species of *Archaeoglobigerina*, was not possible during this study because the topotypes are poorly preserved or infilled with cement, and well-preserved specimens of *A. blowi* from outside the type area were not available. Without comparative data from the type species of *Archaeoglobigerina*, no emendation of this genus is made at this time. Nonetheless, it should be noted that inclusion of the high latitude species *A. australis* and *A. mateola* in *Archaeoglobigerina* is based primarily on the similarity of these species to their presumed ancestral taxon, *A. bosquensis*. If the generic designation of *A. bosquensis* is revised at some later date, similar revision in the generic status of *A. australis* and *A. mateola* would be warranted.

C. pilula

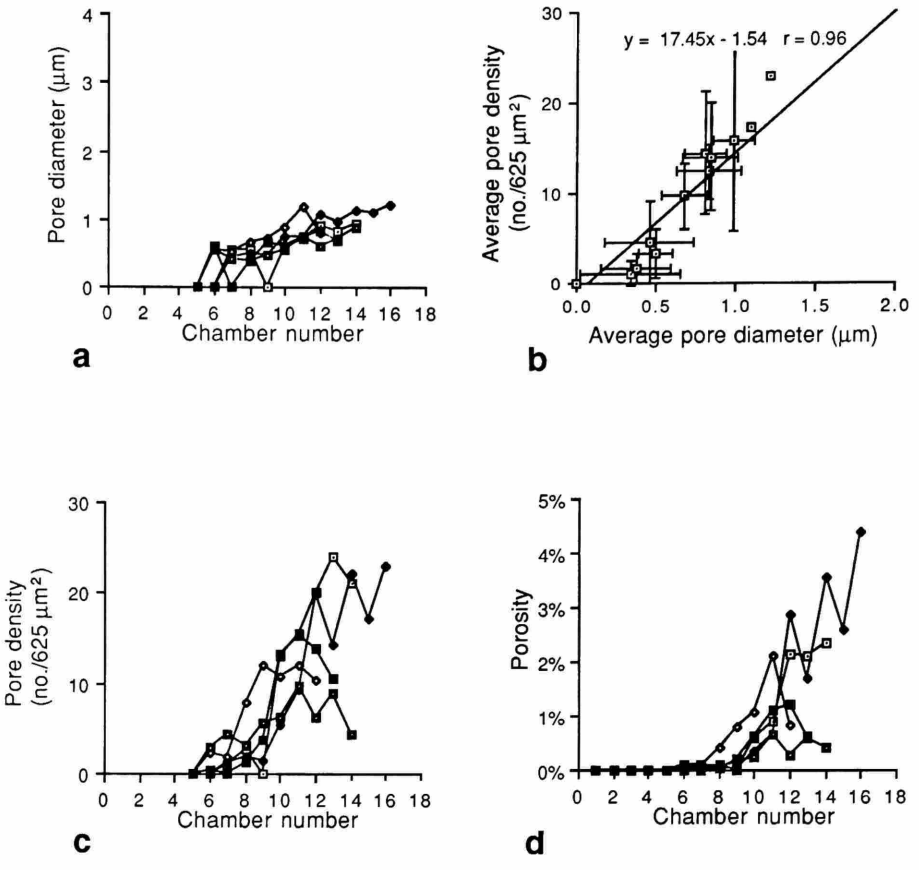

FIGURE 20.—Ontogenetic changes in *a*, pore diameter; *c*, pore density; and *d*, porosity, measured from five adult specimens of *Costellagerina pilula*. *b*, is a linear regression curve calculated from the mean values of pore diameter and pore density of all measured chambers of *C. pilula* with bars representing one standard deviation above and below the mean values. A least squares regression line is also shown.

TABLE 9.—Pore diameter, pore density, and porosity data, including averages, standard deviations, and maximum and minimum values, determined for each chamber within five serially dissected specimens of *Costellagerina pilula*.

Ch. No.	DIAMETER AVG	STD	MAX	MIN	DENSITY AVG	STD	MAX	MIN	POROSITY AVG	STD	MAX	MIN
1	0.00	0.00	0.00	0.00	0.00	0.00	0.00	0.00	0.00%	0.00%	0.00%	0.00%
2	0.00	0.00	0.00	0.00	0.00	0.00	0.00	0.00	0.00%	0.00%	0.00%	0.00%
3	0.00	0.00	0.00	0.00	0.00	0.00	0.00	0.00	0.00%	0.00%	0.00%	0.00%
4	0.00	0.00	0.00	0.00	0.00	0.00	0.00	0.00	0.00%	0.00%	0.00%	0.00%
5	0.00	0.00	0.00	0.00	0.00	0.00	0.00	0.00	0.00%	0.00%	0.00%	0.00%
6	0.34	0.32	0.62	0.00	1.12	1.34	2.90	0.00	0.04%	0.05%	0.10%	0.00%
7	0.38	0.22	0.55	0.00	1.70	1.61	4.30	0.00	0.05%	0.04%	0.09%	0.00%
8	0.50	0.11	0.66	0.39	3.36	2.64	7.90	1.30	0.13%	0.17%	0.43%	0.02%
9	0.46	0.28	0.73	0.00	4.56	4.66	12.00	0.00	0.24%	0.32%	0.80%	0.00%
10	0.68	0.14	0.89	0.55	9.70	3.71	13.20	5.30	0.57%	0.31%	1.06%	0.24%
11	0.83	0.20	1.18	0.71	12.42	2.99	15.60	9.40	1.08%	0.60%	2.11%	0.66%
12	0.84	0.17	1.07	0.60	14.06	5.99	20.00	6.20	1.46%	1.03%	2.85%	0.28%
13	0.81	0.13	0.97	0.69	14.40	6.78	24.00	8.80	1.25%	0.77%	2.11%	0.58%
14	0.99	0.13	1.13	0.89	15.90	9.97	22.10	4.40	2.10%	1.59%	3.56%	0.40%
15	1.10		1.10	1.10	17.20		17.20	17.20	2.59%		2.59%	2.59%
16	1.21		1.21	1.21	23.00		23.00	23.00	4.37%		4.37%	4.37%

Archaeoglobigerina australis Huber, 1990

PLATE 1: FIGURES 6–22, 26, 27, PLATE 5: FIGURES 5–19, PLATE 6: FIGURES 1–18

Hedbergella monmouthensis (Olsson).—Sliter, 1977:542, pl. 3: figs. 1–3.—Krasheninnikov and Basov, 1983:804–805, pl. 6: figs. 5–8.

Rugoglobigerina pilula Belford.—Sliter, 1977:542, pl. 10: figs. 7–9.—Krasheninnikov and Basov, 1983:807, pl. 11: figs. 3–6.

Rugoglobigerina pustulata Brönnimann, Krasheninnikov, and Basov, 1983:806, pl. 10: figs. 10–13.

Rugoglobigerina rotundata Brönnimann, Krasheninnikov, and Basov, 1983:807, pl. 1: figs. 7–11.—Huber, 1988a:206, figs. 28.12–28.14.

Rugoglobigerina? sp. 1.—Huber, 1988a:207, figs. 29.1–29.14, 30.5–30.10.

Archaeoglobigerina australis Huber, 1990:504–505, pl. 2: figs. 11–13, pl. 3: figs. 1–7, pl. 6: figs. 7–9; 1991a:292, pl. 1: figs. 9–12, pl. 2: fig. 1; 1991b:461, pl. 1: figs. 10, 11.

OBSERVATIONS OF THE TEST EXTERIOR.—The test is trochospiral with a moderately high dorsoconvexity, the equatorial periphery is deeply lobate, and the axial periphery is broadly rounded. Average diameter of adult specimens is 280 μm, with some reaching 410 μm, average breadth is 150 μm, and the breadth/diameter ratio averages 0.55 (Table 4). The umbilicus is deep, narrow to broad, comprising an average of 28% of the maximum test diameter. Adult tests have a total of 12 to 15 chambers, with an average of 4.59 and range of 3.75 to 5.75 chambers in the final whorl. Chamber size increase is relatively slow in the final whorl, as shown by the low penultimate/antepenultimate chamber diameter ratio of 1.16. Kummerform frequency is about 36%, and the frequency of dextral forms is 76%. Apertures of gerontic ecomorphs are umbilical to slightly extraumbilical, and are often bordered by a broad porticus. Specimens with a tegillum have not been observed. The test surface is covered with fine to coarse pustules that are randomly situated.

OBSERVATIONS OF THE TEST INTERIOR.—*Initial Whorl:* Proloculus diameters average about 15 μm and range from 10 μm to 19 μm. An average of 4.38 chambers occur in the initial whorl, which ranges from 41 to 93 μm in diameter and has a mean diameter of about 72 μm in adult size specimens and 61 μm in micromorphs (Figures 9–11, Table 5). The initial whorl morphology is low trochospiral with globular chambers and apertures that are extraumbilical in position. Initial whorl chambers are generally smooth (Plate 6: Figures 17, 18).

Penultimate Whorl: From 4.00 to 5.50 chambers occur in the penultimate whorl, which averages 4.66 chambers (Table 4). The aperture moves from an extraumbilical to umbilical-extraumbilical position, and surface ornament becomes more densely pustulose (Plate 5: Figure 10).

Ontogenetic Growth Curves: The rate of chamber size increase in adult specimens is moderately high until the ninth to eleventh chamber, where the rate begins to diminish (Figure 21). Size variability of these forms is quite high by the twelfth to fourteenth chamber due to the frequency of kummerform final chambers. Neanic (or micromorph) forms of *A. australis* initially show a moderately high rate of chamber size increase, but the rate diminishes by the eighth to ninth chamber (Figures 22, 23).

Porosity: Pores are generally absent from the first two to three chambers, then spread from near the spiral suture outward and are evenly scattered across the chamber wall by the sixth to eighth chamber in adult specimens (Figure 16*c*), and by the fifth to sixth chamber in neanic forms (Figure 16*e*). On the interior of adult chambers, a narrow funnel-shaped depression borders the cylindrical portion of the pore openings (Figure 7*a*). Pore diameters are generally less than 0.60 μm prior to the seventh chamber and increase to a maximum of 1.0 μm to 1.2 μm in the final whorl chambers (Tables 10, 11). Pore density increases from less than 10 pores/625 μm^2 to 15–18 pores/625 μm^2 between the eighth and tenth chamber. Maximum observed pore density is 22. Pore density values and pore diameters show a strongly positive correlation (Figures 24, 25). Porosity values generally range below 1% before the eighth to ninth chamber and reach a maximum of 2% to 4% afterwards.

PHENOTYPIC VARIABILITY.—One of the major goals in this study was to establish the taxonomic status, phylogeny, and range of phenotypic variability of *A. australis*. Forms with a wide range of test sizes and shell morphologies in the *A. australis* concept are included for the following reasons: (1) intergrading morphologies occur in all size fractions; (2) the end-member phenotypes share a common stratigraphic and geographic range; (3) the surface architecture is similar for all sizes; and (4) the small- and intermediate-sized phenotypes can be recognized within the the interior of adult-sized tests. Nevertheless, a conventional approach to taxonomic classification would categorize the end-member phenotypes (e.g., Figure 2*a–d, i–l*) in different genera because of the differences in apertural positions and rate of chamber size increase in the final whorls. It is therefore appropriate to explore possible paleobiologic factors and/or evolutionary mechanisms that may have controlled the terminal morphologies of the *A. australis* populations.

Premature Termination of Growth: Pre-adult morphologies of *A. australis* have been identified by backtracking the chamber-by-chamber growth in serially dissected adult tests (e.g., Plates 5, 6). As discussed above, chambers in and prior to the penultimate whorl of large-sized specimens show (1) a more extraumbilical position of the aperture, (2) less dense and finer pustulose surface ornament, and (3) a more rapid rate of chamber size increase than in final whorl chambers. Thus, normalform, small to intermediate-sized specimens (e.g., Figures 2*a–d*) are considered as micromorphs of *A. australis* that died before reaching reproductive maturity.

Relative abundance counts of Maastrichtian samples from ODP Sites 689 and 690 reveal that micromorphs of *A. australis* are quite common in the <150 μm size fraction (Huber, 1990). Thus, juvenile mortality at those high latitude sites must have been quite high considering that shells in the finer fraction have thinner walls and a slower settling rate and therefore are less

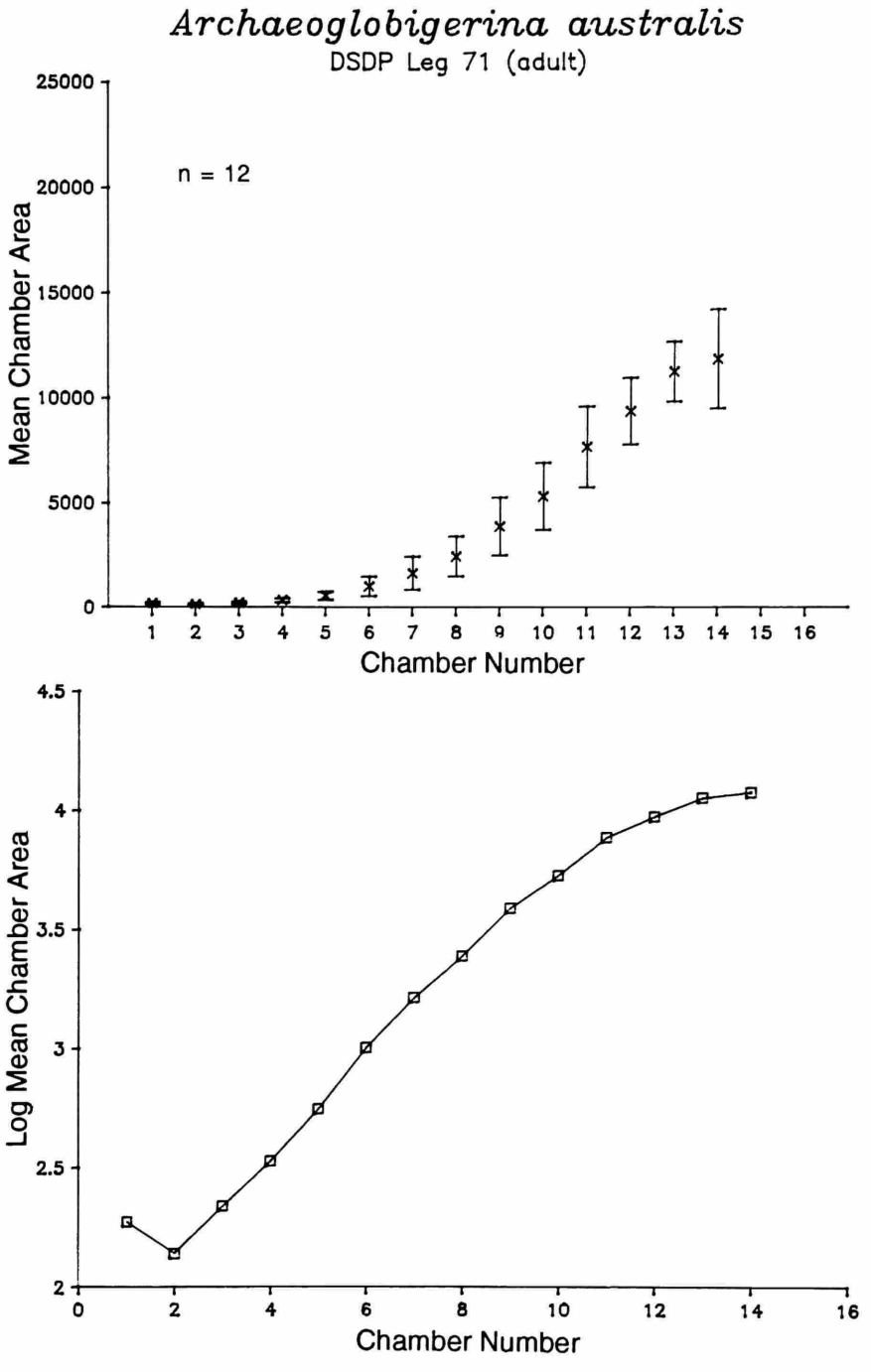

FIGURE 21.—Arithmetic and logarithmic plots of the chamber-by-chamber increase in cross-sectional chamber area (in μm^2) of *Archaeoglobigerina australis* (adult). The arithmetic plots show one standard deviation about the mean and the logarithmic plots show only the mean values. The number (n) of specimens analyzed is also shown.

likely to reach the seafloor due to dissolution within the water column (Hecht et al., 1975; Adelseck and Berger, 1975).

The most important cause of juvenile mortality is probably related to insufficient food availability in the surface waters (Hemleben, pers. comm., 1991). Hemleben et al. (1985) found that there is a large flux of dead juvenile shells of *Globorotalia truncatulinoides* following a peak in adult production and food consumption. A second cause of premature death is predation; grazing by some zooplankton may concentrate undamaged juvenile tests into fecal pellets which rapidly sink to the

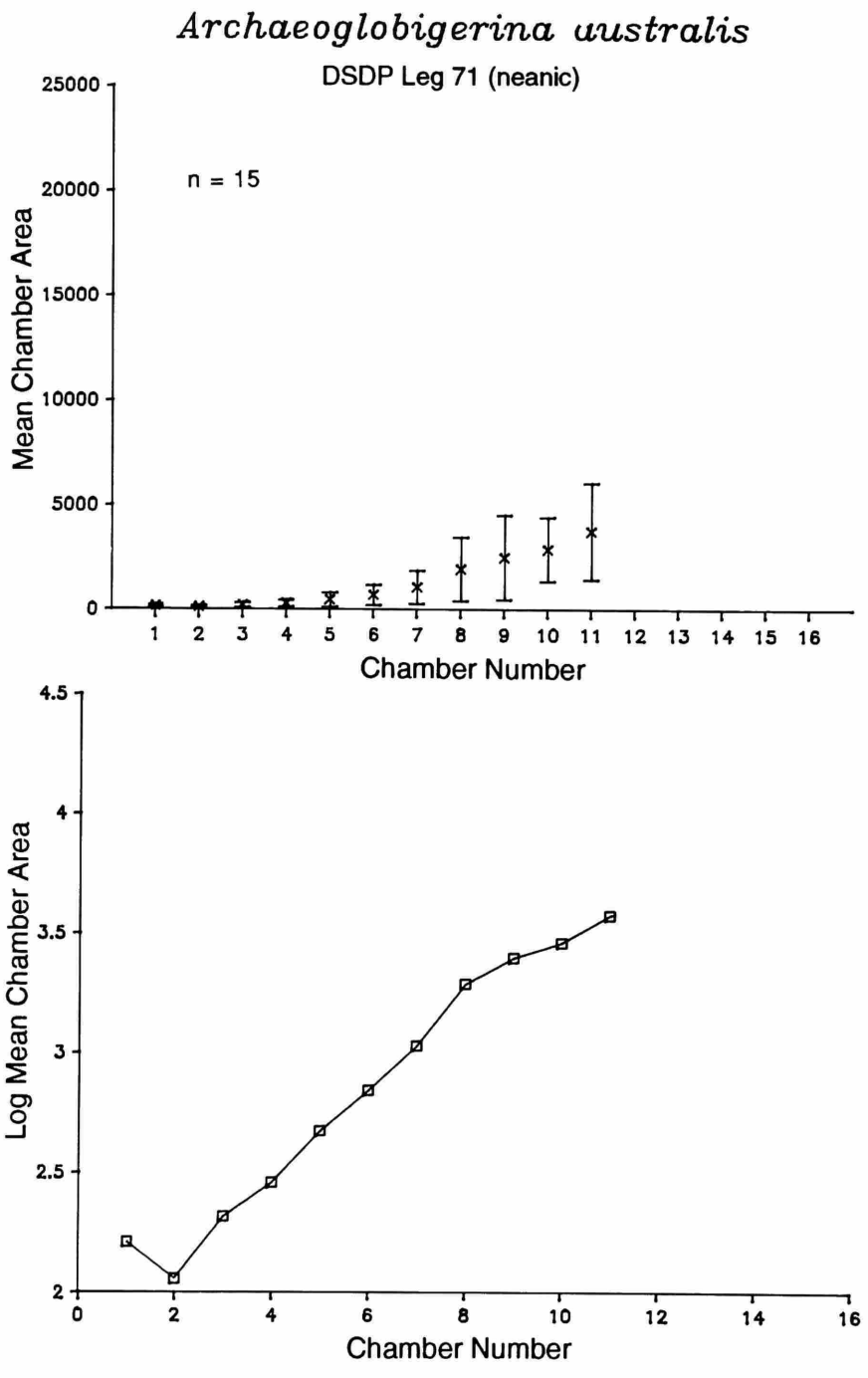

FIGURE 22.—Arithmetic and logarithmic plots of the chamber-by-chamber increase in cross-sectional chamber area (in μm^2) of *Archaeoglobigerina australis* (neanic). The arithmetic plots show one standard deviation about the mean and the logarithmic plots show only the mean values. The number (n) of specimens analyzed is also shown.

seafloor (Bé et, al., 1985). A third cause is aggregation of the smaller foraminiferal size classes with flocculent matter that is sinking through the water column and settling on the seafloor (Hemleben et al., 1988). Finally, pre-adult foraminifera may perish because of displacement into unfavorable environments by advection, mixing, or migration (Berger, 1971b). All of these factors probably contributed to premature death of the Cretaceous assemblages of *A. australis*.

Environmental-related Size and Morphology Differences: The range of morphologic variability of *A. australis* is paralleled to that observed in *Neogloboquadrina pachyderma* (Ehrenberg), *Globigerina bulloides* d'Orbigny, and *Globigerinoides sacculifer* (Brady), which inhabit the modern oceans. Kennett (1968) recognized three latitudinal variants of *N. pachyderma* in surface sediments of the South Pacific based on systematic changes in test size, shell thickness, apertural characteristics, number of chambers, and dominant coiling direction, and indicated that these differences were environmentally controlled. Subsequent studies on *N. pachyderma* (Kennett, 1970; Malmgren and Kennett, 1972; Keller, 1978; Reynolds and Thunell, 1986) and *G. bulloides* (Malmgren and Kennett, 1976, 1977) have correlated changes in morphology primarily to temperature-related phenomena, although some authors have separated the *N. pachyderma* morphogroups into distinct new species (Cifelli, 1961, 1973; Olsson, 1974, 1976).

A number of phenotypic variants of living specimens of *Globigerinoides sacculifer* were produced by varying temperature and salinity conditions in laboratory cultures (Hemleben et al., 1987). These authors found that differences in external appearance were so strong that the morphovariants could not be distinguished at the species level from five other planktonic taxa. Laboratory culture studies have also demonstrated a strong correlation of planktonic foraminiferal test size, chamber morphology, and total lifespan with several important physical and chemical parameters. Rapid onset of gametogenesis, resulting in premature termination of the parent cell and stunted shell growth, was induced by reduction in light intensity (Bé et al., 1981), longer feeding frequency (Caron et al., 1981), and lowered salinity and temperature (Hemleben et al., 1987; Bijma, Faber, and Hemleben, 1990). Hence, maximum test sizes occur under optimum growth conditions, whereas smaller final test sizes developed under sub-optimum growth conditions.

The growth of kummerform chambers in planktonic foraminifera has been interpreted by some authors as a morphological response to stressed environmental conditions (Berger, 1968, 1969, 1971a; Hecht and Savin, 1970, 1971, 1972). However, laboratory culture study of *G. sacculifer* has revealed that formation of kummerform or sac-like chambers is closely tied to the reproductive process (Hemleben and Spindler, 1983; Anderson and Faber, 1984; Hemleben et al., 1988; Bijma, Erez, and Hemleben, 1990). In fact, Bijma, Faber, and Hemleben (1990) found that the frequency of kummerform phenotypes among cultured populations of *G. sacculifer* diminishes toward extreme temperature and salinity conditions. High kummerform frequencies occurred among populations that grew under normal conditions and attained reproductive maturity, whereas, populations with few kummerforms reflect growth under marginal conditions with limited reproductive success (Bijma, Faber, and Hemleben, 1990).

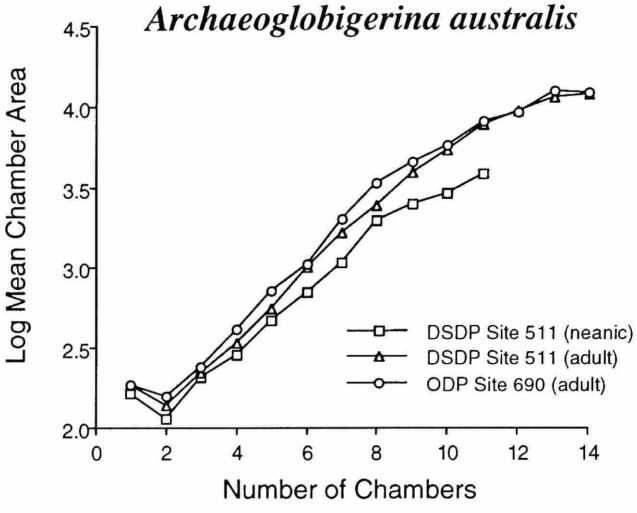

FIGURE 23.—Logarithmic plots of the mean cross-sectional chamber area of neanic and adult specimens of *Archaeoglobigerina australis* from DSDP Leg 71 and adult specimens from ODP Leg 113. Note that the Leg 71 and Leg 113 adult morphotypes compare closely in their mean values, but the mean value of the neanic specimens diminishes particularly after the eighth chamber.

Perhaps some of the size and morphologic variability demonstrated by micromorph and gerontic populations of *A. australis* is caused by its habitation in an intensely seasonal high latitude environment. Micromorphs of this species, which show the most extreme ontogenetic morphometric variability (Figures 9–11, Tables 4, 5), may reflect growth during periods of low light and limited nutrient availability (e.g., early Spring, late Fall, or Winter) and/or stress-induced gametogenesis. Although the higher kummerform frequency among micromorph populations of *A. australis* does not support this premise, based on analogy with the laboratory culture studies of *G. sacculifer*, it is premature to make uniformitarian assumptions about the environmental significance of diminutive final chambers on extinct fossil taxa. The predominance of kummerform *A. australis* phenotypes in nearshore clastic sediments from Seymour and Vega Island (Huber, 1988a) suggests that these forms were tolerant of stressed environmental conditions. Stable isotope analyses of micromorph and gerontic normalform specimens may elucidate their habitat preferences.

Differences in mean proloculus size of the *A. australis* morphotypes (Figures 21–23) may be an indicator of surface water conditions during the Late Cretaceous. Sverdlove and Bé (1985) hypothesized that maximum prolocular size in planktonic foraminifera is attained in conditions of high temperatures, high nutrient availability, and strong light intensity. They suggested that decreasing levels of these three factors lead to diminished prolocular (and successive) chamber sizes. The lower mean proloculus diameters shown for micromorphs of *A. australis* (Figure 23) may provide additional evidence of their stunted growth in a limiting environment. Perhaps these

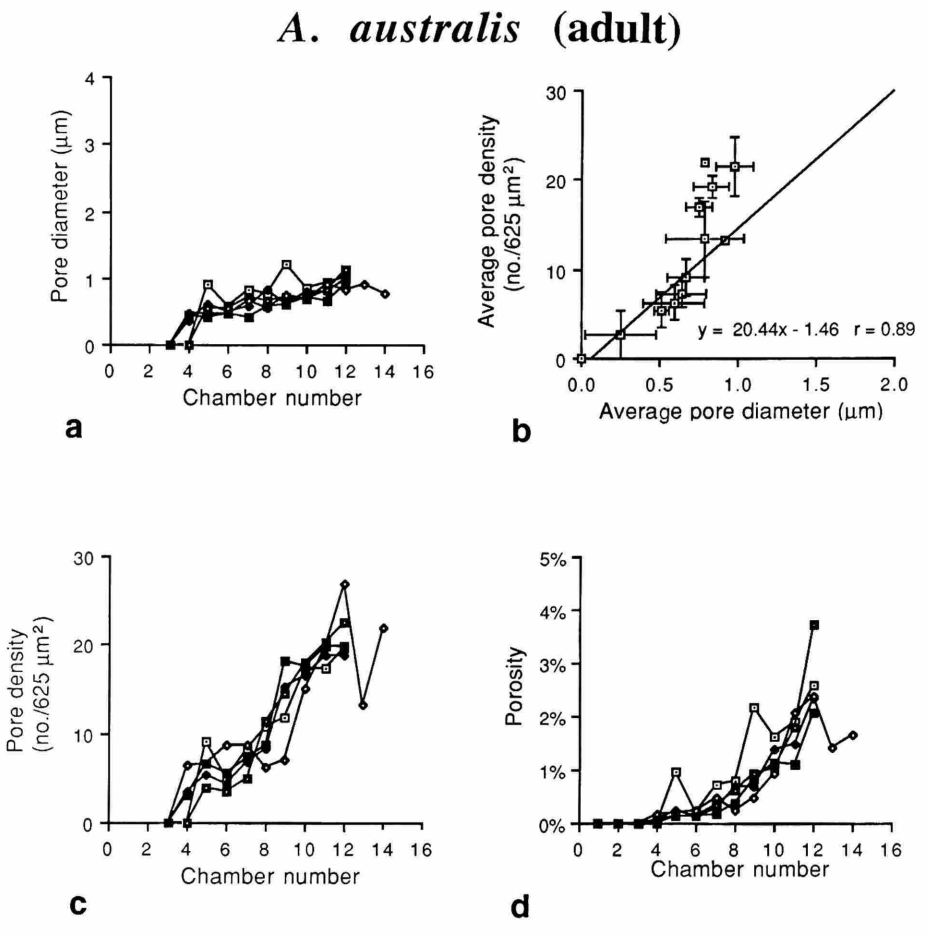

FIGURE 24.—Ontogenetic changes in *a*, pore diameter; *c*, pore density; and *d*, porosity, measured from five adult specimens of *Archaeoglobigerina australis*. *b*, is a linear regression curve calculated from the mean values of pore diameter and pore density of all measured chambers of *A. australis* with bars representing one standard deviation above and below the mean values. A least squares regression line is also shown.

TABLE 10.—Pore diameter, pore density, and porosity data, including averages, standard deviations, and maximum and minimum values, determined for each chamber within five serially dissected adult specimens of *Archaeoglobigerina australis*.

Ch. No.	DIAMETER AVG	STD	MAX	MIN	DENSITY AVG	STD	MAX	MIN	POROSITY AVG	STD	MAX	MIN
1	0.00	0.00	0.00	0.00	0.00	0.00	0.00	0.00	0.00%	0.00%	0.00%	0.00%
2	0.00	0.00	0.00	0.00	0.00	0.00	0.00	0.00	0.00%	0.00%	0.00%	0.00%
3	0.00	0.00	0.00	0.00	0.00	0.00	0.00	0.00	0.00%	0.00%	0.00%	0.00%
4	0.25	0.23	0.46	0.00	2.62	2.73	6.50	0.00	0.06%	0.07%	0.17%	0.00%
5	0.59	0.20	0.92	0.42	6.30	1.89	9.00	3.90	0.34%	0.35%	0.96%	0.14%
6	0.51	0.05	0.58	0.46	5.44	1.96	8.70	3.60	0.17%	0.05%	0.24%	0.14%
7	0.64	0.16	0.84	0.42	7.18	1.43	8.60	5.00	0.39%	0.22%	0.73%	0.16%
8	0.67	0.12	0.82	0.54	9.04	2.07	11.40	6.20	0.54%	0.24%	0.81%	0.23%
9	0.78	0.25	1.21	0.60	13.38	4.19	18.20	7.10	1.02%	0.65%	2.16%	0.50%
10	0.75	0.08	0.86	0.68	16.96	1.12	18.10	15.20	1.22%	0.27%	1.61%	0.94%
11	0.83	0.11	0.94	0.66	19.22	1.19	20.30	17.30	1.66%	0.38%	2.06%	1.10%
12	0.98	0.12	1.14	0.84	21.62	3.31	27.00	18.90	2.62%	0.64%	3.72%	2.07%
13	0.92		0.92	0.92	13.20		13.20	13.20	1.41%		1.41%	1.41%
14	0.78		0.78	0.78	22.00		22.00	22.00	1.66%		1.66%	1.66%

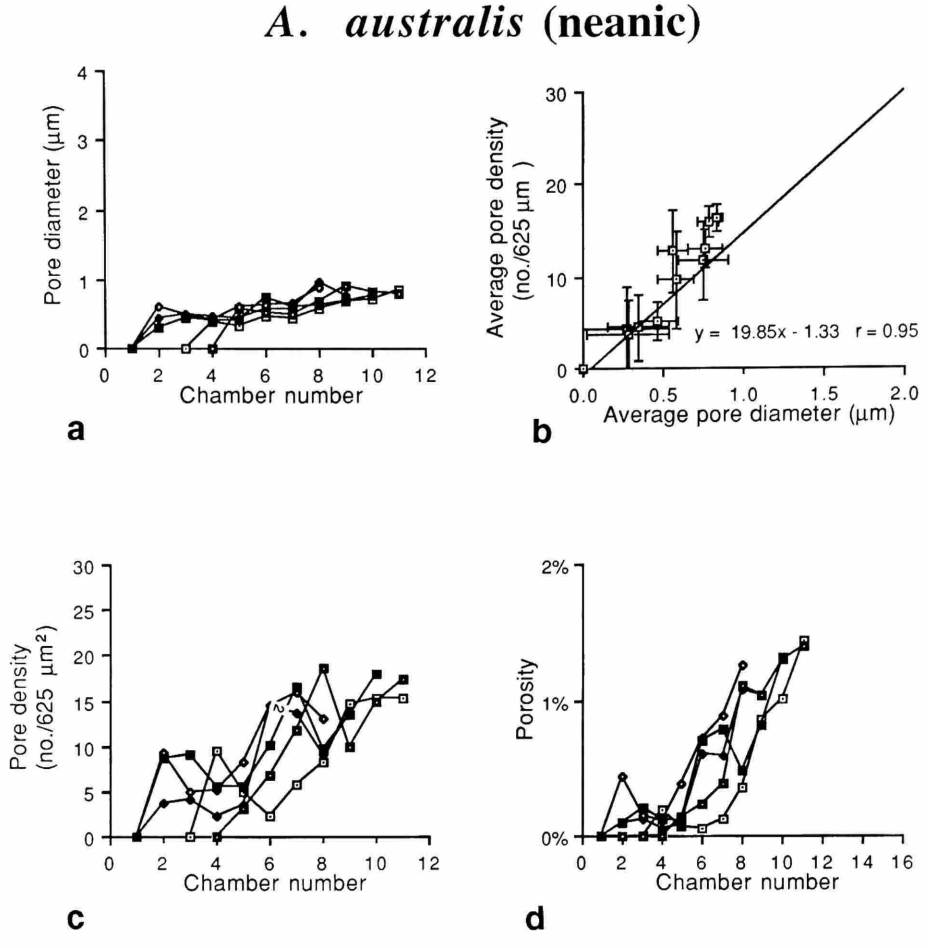

FIGURE 25.—Ontogenetic changes in *a*, pore diameter; *c*, pore density; and *d*, porosity, measured from five neanic specimens of *Archaeoglobigerina australis*. *b*, is a linear regression curve calculated from the mean values of pore diameter and pore density of all measured chambers of *A. australis* micromorphs with bars representing one standard deviation above and below the mean values. A least squares regression line is also shown.

TABLE 11.—Pore diameter, pore density, and porosity data, including averages, standard deviations, and maximum and minimum values, determined for each chamber within five serially dissected micromorph specimens of *Archaeoglobigerina australis*.

Ch. No.	DIAMETER AVG	STD	MAX	MIN	DENSITY AVG	STD	MAX	MIN	POROSITY AVG	STD	MAX	MIN
1	0.00	0.00	0.00	0.00	0.00	0.00	0.00	0.00	0.00%	0.00%	0.00%	0.00%
2	0.27	0.27	0.62	0.00	4.32	4.50	9.30	0.00	0.13%	0.18%	0.44%	0.00%
3	0.28	0.26	0.49	0.00	3.64	3.82	9.10	0.00	0.10%	0.09%	0.21%	0.00%
4	0.34	0.19	0.46	0.00	4.50	3.59	9.50	0.00	0.10%	0.07%	0.19%	0.00%
5	0.47	0.12	0.62	0.34	5.12	2.02	8.30	3.20	0.16%	0.13%	0.39%	0.07%
6	0.58	0.11	0.74	0.46	9.66	5.25	14.50	2.20	0.46%	0.30%	0.72%	0.06%
7	0.56	0.09	0.66	0.43	12.74	4.37	16.60	5.70	0.56%	0.31%	0.88%	0.13%
8	0.75	0.16	0.97	0.59	11.70	4.27	18.60	8.20	0.85%	0.40%	1.25%	0.36%
9	0.76	0.11	0.91	0.68	12.98	2.05	14.70	10.00	0.93%	0.12%	1.04%	0.81%
10	0.78	0.06	0.84	0.73	16.00	1.66	17.90	14.80	1.21%	0.17%	1.31%	1.01%
11	0.83	0.04	0.86	0.80	16.30	1.41	17.30	15.30	1.41%	0.03%	1.43%	1.39%

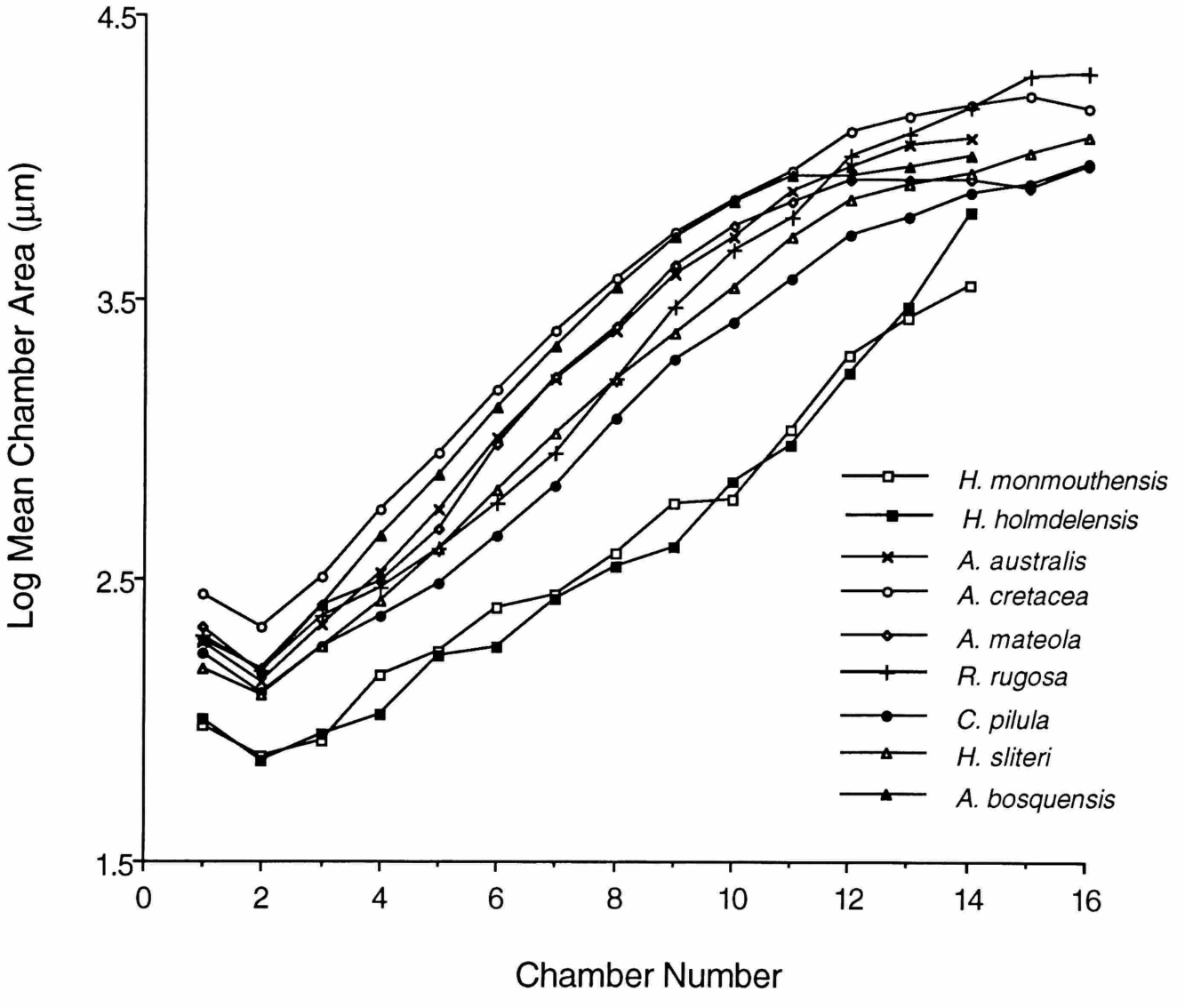

FIGURE 26.—Mean logarithmic values of the chamber-by-chamber increase in cross-sectional chamber areas of all Late Cretaceous planktonic foraminiferal species analyzed in this study. Changes in slope reflect ontogenetic changes in the rate of chamber size increase. Note the smaller value of the deuteroconch (#2 chamber) relative to the proloculus (#1 chamber). Data sets from measurement of adult specimens of *Archaeoglobigerina australis* from DSDP Site 511 and ODP Site 690 were combined on this graph.

micromorphs should be considered as dwarfs that did not attain adult size, but may have attained reproductive maturity.

Heterochrony: An alternative interpretation of the taxonomy of the micromorph populations is that they represent a distinct new species that evolved by the heterochronic process of paedomorphosis, where the juvenile characteristics of ancestral *A. australis* populations became the adult characteristics of the descendant micromorph populations. Evidence for this hypothesis is gained from the observed similarity between the penultimate whorl morphologies of dissected gerontic *A. australis* specimens and the exterior morphologies of micromorph specimens (e.g., compare Plate 6: Figures 1, 2, 7 with Plate 5: Figure 10). This may have been achieved by progenesis, since the onset of reproductive maturity would have occurred at an earlier stage of development in the descendant populations. Independent proof for this view is lacking, however, as the stratigraphic range and areal distribution of the micromorph and gerontic populations are the same.

GENERAL REMARKS.—The "typical" initial whorl morphology of *A. australis* is characterized by normalform gerontic specimens from both the Falkland Plateau and the Maud Rise (Plate 5: Figures 9, 13–15, 16, 17, 19). Qualitative comparison

with the initial whorls of dissected micromorphs on Plate 6 and specimens from Seymour Island reveals strong similarities, such that placement in *A. australis* seems justified. However, some of the Seymour Island forms differ in their external morphology in having faint development of meridional costellae and a tegillum covering the umbilical region (Plate 9: Figures 9, 13), suggesting a strong affinity to *R. rugosa*, but the ontogenetic morphology (e.g., Plate 9: Figure 16) is typical of *A. australis*. The specimen illustrated on Plate 5: Figures 1–4 also features characteristics similar to *R. rugosa* and *A. australis*. Unfortunately, the serial dissection approach did not help clarify the taxonomic position of these latter forms.

The homeomorphic similarity between *A. australis* and *C. pilula* is problematical in external views only, as the interior morphologies show a number of distinct differences. For example, *C. pilula* has a more evolute coiling arrangement in the earlier whorls, a greater number of chambers in the initial and penultimate whorls, and a slower rate of chamber size increase (Figure 26). These differences coupled with the fact that a number of *C. pilula* specimens bear meridionally aligned costellae indicate that *A. australis* is not closely related to *C. pilula*.

Comparison of the developmental morphology of *A. australis* with that of *R. rugosa*, the type species of *Rugoglobigerina*, also shows a number of distinct differences. The interior chamber morphologies of *R. rugosa* are more reniform than in *A. australis*, and the maximum shell porosity is over six times greater. The presence of well-developed meridional costellae and tegilla on *R. rugosa* further separates this taxon from *A. australis*.

Archaeoglobigerina australis is most likely descended from *A. bosquensis* (Figure 18), as these taxa are very similar in ontogenetic and external morphologies (see discussion in *A. bosquensis*) and *A. bosquensis* occurs in older sediments without *A. australis*. They differ in that the final whorl of *A. australis* is more broadly coiled, the test is not as high-spired, and portici are usually present. The stratigraphic range of *A. bosquensis* is reported to have been restricted to the Santonian (Pessagno, 1967), but probably extends into the lower Campanian at the Falkland Plateau (Huber, in prep.). The earliest unequivocal identification of *A. australis* is in upper Campanian sediments, as older occurrences cannot be verified due to poor preservation (Huber, 1991a).

Archaeoglobigerina bosquensis Pessagno, 1967

PLATE 7: FIGURES 1–11

Archaeoglobigerina bosquensis Pessagno, 1967:316, pl. 60: figs. 7–12.—Sliter, 1977:542, pl. 9: figs. 3–5.—Krasheninnikov and Basov, 1983:805-806, pl. 8: figs. 1–8.

OBSERVATIONS OF THE TEST EXTERIOR.—The test is coiled in a moderately low trochospire and forms a quadrate to subcircular outline with a broadly rounded axial periphery and a lobate equatorial periphery. Test diameter averages 285 μm with a maximum of 340 μm, test breadth averages 194 μm, and the breadth/diameter ratio averages 0.68 (Table 4). The umbilicus is narrow, deep, comprising an average of 19% of the maximum test diameter. Adult specimens have a total of 12, 13, or rarely 14 chambers, with an average of 4.23 chambers in the final whorl, and a range of 3.00 to 5.50 chambers. Over half of the studied population have kummerform ultimate chambers, and 86% are dextrally coiled. Apertures are umbilical to slightly extraumbilical in position, bordered by a lip or a narrow porticus. A tegillum has not been observed on any specimens. The wall is medioperforate and the surface is covered by randomly situated, noncoalescent, fine to coarse pustules.

OBSERVATIONS OF THE TEST INTERIOR.—*Initial Whorl:* The initial whorl morphology of *A. bosquensis* is nearly identical to that of *A. australis*. The mean proloculus diameter is 15.3 μm, the mean initial whorl diameter is 74.9 μm, and there are an average of 4.36 chambers in the initial whorl (Figures 9–11, Table 5). Correlation between the proloculus and initial whorl diameters is quite low, with a correlation coefficient of 0.67. Chamber morphology within the initial whorl is globular and the the apertural position remains extraumbilical.

Penultimate Whorl: An average of 4.64 chambers occur in the penultimate whorl (Table 4). Apertural position moves from extraumbilical to umbilical-extraumbilical, chamber morphology is globular, and surface ornament becomes more densely pustulose within this part of the ontogeny.

Ontogenetic Growth Curves: The rate of chamber size increase is log-linear and moderately rapid for the first nine to ten chambers, and is considerably diminished by the final whorl chambers (Figure 27).

Porosity: Pores are absent from the proloculus and one to several occur in the subsequent initial whorl chambers, mostly concentrated near the inner spiral suture until after about the fourth chamber, then become more evenly distributed (Figure 16*d*). The pore openings are cylindrical except for the funnel-shaped opening from the external wall surface (Figure 6*c,d*). Pore diameters of *A. bosquensis* fall within the lower range of the medioperforate classification, with maximum values gradually increasing through ontogeny to less than 1.6 μm (Figure 28). Pore densities rapidly increase between the sixth and eighth chambers from less than 8 pores/625 μm^2 to more than 17 pores/625 μm^2 and reach a maximum of 27 pores/625 μm^2 (Table 12). Porosity values are 3% to 5% by the eleventh chamber and reach a maximum of nearly 7% by the final chamber (Figure 28).

GENERAL REMARKS.—The ontogenetic morphology of *A. bosquensis* is nearly identical to that of *A. australis*. Although the differences are subtle, the Falkland Plateau specimens of *A. bosquensis* can be distinguished by having a higher spire, a tighter mode of coiling, and absence of wide portical flaps. Maximum shell porosity is also higher for *A. bosquensis*, but

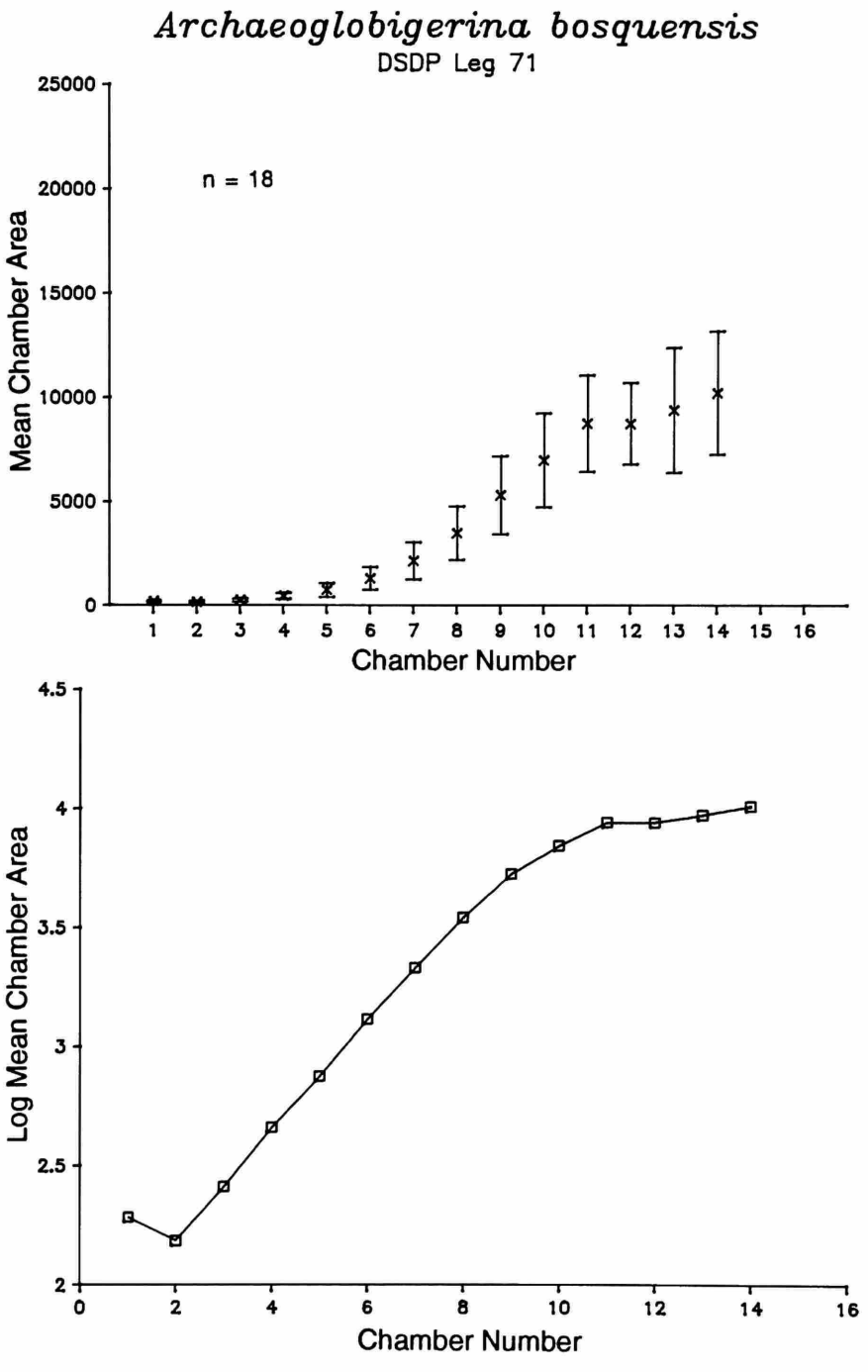

FIGURE 27.—Arithmetic and logarithmic plots of the chamber-by-chamber increase in cross-sectional chamber area (in μm^2) of *Archaeoglobigerina bosquensis*. The arithmetic plots show one standard deviation about the mean and the logarithmic plots show only the mean values. The number (n) of specimens analyzed is also shown.

the warmer surface water temperatures prevalent during the Santonian may account for the larger values.

The Gulf Coast holotype and paratype of *A. bosquensis* are not nearly as well preserved as the Falkland Plateau specimens as their tests are completely infilled with cement. The Site 511 forms differ from the primary type specimens by having a higher coiling axis and more tightly coiled chambers. The greater range of morphologic variability exhibited by the Falkland Plateau specimens may be related to their habitation in a more seasonally variable high latitude environment.

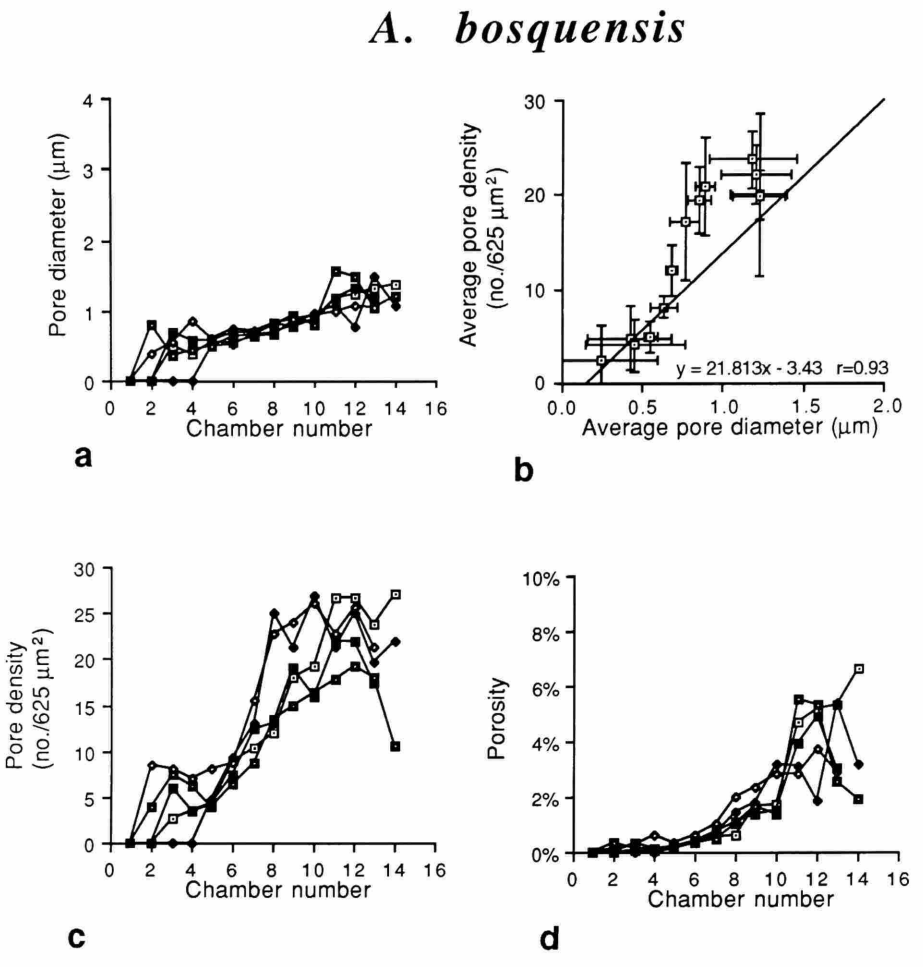

FIGURE 28.—Ontogenetic changes in *a*, pore diameter; *c*, pore density; and *d*, porosity, measured from five adult specimens of *Archaeoglobigerina bosquensis*. *b*, is a linear regression curve calculated from the mean values of pore diameter and pore density of all measured chambers of *A. bosquensis* with bars representing one standard deviation above and below the mean values. A least squares regression line is also shown.

TABLE 12.—Pore diameter, pore density, and porosity data, including averages, standard deviations, and maximum and minimum values, determined for each chamber within five serially dissected specimens of *Archaeoglobigerina bosquensis*.

Ch. No.	DIAMETER AVG	STD	MAX	MIN	DENSITY AVG	STD	MAX	MIN	POROSITY AVG	STD	MAX	MIN
1	0.00	0.00	0.00	0.00	0.00	0.00	0.00	0.00	0.00%	0.00%	0.00%	0.00%
2	0.24	0.36	0.80	0.00	2.50	3.77	8.50	0.00	0.10%	0.15%	0.32%	0.00%
3	0.42	0.26	0.68	0.00	4.86	3.45	8.15	0.00	0.17%	0.15%	0.35%	0.00%
4	0.45	0.31	0.86	0.00	4.06	2.75	7.00	0.00	0.20%	0.26%	0.65%	0.00%
5	0.55	0.04	0.60	0.51	5.04	1.67	8.00	4.00	0.20%	0.10%	0.37%	0.13%
6	0.63	0.09	0.75	0.53	8.14	1.18	9.30	6.40	0.41%	0.12%	0.61%	0.33%
7	0.68	0.04	0.73	0.64	12.02	2.63	15.60	8.70	0.70%	0.22%	1.03%	0.47%
8	0.76	0.09	0.84	0.65	17.20	6.15	25.00	11.90	1.25%	0.51%	2.00%	0.64%
9	0.85	0.07	0.94	0.76	19.46	3.45	24.00	14.90	1.76%	0.37%	2.37%	1.39%
10	0.89	0.06	0.97	0.81	20.88	5.19	26.80	16.00	2.14%	0.83%	3.18%	1.36%
11	1.20	0.22	1.58	1.00	22.12	3.18	26.70	17.80	4.02%	1.13%	5.55%	2.84%
12	1.18	0.27	1.48	0.76	23.72	3.02	26.70	19.30	4.17%	1.46%	5.29%	1.83%
13	1.22	0.18	1.48	1.05	20.00	2.62	23.80	17.40	3.83%	1.38%	5.37%	2.52%
14	1.22	0.16	1.39	1.07	19.90	8.55	27.20	10.50	3.90%	2.43%	6.61%	1.92%

Archaeoglobigerina cretacea (d'Orbigny, 1840)

PLATE 8: FIGURES 1–8

Globigerina cretacea d'Orbigny, 1840:34, pl. 3: figs. 12–14.—Banner and Blow, 1960:8–10, pl. 7: fig. 1a–c.

Archaeoglobigerina cretacea (d'Orbigny).—Pessagno, 1967:317, pl. 70: figs. 3–8, pl. 94: figs. 4, 5.—Robaszynsky et al., 1984:278, pl. 47: figs 3–6, pl. 48: fig. 2.

Globotruncana cretacea (d'Orbigny).—Krasheninnikov and Basov, 1983:806, pl. 8: figs. 13–15.

OBSERVATIONS OF THE TEST EXTERIOR.—The test is coiled in a low trochospire, forming a moderately lobate, subcircular equatorial outline. The subrounded axial periphery bears an imperforate band which is frequently bordered on the last several chambers by two weakly developed and broadly spaced keels formed from parallel alignment and coalescence of surface rugosities. The mean test diameter of adult specimens is 356 μm, the maximum is 468 μm, the mean breadth is 167 μm, and the mean breadth/diameter ratio is 0.47 (Table 4). The umbilicus is moderately broad and shallow, comprising an average of 29% of the maximum test diameter. Adult tests have from 2.5 to 3 whorls with 13 to 17 total number of chambers and final whorl chambers ranging from 4.50 to 5.75 and averaging 5.16 (Table 4). The penultimate/antepenultimate chamber size ratio averages 1.11 and ranges from 0.92 to 1.28. Nearly all specimens are dextrally coiled and about one-third have kummerform final chambers. The aperture of adult specimens is wholly umbilical and is bordered by a narrow porticus, but tegilla have not been observed on any of the Falkland Plateau specimens. Relict portical flaps occur in the umbilical margin. The wall is medioperforate and the surface is covered with randomly situated, fine to medium-sized pustules, except for the final one or two chambers which are nearly smooth.

OBSERVATIONS OF THE TEST INTERIOR.—*Initial Whorl:* The proloculus and initial whorl diameters of *A. cretacea* are the largest of the species studied. Proloculus diameters range from 16.2 to 23.4 μm, averaging 19.8 μm, and initial whorl diameters range from 77.1 to 115.2 μm, averaging 92.2 μm (Figures 9–11, Table 5). Linear regression of proloculus and initial whorl diameter plots results in a relatively low correlation coefficient. Initial whorl chambers number from 4.00 to 5.00 chambers, with an mean of 4.57. Throughout the initial whorl, chamber morphology is globular, apertural position is extraumbilical, the axial periphery is imperforate, and surface ornamentation is finely hispid.

Penultimate Whorl: The number of chambers in the penultimate whorl averages 5.00, slightly less than in the ultimate whorl, and ranges from 4.50 to 5.75 (Table 4). Morphologic changes that occur in the penultimate whorl include movement of the aperture to an umbilical-extraumbilical position and increasing axial compression of the chambers, leading to a reniform cross-sectional morphology. The axial periphery is imperforate throughout the penultimate whorl, and it occasionally bears concentrations of enlarged rugosities on the axial periphery

Ontogenetic Growth Curves: Plots of mean cross-sectional chamber areas show a log-linear increase in chamber size until about the ninth to tenth chamber, where the rate of chamber size increase begins to gradually diminish (Figure 29). Variability in chamber size strongly increases between the eleventh and twelfth chambers. The mean growth trajectory of *A. cretacea* is surpassed in size only by *R. rugosa* after the fourteenth chamber (Figure 26).

Porosity: Pores generally appear by the third chamber, but single pores were observed in the proloculus and deuteroconch in a few specimens. By the fifth or sixth chamber, pores have spread outward from the inner spiral suture of the chambers (Figure 30*a,c*), but the axial periphery remains poreless throughout the ontogeny (Figure 30*b*). Adult chambers have cylindrically shaped pores that are bordered by a narrow funnel-shaped opening (Figure 7*c*). Pore diameters change very little, averaging about 0.80–0.92 μm between the third and seventh chambers, then increase to a maximum of 1.70–1.90 μm in the following chambers (Figure 31, Table 13). Pore densities show a greater ontogenetic change, increasing from an average of 5.30–7.80 pores/625 μm^2 in the initial whorl to a maximum of 15.75–23.50 pores/625 μm^2 in the penultimate and ultimate whorls. The mean pore diameters and pore densities show a strong positive correlation. Porosity steadily increases to an average of 4.5%–6.0% in the final whorl chambers with maximum values of 6.7%–8.7%.

GENERAL REMARKS.—Because of wide disagreement in the concept of *A. cretacea* d'Orbigny, Banner and Blow (1960) conducted an extensive study of d'Orbigny's type material stored at the National Museum of Natural History in Paris. They found one vial containing six specimens from the Saint Germain Basin and selected the best preserved of these as the lectotype of *Globigerina cretacea* d'Orbigny. Although d'Orbigny's (1840) illustrated syntype shows a rounded, unkeeled axial periphery, Banner and Blow observed weak, broadly spaced double keels on d'Orbigny's specimens, and suggested that these features were overlooked by d'Orbigny because his optical equipment did not provide adequate optical resolution. Banner and Blow further noted that a fragile tegillum is preserved on several of the d'Orbigny syntypes, but not on the lectotype. Based on these observations, Banner and Blow removed *A. cretacea* from *Globigerina* and placed it in *Globotruncana.*

Pessagno (1967) subsequently removed *A. cretacea* from *Globotruncana* and placed it instead in his new genus *Archaeoglobigerina* because of (1) the lack of strongly developed keels, (2) the presence of strongly depressed rather than raised, beaded sutures, (3) the lack of a truncate or angled periphery, and (4) the spherical to ovoid chamber shape. He also stated that *Archaeoglobigerina blowi* Pessagno, the type species of *Archaeoglobigerina*, is the ancestral species of *A.*

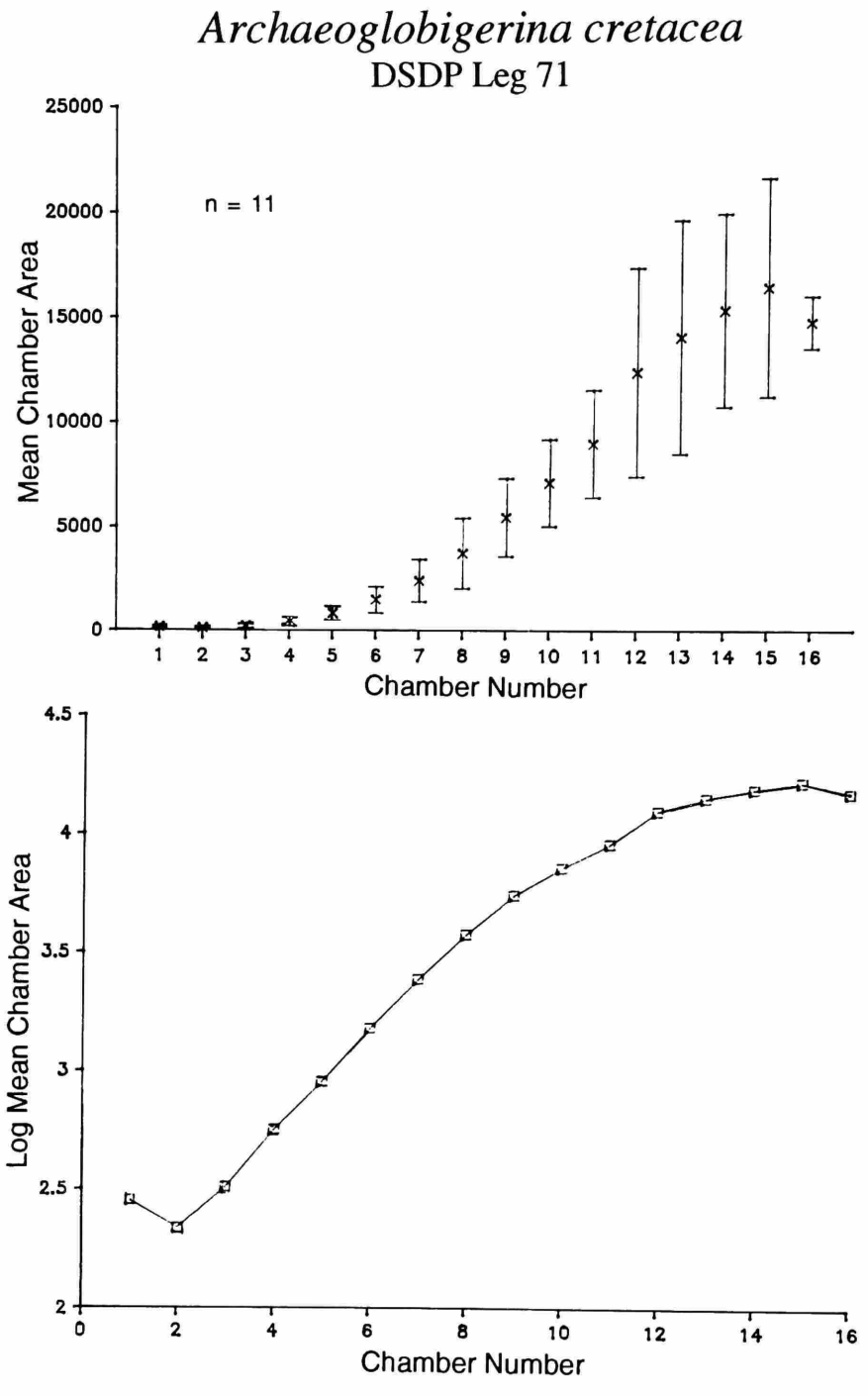

FIGURE 29—Arithmetic and logarithmic plots of the chamber-by-chamber increase in cross-sectional chamber area (in μm^2) of *Archaeoglobigerina cretacea*. The arithmetic plots show one standard deviation about the mean and the logarithmic plots show only the mean values. The number (n) of specimens analyzed is also shown.

cretacea, and forms that are transitional between these two species are common.

Opinions of succeeding authors on the generic designation of *A. cretacea* have varied. Those preferring to include *A. cretacea* in *Globotruncana* place major emphasis on the presence of an imperforate peripheral band and faint double keels (Hanzlíková, 1972; Masters, 1977; Krasheninnikov and Basov, 1983). Others (e.g., McNeil and Caldwell, 1981; Robaszynski

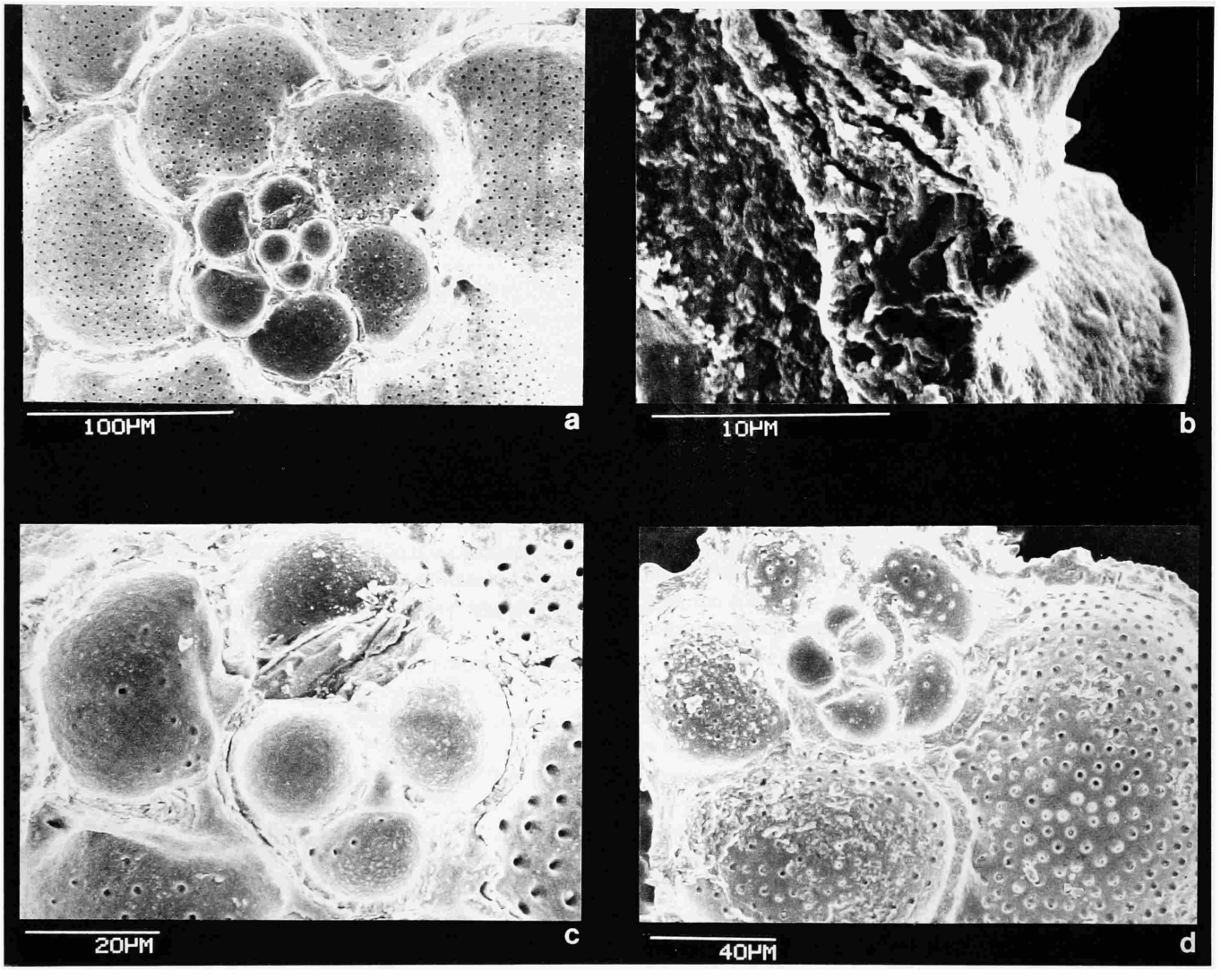

FIGURE 30.—Ontogenetic patterns of pore distribution on the ventral chamber surfaces of *a,c, Archaeoglobigerina cretacea* and *d, Rugoglobigerina rugosa*. Note that pores are absent from the proloculi and are initially concentrated along the spiral sutures in both species. *b*, is a cross-sectional view of the poreless peripheral margin of the twelfth chamber of *A. cretacea*. See Figure 16 for comparison with other species.

et al., 1984; Caron, 1985) place greater significance in the absence of an angulotruncate periphery and beaded sutures.

Serial dissection of Falkland Plateau specimens of *A. cretacea* reveals that the ontogenetic morphology is distinctive from other species assigned to *Archaeoglobigerina*. Significant differences include: (1) larger mean proloculus and initial whorl diameters; (2) more reniform penultimate and ultimate whorl chamber morphologies; (3) the presence of an imperforate axial periphery throughout ontogeny; (4) greater axial compression of the test; and (5) the presence of rugosities that become aligned and fused in double rows on the equatorial periphery. Unfortunately, topotypes of *A. blowi* are too poorly preserved and infilled with sediment or cement for detailed ontogenetic biometric comparison with the Falkland Plateau specimens of *A. cretacea*. But the presence of an imperforate peripheral band and tegilla on both of these species suggests they are closely related, whereas *A. bosquensis, A. australis*, and *A. mateola* lack these features and were probably derived separately. Until further investigation reveals otherwise, *Whiteinella* is considered to be the common ancestor to all of these species (Figure 18).

Archaeoglobigerina mateola Huber, 1990

PLATE 9: FIGURES 1–16

Rugoglobigerina? sp. 2.—Huber, 1988a:207, figs. 31.12, 31.15, 31.16.

Archaeoglobigerina mateola Huber, 1990:505, pl. 3: figs. 8–10, pl. 4: figs. 1–3, pl. 6: fig. 6; 1991a:292, pl. 2: figs. 2, 3; 1991b:461, pl. 1: figs. 12, 13.

A. cretacea

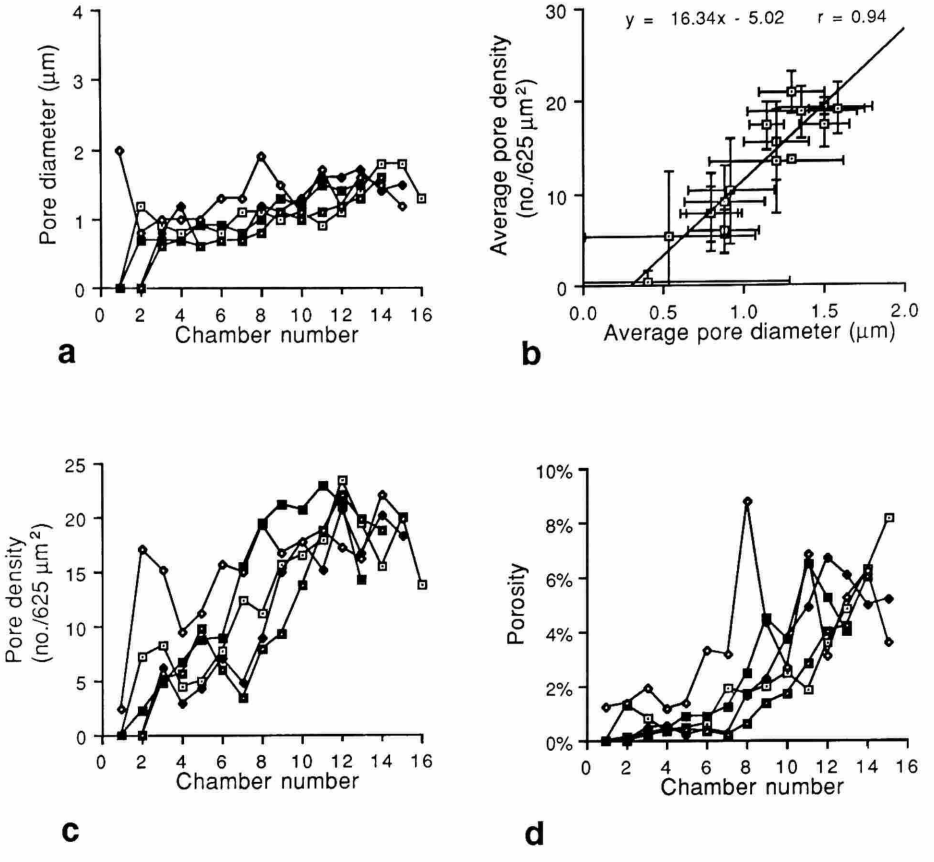

FIGURE 31.—Ontogenetic changes in *a*, pore diameter; *c*, pore density; and *d*, porosity, measured from five neanic specimens of *Archaeoglobigerina cretacea*. *b*, is a linear regression curve calculated from the mean values of pore diameter and pore density of all measured chambers of *A. cretacea* with bars representing one standard deviation above and below the mean values. A least squares regression line is also shown.

TABLE 13.—Pore diameter, pore density, and porosity data, including averages, standard deviations, and maximum and minimum values, determined for each chamber within five serially dissected specimens of *Archaeoglobigerina cretacea*.

Ch. No.	DIAMETER AVG	STD	MAX	MIN	DENSITY AVG	STD	MAX	MIN	POROSITY AVG	STD	MAX	MIN
1	0.40	0.89	2.00	0.00	0.50	1.12	2.50	0.00	0.25%	0.56%	1.26%	0.00%
2	0.54	0.53	1.20	0.00	5.30	7.18	17.00	0.00	0.56%	0.71%	1.37%	0.00%
3	0.80	0.16	1.00	0.60	7.95	4.30	15.25	4.75	0.76%	0.69%	1.92%	0.24%
4	0.88	0.22	1.20	0.70	5.90	2.45	9.50	3.00	0.57%	0.35%	1.19%	0.35%
5	0.80	0.19	1.00	0.60	7.80	3.04	11.25	4.25	0.69%	0.48%	1.41%	0.19%
6	0.88	0.25	1.30	0.70	9.10	3.88	15.75	6.00	1.14%	1.25%	3.34%	0.37%
7	0.92	0.27	1.30	0.70	10.25	5.72	15.50	3.50	1.37%	1.23%	3.19%	0.22%
8	1.20	0.42	1.90	0.80	13.40	5.58	19.50	8.00	3.03%	3.25%	8.73%	0.64%
9	1.20	0.20	1.50	1.00	15.60	4.30	21.25	9.25	2.91%	1.43%	4.51%	1.41%
10	1.14	0.11	1.30	1.00	17.30	2.53	20.75	13.75	2.89%	0.87%	3.77%	1.73%
11	1.36	0.34	1.70	0.90	18.75	2.78	23.00	15.25	4.58%	2.20%	6.81%	1.83%
12	1.30	0.20	1.60	1.10	20.95	2.31	23.50	17.25	4.52%	1.44%	6.68%	3.12%
13	1.50	0.16	1.70	1.30	17.30	2.32	19.75	14.25	4.87%	0.83%	6.08%	4.03%
14	1.58	0.17	1.80	1.40	19.13	2.76	22.00	18.75	5.89%	0.61%	6.31%	4.99%
15	1.50	0.30	1.80	1.20	19.33	0.95	20.00	18.25	5.63%	2.32%	8.14%	3.57%
16	1.30		1.30	1.30	13.75		13.75	13.75				

OBSERVATIONS OF THE TEST EXTERIOR.—The test is coiled in a moderate to high spire, equally to inequally biconvex with the spiral side often more convex than umbilical side. The axial periphery is broadly rounded and the equatorial periphery is often quadrate and moderately to strongly lobate. The average maximum diameter of adult specimens is 270 μm, whereas the largest specimen is 415 μm in diameter. With the test breadth averaging 186 μm, the average breadth/diameter ratio of 0.69 is the highest of the species measured in this study (Table 4). The umbilicus is generally small and deep, comprising an average of 19% of the total test diameter. The total number of chambers in adult tests generally ranges from 11 to 14, with a maximum of 16 observed, and the final whorl is comprised of between 3.00 and 5.50 chambers with an average of 4.23. A diminished rate of final whorl chamber size increase is demonstrated by the average penultimate/antepenultimate chamber size ratio of 0.99, which is lower than the other species analyzed. Kummerform morphotypes dominate at 80% of the studied population, and 78% are dextrally coiled. The aperture is umbilical in position, but is usually obscured by a broad porticus or a bullate extension of the final chamber. The wall is medioperforate and the test surface is distinctly ornamented with large, randomly situated pustules or elongate "pseudospines" that differ from true foraminiferal spines by lacking a hollow base.

OBSERVATIONS OF THE TEST INTERIOR.—*Initial Whorl:* Proloculus diameters show a bimodal size distribution (Plate 8: Figures 13, 14), with most ranging from 13 to 17 μm and two that are between 27 and 28 μm (Figures 9–11, Table 5). Although these size differences may be interpreted as representing alternating asexual (microspheric) and sexual (megalospheric) modes of reproduction, measurement of additional specimens is warranted since only 13 were successfully dissected. Because of the considerable variation in proloculus sizes, there is also an large range of initial whorl diameters, with most between 50–83 μm and two between 113–117 μm. The initial whorl chamber number averages 4.48 and ranges from 4.00 to 5.00.

Penultimate Whorl: An average of 4.43 chambers occur in the penultimate whorl (Table 4). Surface ornament on those chambers includes fine to medium pustules, and the apertural position is umbilical-extraumbilical.

Ontogenetic Growth Curves: The growth curves of *A. mateola* are the most irregular of the species studied. Most specimens show a moderate rate of size increase until about the eighth to tenth chamber, then a decreasing rate in the final two to four chambers, where the rates of some specimens become negative (Figure 32).

Porosity: Calcite overgrowth is apparent in most of the dissected specimens of *A. mateola* causing an underestimation of shell porosity. No pores were observed in the first three chambers and very few occur near the spiral suture of the sixth to seventh chamber, where the pores become more evenly scattered through the remaining ontogenetic sequence (Figure 16*f*). A narrow funnel-shaped depression borders the cylindrical pores on the interior of adult chambers (Figure 7*b*). The pore diameters are generally less than 1 μm except for a few specimens that reached up to the medioperforate range of 1.19 μm in the final whorl chambers. Pore density is generally less than 10 pores/625 μm^2 until about the tenth or eleventh chamber, then increases to a maximum of 15–25 pores/625 μm^2 whorl chambers (Figure 33). Pore diameters and pore density show a high positive correlation throughout the ontogenetic series. Shell porosity shows a large increase from an average of 0.67% in the ninth chamber to 1.25% in the tenth chamber and reaches a maximum of 2.00%–2.75% (Table 14).

GENERAL REMARKS.—The compact chamber arrangement, relatively high coiling axis, occurrence of a kummerform or bullate final chamber, and presence of coarse pustules that may be raised to form pseudospines together distinguish most specimens of *A. mateola* from other species included in *Archaeoglobigerina*. Similarity in the initial and penultimate whorl morphologies of most specimens of *A. mateola* to those of *A. australis* and *A. bosquensis* testifies to their close phylogenetic relationship (Figure 18).

Other spinosopapillate species that occur in Maastrichtian sediments include *Helvetiella atlantica* Longoria and Gamper, *Helvetiella helvetia* Longoria and Gamper, and *Bucherina sandidgei* Brönnimann and Brown (Longoria and Gamper, 1984). *Bucherina sandidgei* differs from *A. mateola* by having (1) a well-developed spiral system of tegilla, (2) a truncate axial periphery, (3) flattened dorsal chambers, and (4) a dorsal keel. The primary feature that distinguishes *A. mateola* from *Helvetiella* spp. is the absence of a spiral system of tegilla. Absence of tegilla from *A. mateola* cannot be a factor of poor preservation as not one has been observed of the hundreds of well-preserved specimens that have been studied.

The oldest occurrence of *A. mateola* is uncertain, as this species was found in the oldest (latest Campanian) sediments recovered at ODP Site 690, but was not found at the Falkland Plateau (see Huber, 1990). It's absence from pre-Maastrichtian sediments of Leg 114 Hole 700C may be an artifact of poor preservation of the Campanian sediments (Huber, 1991a). Nevertheless, the first appearance of *A. mateola* considerably predates that of *B. sandidgei, H. atlantica*, and *H. helvetia*, which have not been reported from sediments older than late Maastrichtian.

Several authors have demonstrated wide intraspecific variability in proloculus diameters among modern populations of *Globigerinoides* (Brummer et al., 1987) and several other living planktonic foraminiferal species (Huang, 1981; Sverdlove and Bé, 1985; Brummer et al., 1987). However, only broadly unimodal size distributions have been recognized, suggesting that alternation of sexual (microspheric) and asexual (megalospheric) generations does not occur among the planktonic foraminifera. In fact, Brummer et al. (1987) proposed that the terms megalospheric and microspheric may

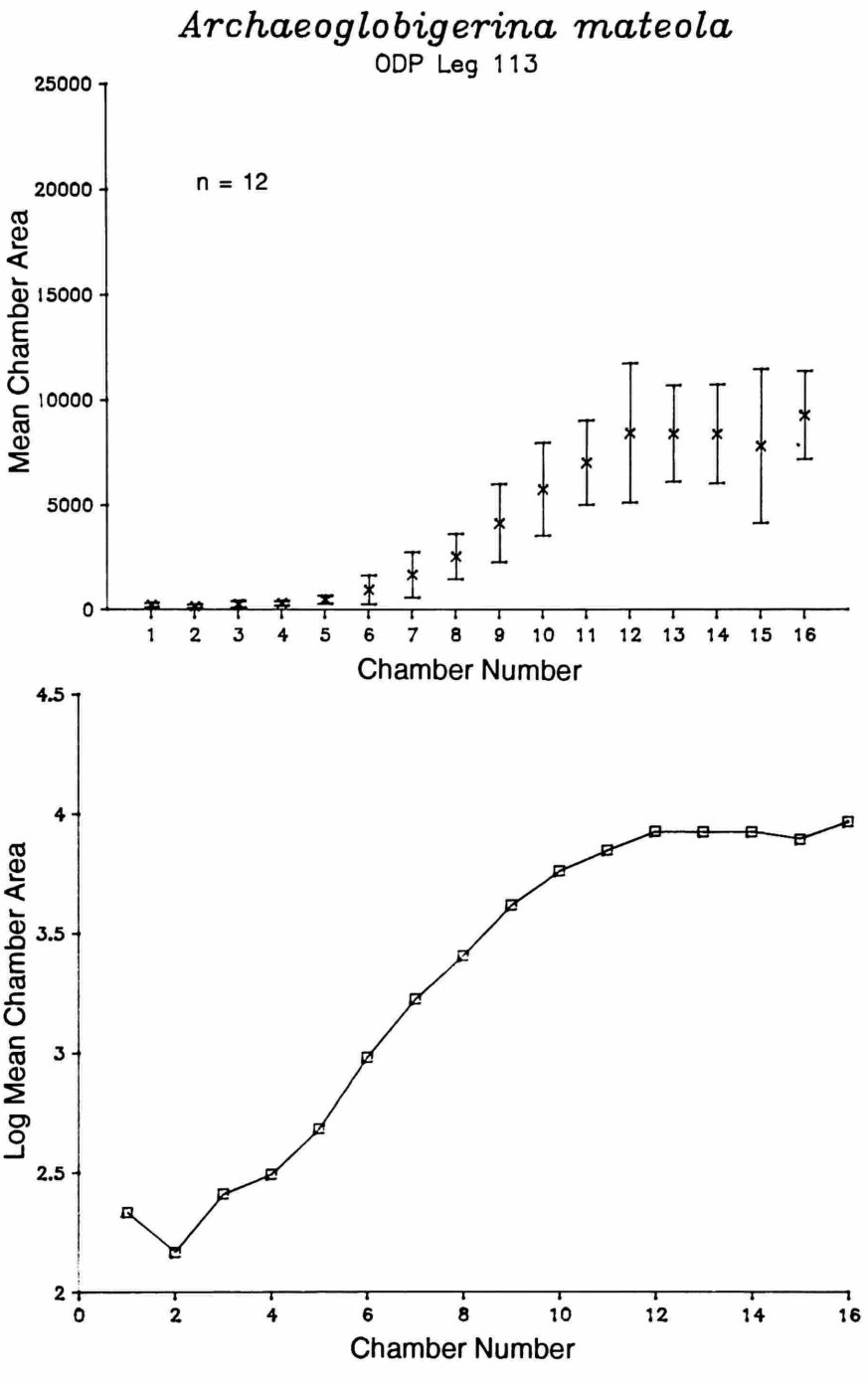

FIGURE 32.—Arithmetic and logarithmic plots of the chamber-by-chamber increase in cross-sectional chamber area (in μm^2) of *Archaeoglobigerina mateola*. The arithmetic plots show one standard deviation about the mean and the logarithmic plots show only the mean values. The number (n) of specimens analyzed is also shown.

not be applicable to globigerinid species. A predominant or exclusive sexual reproductive mode was suggested by Brummer et al. (1987), based on prolocular measurements and the fact that asexual reproductive modes have never been observed in laboratory cultures of planktonic foraminifera. The absence of mean proloculus diameter values between the two clusters in *A. mateola* (Figure 6; see also Plate 8: Figures 13–15) may suggest alternation of generations in the life cycle of this species, but serial dissections of more specimens are needed to verify this bimodal distribution.

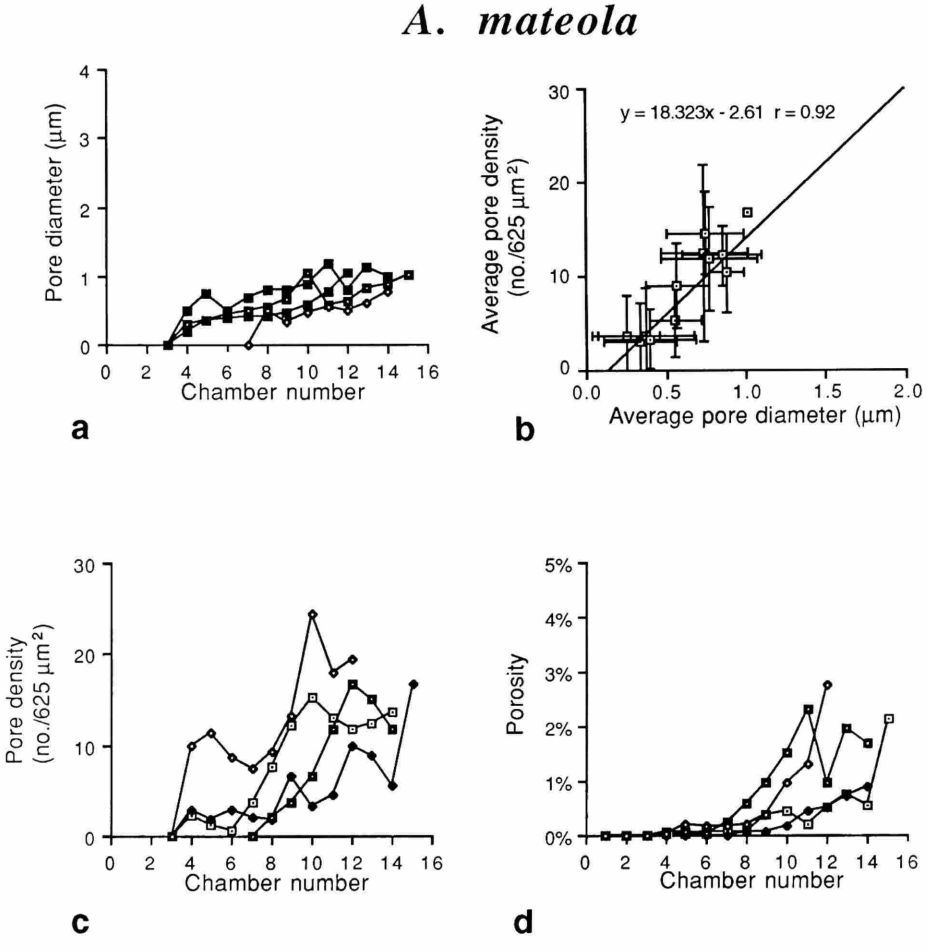

FIGURE 33.—Ontogenetic changes in *a*, pore diameter; *c*, pore density; and *d*, porosity, measured from five adult specimens of *Archaeoglobigerina mateola*. *b*, is a linear regression curve calculated from the mean values of pore diameter and pore density of all measured chambers of *A. mateola* with bars representing one standard deviation above and below the mean values. A least squares regression line is also shown.

TABLE 14.—Pore diameter, pore density, and porosity data, including averages, standard deviations, and maximum and minimum values, determined for each chamber within five serially dissected specimens of *Archaeoglobigerina mateola*.

Ch. No.	DIAMETER AVG	STD	MAX	MIN	DENSITY AVG	STD	MAX	MIN	POROSITY AVG	STD	MAX	MIN
1	0.00	0.00	0.00	0.00	0.00	0.00	0.00	0.00	0.00%	0.00%	0.00%	0.00%
2	0.00	0.00	0.00	0.00	0.00	0.00	0.00	0.00	0.00%	0.00%	0.00%	0.00%
3	0.00	0.00	0.00	0.00	0.00	0.00	0.00	0.00	0.00%	0.00%	0.00%	0.00%
4	0.25	0.21	0.49	0.00	3.77	4.28	9.90	0.00	0.05%	0.02%	0.07%	0.00%
5	0.37	0.30	0.74	0.00	3.58	5.20	11.30	0.00	0.14%	0.08%	0.19%	0.00%
6	0.34	0.23	0.49	0.00	3.10	3.95	8.70	0.00	0.10%	0.11%	0.17%	0.00%
7	0.40	0.29	0.69	0.00	3.33	3.13	7.40	0.00	0.19%	0.04%	0.23%	0.00%
8	0.56	0.16	0.79	0.41	5.23	3.84	9.30	1.90	0.40%	0.29%	0.60%	0.06%
9	0.57	0.20	0.79	0.34	8.93	4.54	13.20	3.70	0.67%	0.40%	0.95%	0.06%
10	0.74	0.27	1.05	0.47	12.45	9.46	24.40	3.30	1.25%	0.38%	1.52%	0.18%
11	0.77	0.30	1.19	0.55	11.80	5.54	17.90	4.50	1.81%	0.71%	2.32%	0.19%
12	0.75	0.24	1.06	0.49	14.53	4.39	19.50	10.00	1.86%	1.25%	2.75%	0.51%
13	0.85	0.25	1.12	0.62	12.20	3.16	15.20	8.90	1.97%		1.97%	0.72%
14	0.88	0.11	1.00	0.78	10.33	4.20	13.60	5.60	1.69%		1.69%	0.54%
15	1.01		1.01	1.01	16.70		16.70	16.70			2.14%	2.14%

Genus *Rugoglobigerina* Brönnimann, 1952

TYPE SPECIES.—*Globigerina rugosa* Plummer, 1927.

DESCRIPTION.—Test is a flat to high trochospire, biconvex, outline strongly lobate and ovate to subcircular, axial periphery moderately to broadly rounded. Chambers increase gradually to rapidly in size, strongly inflated, globular to reniform in shape, and may be slightly compressed in the axial direction. Aperture interiomarginal, umbilical, bordered by a thick lip, and covered by a tegillum in adult specimens. Wall is medium to coarsely perforate, surface covered by coarse pustules usually coalescing to form costellae that are meridionally aligned.

REMARKS.—At the initiation of this study, it was hoped that serial dissection of high latitude morphotypes considered as rugoglobigerinids because of the presence of faint meridionally aligned costellae and tegilla (e.g., Plate 5: Figures 1–4, Plate 9: Figures 9–15) would reveal distinctive ontogenetic features associating them with serially dissected topotypes of *Rugoglobigerina*. The dissections, however, reveal ontogenetic morphologies that more strongly resemble the interior morphologies of *A. australis*. Unfortunately, resolution of the taxonomic uncertainties among this group was not achieved in this study.

Rugoglobigerina rugosa (Plummer, 1927)

PLATE 10: FIGURES 1–15

Globigerina rugosa Plummer, 1927:38, pl. 2: fig. 10.

Rugoglobigerina rugosa (Plummer).—Smith and Pessagno, 1973:58–60, pl. 25: figs. 1–4.—Webb, 1973:552, pl. 3: figs. 3–8.—Huber, 1991b:461, pl. 1: fig. 17.

Rugoglobigerina macrocephala macrocephala Brönnimann, 1952:25–27, text-fig. 9, pl. 2: figs. 1–3.

Rugoglobigerina macrocephala ornata Brönnimann, 1952:27, text-fig. 10, pl. 2: figs. 4–6.

Rugoglobigerina macrocephala Smith and Pessagno, 1973:55-56, pl. 23: figs. 1–3, 7–10.

OBSERVATIONS OF THE TEST EXTERIOR.—The test of *R. rugosa* is coiled in a low to medium trochospire, with a somewhat flattened spiral side and a strongly lobate equatorial outline, and a broadly rounded, non-keeled axial periphery. Adult tests analyzed in this study reach a maximum diameter of 410 μm, have an average diameter of 256 μm, a mean breadth of 164 μm, and a mean breadth/diameter ratio of 0.64 (Table 4). The umbilicus is moderately narrow and deep, comprising an average of 21% and a range of 9% to 30% of the maximum test diameter. Adult tests have from 12 to 16 chambers arranged in 2–2.5 whorls, with final whorl chambers numbering from 3.75 to 5.25 and averaging 4.43. The penultimate/antepenultimate ratio of 1.29 is the highest of the adult species analyzed. Nearly all species studied show dextral coiling and no kummerform specimens were found. The apertural position is wholly umbilical, and it is covered by an imperforate tegillum (Plate 10: Figure 7). The wall is generally medioperforate, but may be macroperforate in the final whorl chambers, and the surface is ornamented with coarse costellae that form a meridional pattern that radiates from the equatorial center of each chamber.

OBSERVATIONS OF THE TEST INTERIOR.—*Initial Whorl:* Proloculus diameters range from 10.9 to 18.5 μm and average 15.3 μm, and initial whorl diameters range from 57.4 to 78.2 μm and average 62.7 μm (Figures 9–11, Table 5). The initial whorl is comprised of an average of 4.75 chambers, a minimum 4.50 chambers and a maximum of 5.00 chambers. The coefficient of correlation of proloculus and initial whorl diameters is 0.73 (Figure 9). Most chambers following the proloculus are slightly compressed in the axial direction, giving a reniform appearance in cross-section (Plate 10: Figures 6, 13–15). The apertural position is extraumbilical throughout the initial whorl.

Penultimate Whorl: A greater mean number of chambers (5.31) occurs in the penultimate whorl than in the final whorl (Table 4). Apertural position changes from extraumbilical in the early part of the penultimate whorl to umbilical in the later chambers, and surface ornamentation coarsens from hispid to coarsely pustulose or costellate by the last penultimate whorl chamber.

Ontogenetic Growth Curves: The rate of chamber size increase is log-linear throughout most of the ontogeny of *R. rugosa*, and dimishes only slightly in the final whorl (Figure 34). The final chambers of this species attain the largest size of all the species examined, reaching over 25,000 μm^2 in some specimens.

Porosity: Rugoglobigerina rugosa attains the highest porosity of the species studied. Pores are absent or few in number in the initial whorl (Figure 30*d*), then are concentrated near the inner spiral suture until about the seventh chamber, where they become more evenly scattered. They are cylindrical in cross-section and are bordered by a narrow funnel-shaped depression on the interior wall of adult chambers (Figure 7*d*). Pore diameters are 1 μm or less until the seventh to eighth chamber, where they steadily increase to a maximum of 2.70 μm (Figure 35). Pore densities are generally less than 8 prior to the sixth to seventh chamber, then increase to a maximum of 12 to 20 (Table 15). Accordingly, porosities remain low (<1%) until about the sixth to eighth chamber, then rapidly increase to values >5%, reaching a maximum of 10%–23% in some specimens. High latitude forms of this species should be studied to determine whether the large porosity values are invariable between contrasting surface water habitats or if they are to some degree controlled by the ambient environment.

GENERAL REMARKS.—The topotypes of *R. rugosa* selected for dissection and illustrated on Plate 10 are very characteristic of this species; their chambers have a rapid rate of inflation and are slightly compressed in the axial direction, meridionally aligned costellae ornament the surface of final whorl chambers, and their umbilici are covered by tegilla. One of the reasons *R. rugosa* is included in this biometric study is that it is the type species of the genus *Rugoglobigerina* Brönnimann (1952).

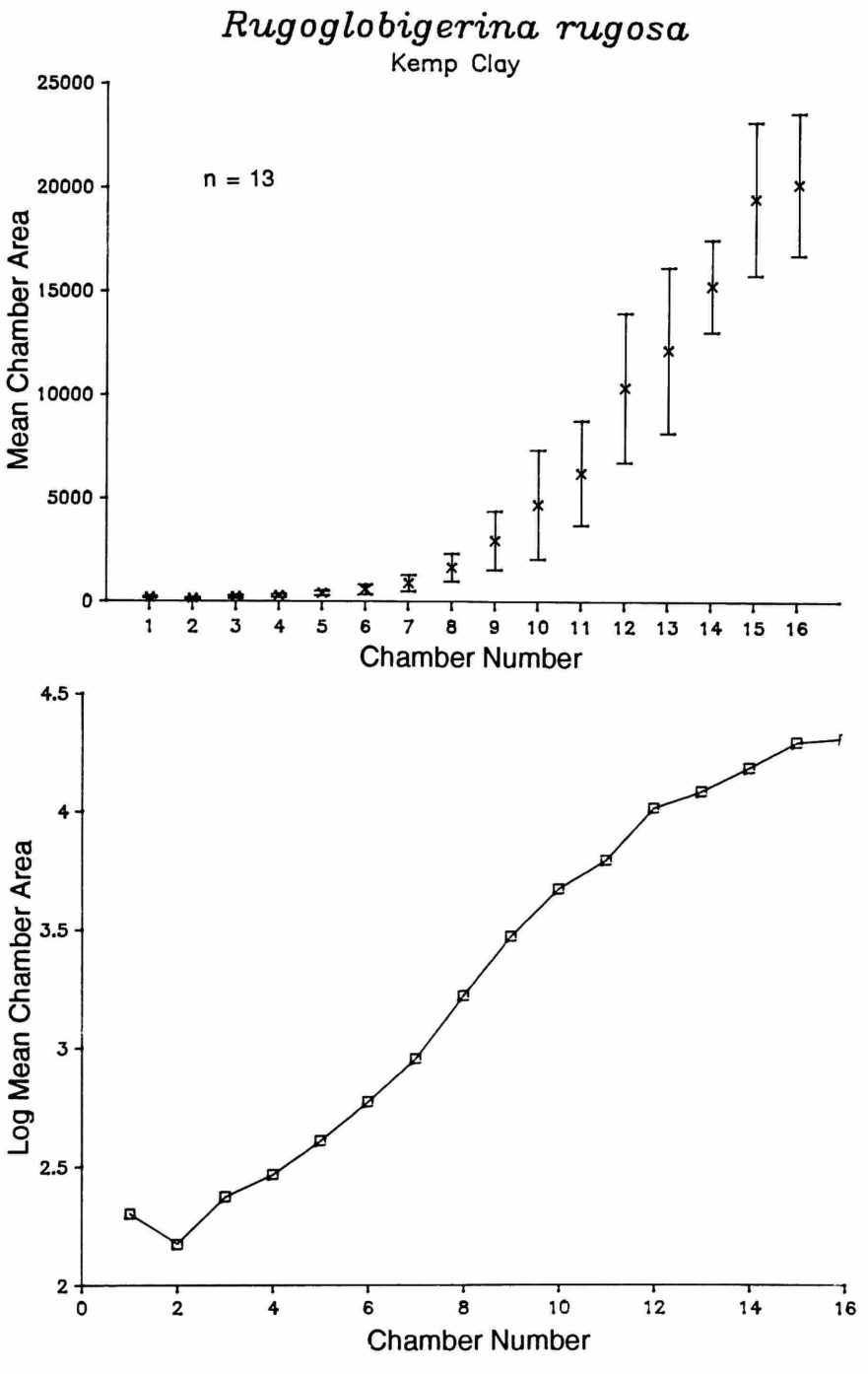

FIGURE 34.—Arithmetic and logarithmic plots of the chamber-by-chamber increase in cross-sectional chamber area (in μm^2) of *Rugoglobigerina rugosa*. The arithmetic plots show one standard deviation about the mean and the logarithmic plots show only the mean values. The number (n) of specimens analyzed is also shown.

Therefore, the obtained ontogenetic data provide additional criteria for comparison with *Costellagerina pilula*, which is the type species of the only other meridionally costellate genus of the Late Cretaceous (Tables 2, 3). Results demonstrate that the ontogenetic morphologies of these two species are distinctly different. *Rugoglobigerina rugosa* has (1) fewer chambers in the initial whorl, (2) a more rapid rate of chamber size increase (Figure 26), (3) a reniform rather than rounded cross-sectional chamber morphology, (4) an umbilically positioned aperture in the final whorl chambers, and (5) a tegillum covering the

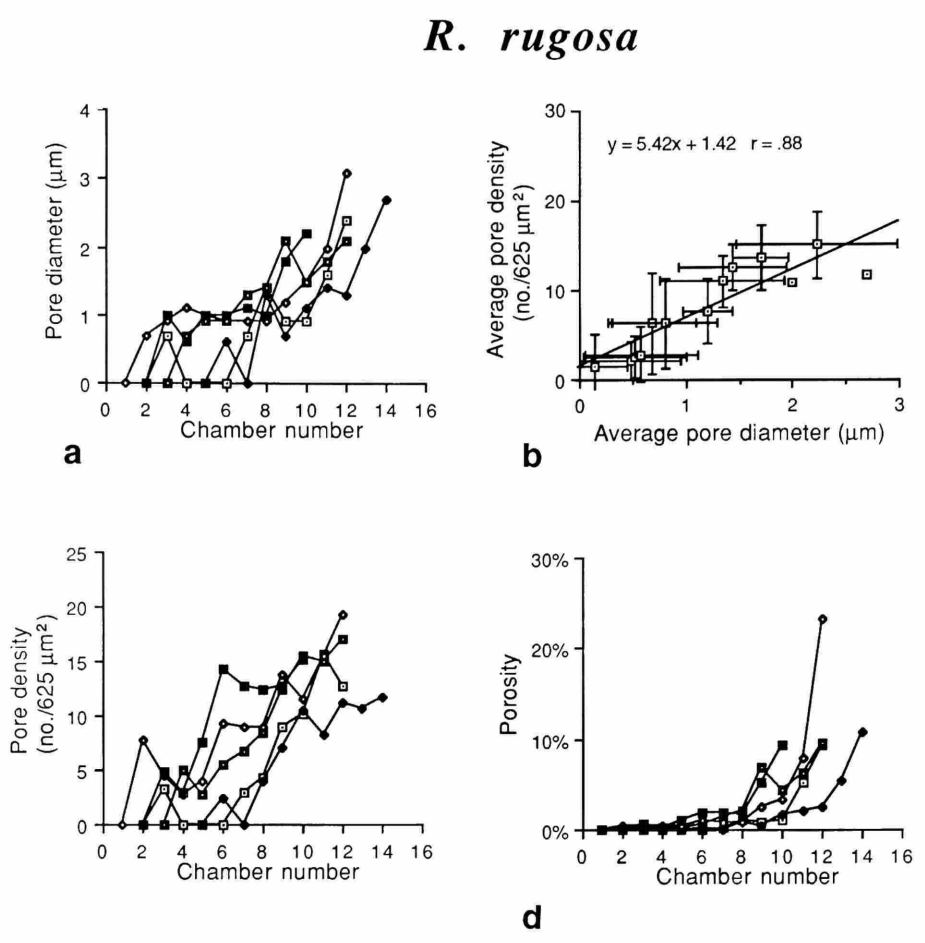

FIGURE 35.—Ontogenetic changes in *a*, pore diameter; *c*, pore density; and *d*, porosity, measured from five adult specimens of *Rugoglobigerina rugosa*. *b*, is a linear regression curve calculated from the mean values of pore diameter and pore density of all measured chambers of *R. rugosa* with bars representing one standard deviation above and below the mean values. A least squares regression line is also shown.

TABLE 15.—Pore diameter, pore density, and porosity data, including averages, standard deviations, and maximum and minimum values, determined for each chamber within five serially dissected specimens of *Rugoglobigerina rugosa*.

Ch. No.	DIAMETER AVG	STD	MAX	MIN	DENSITY AVG	STD	MAX	MIN	POROSITY AVG	STD	MAX	MIN
1	0.00	0.00	0.00	0.00	0.00	0.00	0.00	0.00	0.00%	0.00%	0.00%	0.00%
2	0.14	0.31	0.70	0.00	1.55	3.47	7.75	0.00	0.10%	0.21%	0.48%	0.00%
3	0.52	0.49	1.00	0.00	2.50	2.35	4.75	0.00	0.25%	0.27%	0.60%	0.00%
4	0.48	0.48	1.10	0.00	2.15	2.15	5.00	0.00	0.17%	0.19%	0.42%	0.00%
5	0.58	0.53	1.00	0.00	2.85	3.13	7.50	0.00	0.35%	0.40%	0.94%	0.00%
6	0.68	0.41	1.00	0.00	6.30	5.63	14.25	0.00	0.68%	0.72%	1.79%	0.00%
7	0.80	0.50	1.30	0.00	6.30	4.99	12.75	0.00	0.89%	0.82%	1.94%	0.00%
8	1.20	0.23	1.40	0.90	7.65	3.57	12.50	4.00	1.30%	0.53%	2.09%	0.85%
9	1.34	0.59	2.10	0.70	11.00	2.87	13.75	7.00	3.19%	2.79%	6.93%	0.43%
10	1.44	0.50	2.20	0.90	12.60	2.58	15.50	10.25	3.91%	3.28%	9.28%	1.04%
11	1.70	0.79	2.00	1.40	13.63	3.60	15.75	8.25	5.25%	2.42%	7.79%	2.03%
12	2.23	1.19	3.10	1.30	15.06	3.70	19.25	11.25	11.07%	8.75%	23.25%	2.39%
13	2.00		2.00	2.00	10.75		10.75	10.75	5.40%		5.40%	5.40%
14	2.70		2.70	2.70	11.75		11.75	11.75	10.76%		10.76%	10.76%

umbilical region. Hence, these species were probably not closely related (Figure 18).

The morphology of isolated "neanic" specimens of *R. rugosa* (Plate 10: Figures 1–3) can be identified within the larger shells of adult forms of this species (Plate 10: Figure 12). The surface ornamentation of the neanic forms consists of faint costellae or randomly situated pustules and the final whorl chambers increase quite rapidly in size, giving it a "big-headed" ("macrocephala") appearance. These pre-adult forms are essentially identical to specimens previously recognized as *Rugoglobigerina macrocephala* (see Brönnimann, 1952; Robaszynski et al., 1984:284, pl. 49: fig. 7a–c). These observations suggest that *R. macrocephala* is a pre-adult form of *R. rugosa* and, accordingly, *R. macrocephala* should be treated as a junior synonym.

Surface ornamentation is not only variable within the ontogeny of *R. rugosa*, but it also varies latitudinally. Tropical forms, such as the Kemp Clay specimens illustrated in this study, show a massive development of meridionally arranged costellae on adult chamber surfaces, but middle to high latitude forms are more weakly ornamented with randomly situated pustules and fewer costellae that show a meridional alignment (e.g., Berggren, 1962, pl. XI: figs. 1a–5b; Olsson, 1964, pl. 7: figs. 2–5; Webb, 1973, pl. 3: figs. 3–9; McNeil and Caldwell, 1981, pl. 2a–3c; Huber, 1991b, pl. 1: fig. 17). Hence, the surface water habitat exerted some control on the architectural features developed on the chamber surface. Temperature was presumably the most significant variable affecting the observed morphologic differences.

Ontogenetic Comparisons

Criteria used to distinguish transitions from one ontogenetic stage to another within the Cretaceous taxa in this study are based on qualitative observations, such as changes in apertural position, chamber surface ornamentation, width and depth of the umbilicus, and chamber morphology (Figure 9), and quantitative data, including abrupt changes in the rate of chamber size increase (Figure 36). An additional method for characterizing growth transitions is the measurement of ontogenetic changes in mean shell porosity (Figure 37). This is based on the premise that porosity, in combination with the surface area to biomass ratio, is directly related to metabolic activity or growth rates (Bijma, Faber and Hemleben, 1990). Shell porosity is also known to be positively correlated with temperature (Bé, 1968; Frerichs et al., 1972). Hence, ontogenetic changes in porosity are constrained by genetic inheritance, but may vary according to: (1) vertical and latitudinal differences in surface water temperature; (2) resource availability (e.g., light, food, oxygen, nutrients); (3) surface water convection; (4) seasonality; and (5) presence or absence of symbionts. Additional study of the same species from different environments will enable a more accurate portrayal of variance in chamber-by-chamber porosity values.

Unlike studies of shell porosity in modern species (e.g., Bé, 1968; Frerichs et al., 1972; Bé et al., 1973, 1976; Bijma, Faber, and Hemleben, 1990), pore densities and pore diameters of most of the Cretaceous species studied are positively correlated, with high correlation coefficients (>0.89) (Figures 20, 24, 25, 28, 31, 33, 35). Exceptions to this are the hedbergellids, which have poor or no correlation between pore diameters and pore density (Figures 12, 13, 17). In most specimens, the ontogenetic change in pore densities is greater than that of pore diameters. Only *R. rugosa* exhibits a relatively even magnitude of changes in these two variables (Figure 35). Pore densities and pore diameters generally show positive trends throughout ontogeny, although the values for ultimate and penultimate chambers may diminish.

Abrupt increases in shell porosity that occur within the first ten chambers of the averaged plots (Figure 37) are used to identify the transition from juvenile to neanic stages. Subsequent escalations to maximum values distinguish the onset of the adult stage. The chamber positions where the developmental transitions occur are compared with the chamber growth trajectories of five specimens per species to examine whether changes in growth rates occur at similar positions in the ontogeny (Figure 36). Ontogenetic stages are not recognized in species that do not show significant shifts in growth trajectories and/or porosity values.

Hedbergella holmdelensis, H. monmouthensis, and *H. sliteri*

These species exhibit such a remarkably uniform increase in chamber size that only the prolocular stage can be distinguished in the chamber area plots (Figures 12, 36). The surface texture of the hedbergellids also show no abrupt changes during ontogeny (Plate 2: Figures 6, 14, Plate 3: Figure 5). The inflection shown between the twelfth and thirteenth chambers on the mean logarithmic growth curve plot of *H. sliteri* (Figure 15) is not indicative of transition between developmental stages. Instead, it probably reflects a diminished size increase of terminal chambers that occur from one to four chambers after the twelfth chamber.

Pore distributions also show a very gradual dispersal from the spiral suture across the chamber wall (Figure 16*a*, Plate 2: Figures 7, 8, 15, 16). Porosity values, on the other hand, show a steady increase until about the eleventh to twelfth chamber, where maximum values are attained (Figures 13, 14, 17). Thus, a transition from the juvenile to adult stage is inferred between the tenth and twelfth chambers based only on the porosity data for *H. sliteri* (Figure 37*a*), whereas a neanic stage is not recognized.

Costellagerina pilula

The growth curves of *C. pilula* are quite uniform in some specimens, but slightly varying in others (Figure 36). The

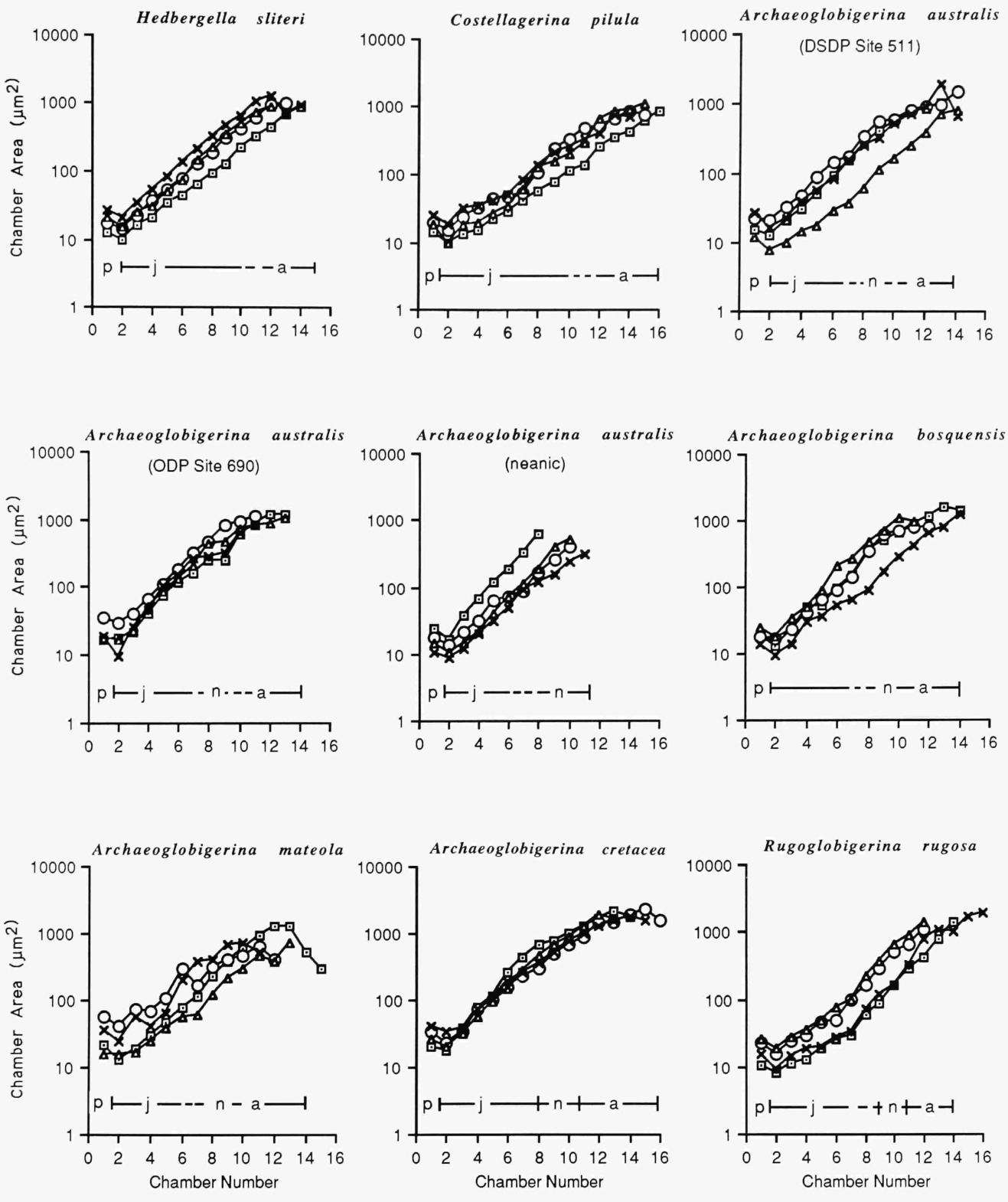

FIGURE 36.—Logarithmic plots of the ontogenetic changes in cross-sectional areas for four specimens of some of the species included in this study. Ontogenetic stages are inferred or determined for each species based on several criteria, including (1) inflections in the growth curves, (2) abrupt changes in shell porosity (see Figure 37), and (3) qualitative observations of serially dissected specimens. See text for further explanation.

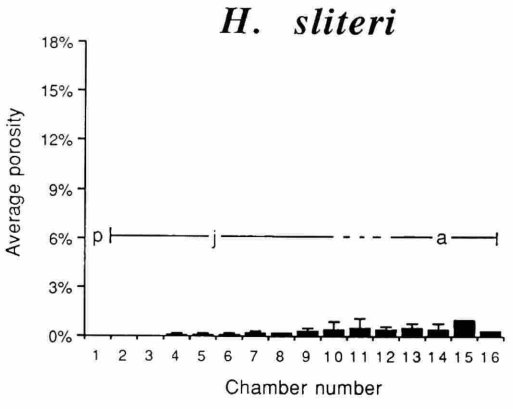
H. sliteri
Average porosity
18%
15%
12%
9%
6%
3%
0%
p
j
a
1 2 3 4 5 6 7 8 9 10 11 12 13 14 15 16
Chamber number

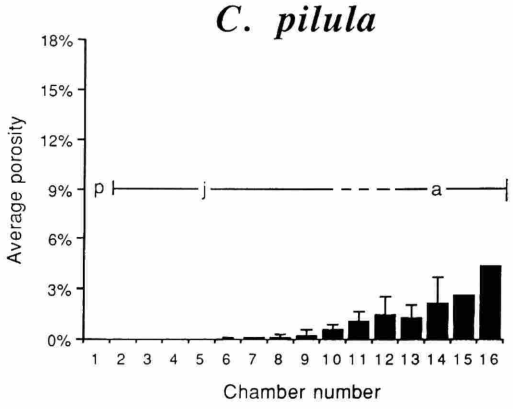
C. pilula
Average porosity
18%
15%
12%
9%
6%
3%
0%
p
j
a
1 2 3 4 5 6 7 8 9 10 11 12 13 14 15 16
Chamber number

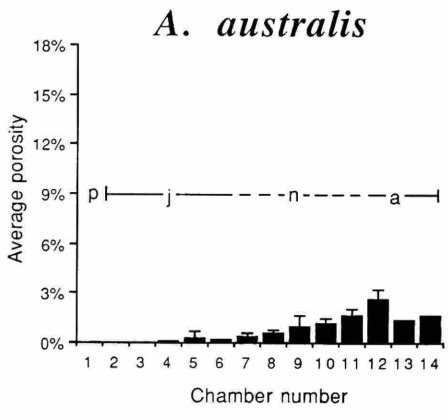
A. australis
Average porosity
18%
15%
12%
9%
6%
3%
0%
p
j
n
a
1 2 3 4 5 6 7 8 9 10 11 12 13 14
Chamber number

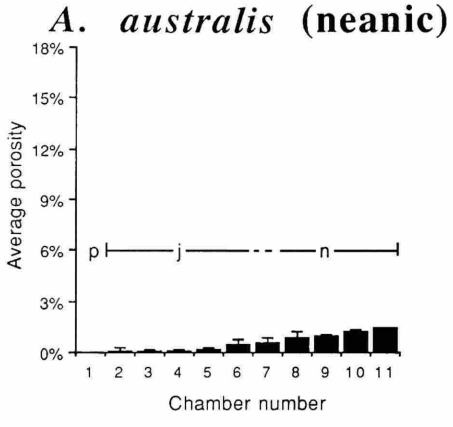
A. australis (neanic)
Average porosity
18%
15%
12%
9%
6%
3%
0%
p
j
n
1 2 3 4 5 6 7 8 9 10 11
Chamber number

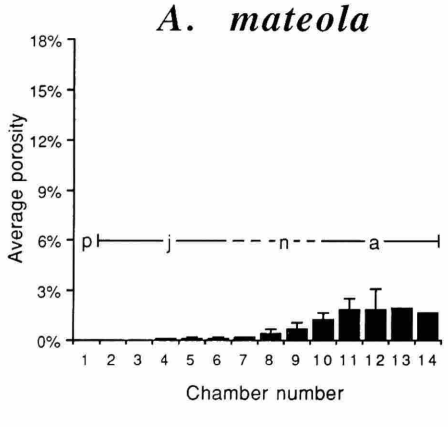
A. mateola
Average porosity
18%
15%
12%
9%
6%
3%
0%
p
j
n
a
1 2 3 4 5 6 7 8 9 10 11 12 13 14
Chamber number

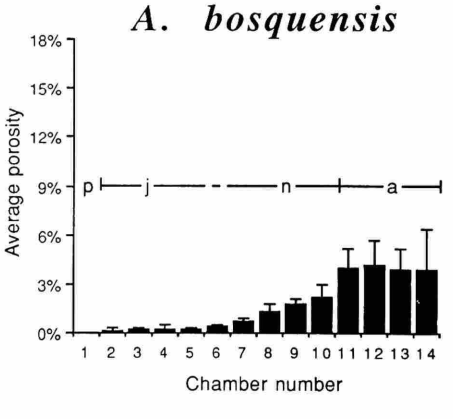
A. bosquensis
Average porosity
18%
15%
12%
9%
6%
3%
0%
p
j
n
a
1 2 3 4 5 6 7 8 9 10 11 12 13 14
Chamber number

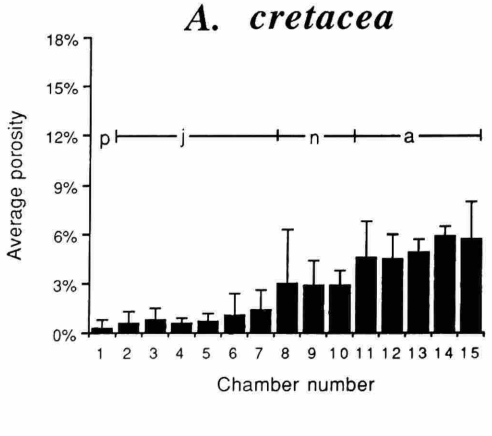
A. cretacea
Average porosity
18%
15%
12%
9%
6%
3%
0%
p
j
n
a
1 2 3 4 5 6 7 8 9 10 11 12 13 14 15
Chamber number

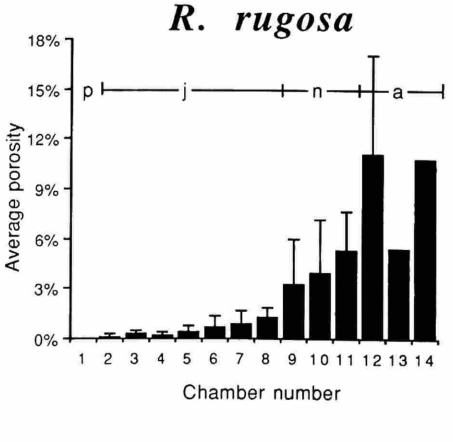
R. rugosa
Average porosity
18%
15%
12%
9%
6%
3%
0%
p
j
n
a
1 2 3 4 5 6 7 8 9 10 11 12 13 14
Chamber number

FIGURE 37 (facing page).—Ontogenetic changes in mean porosity for each chamber of five specimens of each species measured. Vertical bars represent one standard deviation from the mean values obtained for each chamber. See Figure 36 and text for explanation of how ontogenetic stages were identified.

averaged porosity plots also show a relatively uniform increase throughout ontogeny (Figure 37). The growth stages of this species can only be identified based on SEM observations of the test interior. The juvenile stage is recognized in a series of chambers that lack surface ornament and have a relatively open umbilicus (Plate 4: Figure 3). Neanic chambers are distinguished by development of a pustulose surface texture and tightening of the coil (Plate 4: Figure 8). The onset of the adult stage is identified by the appearance of meridionally aligned pustules on the chamber surface. This usually occurs after the tenth to eleventh chamber in specimens that are larger than 200 μm (Plate 4: Figures 2, 7, 11).

Archaeoglobigerina australis

Growth curves for *A. australis* from Site 511 both show a uniform escalation in chamber size up to the seventh to ninth chamber, where there is a rate increase (Figure 36). The subsequent curves do not show an inflection point that is consistent between specimens until the twelfth to thirteenth chamber. Porosity elevates significantly between the eight and ninth chambers in some specimens, due primarily to an increase in pore concentration (Figure 24), but other specimens show a quite regular increase throughout their ontogeny. Maximum values are attained by about the twelfth chamber (Figure 35).

Serial dissection of neanic and adult specimens of *A. australis* enables visual observation of the juvenile, neanic, and adult stages. Juvenile forms have a low coiling axis, a broad, shallow umbilicus, a nearly smooth surface texture, and apertures that are extraumbilical in position (Plate 6: Figures 17, 18). Chambers formed in the neanic stage, beginning at the seventh to ninth chamber, are more tightly coiled, have a more rapid size expansion, have umbilical to slightly extraumbilical apertures, and show development of a finely to moderately pustulose surface texture (Plate 5: Figure 10). Based on these observations, all of the specimens illustrated in Plate 6: Figures 1–10 are considered to be neanic morphotypes.

The adult stage appears by about the twelfth chamber and is characterized by having chambers that slowly increase in size, umbilically positioned apertures, a coarse surface ornament consisting of randomly arranged pustules, and the presence of a portical flap (Plate 5: Figures 5–7, 11, 12).

Archaeoglobigerina bosquensis

Most of the growth trajectories for *A. bosquensis* show an increase in growth rates between the seventh and ninth chambers, suggesting onset of the neanic stage (Figure 36). This is followed by a diminished rate of chamber size increase occurring at the tenth to twelfth chamber. The pore density curves show a similar trend, first with a large increase occurring between the seventh to ninth chamber and then reaching a maximum by the eleventh to twelfth chamber (Figure 28). The transition from the juvenile to neanic stage is not so obvious in the porosity plots (Figures 27, 36). Nevertheless, this developmental phase change is inferred between the seventh to eighth chamber. Maximum porosity is reached by the eleventh chamber, marking the beginning of the adult stage for most specimens.

Pre-adult growth stages of *A. bosquensis* that are revealed by serial dissection are very similar to those of *A. australis*. Juvenile chambers increase slowly in size and have little in the way of surface ornament, apertures that are positioned near the equatorial periphery, and a broad and shallow umbilicus (Figure 8*c,d*). Neanic chambers (Figure 8*e,f*; Plate 7: Figure 5) increase more rapidly in size, have a moderately pustulose surface texture, and umbilical-extraumbilical apertures. The adult stage is characterized by a slowed increase in chamber size, coarsely pustulose surface texture, an umbilically positioned aperture, and, frequently, a kummerform ultimate chamber (Figure 8*g,i*; Plate 7: Figures 1–3).

Archaeoglobigerina cretacea

There is no distinct change in the ontogenetic chamber area trajectories for *A. cretacea* until about the twelfth to thirteenth chamber, where the growth rate gradually diminishes (Figure 36). However, the averaged porosity plots (Figure 37) show significant porosity increases between the seventh and eighth chambers, marking the transition from juvenile to neanic stage, and the tenth and eleventh chambers, marking the transition from neanic to adult stage. Changes in pore distribution do not coincide with these growth stages, as an even scattering of pores is achieved on the ventral chamber wall by the sixth to seventh chamber (Figure 30*a,c*), before onset of the neanic stage.

Serially dissected specimens of *A. cretacea* reveal no abrupt changes in morphology with increasing ontogeny. Surface ornament is lacking in the early juvenile stage, but is characterized by an increasingly pustulose texture in later chambers (Plate 8: Figures 5, 6). Although the peripheral margin is imperforate throughout ontogeny, faint keels do not develop until late in the neanic stage, and are generally present until the penultimate chamber of adult specimens (Plate 8: Figures 1, 2). The neanic stage is characterized by having a more globular chamber morphology and a smaller umbilical area than in the juvenile and adult stages, but these differences are transitional.

Archaeoglobigerina mateola

The growth curves for *A. mateola* are much more erratic than those of the other species. One specimen plot shows a uniform

log-linear size increase up to the twelfth chamber, while another shows a steady size increase to about the seventh chamber, then a more rapid chamber size increase, until the twelfth chamber which is follow by a size decrease, whereas two others show several chamber size increases and decreases during their developmental history (Figure 36). Interestingly, the seventh chamber of one of the latter specimens is kummerform, suggesting that formation of this chamber type is not always associated with attainment of reproductive maturity.

The porosity plots show a much more uniform ontogenetic change than the growth curves (Figures 32, 36). Porosity increase is slow and uniform until about the eighth chamber, where the rate of increase becomes more rapid. This is inferred to be the transition from the juvenile to neanic stage. Maximum porosity is reached by about the eleventh to twelfth chamber, marking the onset of the adult stage.

Pre-adult chambers gradually increase in surface ornament density from nearly smooth-walled juveniles (Plate 9: Figure 12), to moderately pustulose neanic forms (Plate 9: Figure 15), to coarsely pustulose, kummerform adults (Plate 9: Figures 10, 11).

Rugoglobigerina rugosa

Transition from the juvenile to neanic stage of *R. rugosa* shows up as an abrupt chamber size increase between the seventh and ninth chambers (Figure 36). However, only one specimen shows a diminished growth rate that could be interpreted as the onset of the adult stage. This occurs between the twelfth and thirteenth chambers. The other ontogenetic curves have quite uniform rates of chamber size increase after onset of the neanic stage.

The averaged porosity data indicate a sudden porosity increase between the eighth and ninth chambers followed by another between the eleventh and twelfth chambers (Figure 37). These denote the transition from juvenile to neanic and neanic to adult stages, respectively. Plots of pore diameters, pore density, and porosity from individual specimens of *R. rugosa* indicate that the chamber at which these transitions occur (Figure 35) may vary by one or two chambers above or below the growth stage boundaries determined from the averaged plots.

Pores are evenly distributed by the end of the juvenile stage in most of the studied specimens, and show no difference in distribution during transition from the neanic to adult stage (Figure 30*d*).

The growth stages are easily differentiated in serially dissected specimens based on changes in surface ornamentation and chamber arrangement. Juvenile morphotypes are generally unornamented and gradually increase in size (Plate 10: Figures 5, 12). Neanic morphotypes have an increasingly pustulose surface texture with a faint meridional alignment in the later chambers, a rapid rate of chamber size increase, and are more tightly coiled than juvenile or adult morphotypes (Plate 10: Figures 1–3, 5, 12). Adult morphotypes bear meridionally aligned costellae on the chamber surfaces and a broad, deep umbilicus covered by a tegillum (Plate 10: Figures 8–10). It is not clear from serial dissection as to what stage the tegillum first appears, but this feature has not been observed on isolated specimens smaller than 200 μm.

Summary and Conclusions

Previous studies of planktonic foraminifera from upper Campanian–Maastrichtian sequences in the circum-antarctic region (e.g., Webb, 1973; Sliter, 1977; Krasheninnikov and Basov, 1983) have identified a combined total of six non-keeled trochospiral species. Of these, two were included in the genus *Hedbergella*, four were placed in the genus *Rugoglobigerina*, and all were assigned pre-existing names of species recorded from low to middle latitude sites. Subsequent examination of coeval foraminifera from the Antarctic Peninsula (Huber, 1988a) and deep-sea sites in the region of the Southern Ocean (Huber, 1990, 1991a, b) revealed that (1) the morphologies of the high-latitude "rugoglobigerine" taxa intergrade and are highly variable, (2) most of the previously illustrated trochospiral morphotypes from the circum-antarctic region were assigned incorrect species names, (3) three of the four "rugoglobigerine" morphotypes could be lumped into the new species *Archaeoglobigerina australis*, (4) one of the previously identified "ruglobigerine" and one of the hedbergellid morphotypes belong to the new species *Archaeoglobigerina mateola* and *Hedbergella sliteri*. Currently, a total of seven non-keeled trochospiral species belonging to *Hedbergella* (*H. holmdelensis, H. monmouthensis, H. sliteri*), *Archaeoglobigerina* (*A. australis, A. mateola*), and *Rugoglobigerina* (*R. pennyi, R. rugosa*) are considered as valid among southern high latitude assemblages of late Campanian–Maastrichtian age.

The present study was initiated in an effort to resolve taxonomic uncertainties and clarify phyletic relationships among the Late Cretaceous trochospiral taxa. One major goal was to compare the new high latitude species assigned to *Archaeoglobigerina* with topotypes of *Rugoglobigerina* and *Costellagerina* to establish their proper generic designation. Clearly, a conventional taxonomic approach based on observations from adult shells had led to the previous confusion, so a comprehensive analysis of ontogenetic morphometry was deemed necessary to obtain additional criteria for species comparisons. Two methods were employed to acquire these ontogenetic data. Whereas the x-radiograph approach is the simplest, fastest, and least expensive of the two methods, resolution of initial whorl chamber morphologies could only be obtained from the most evolute trochospiral taxa. Another limitation of this method is that it cannot provide information on ontogenetic changes in apertural position and chamber surface ornamentation. Nonetheless, information accurately and efficiently obtained from the microradiographs includes (1) penultimate whorl chamber number, (2) ultimate whorl

chamber number, (3) kummerform frequency, (4) penultimate/antepenultimate chamber size ratio, and (5) umbilicus/test diameter ratio.

The best technique for characterizing planktonic foraminiferal ontogenies requires whorl-by-whorl dissections of the foraminiferal shells and an SEM micrograph record of each whorl dissection. Although tedious and time-consuming, this approach provides an accurate three-dimensional record of changes in chamber shape, size and ornamentation, coiling arrangement, and apertural position throughout the developmental history of the foraminiferal shell. Biometric data obtained using this approach include (1) proloculus diameter, (2) initial whorl diameters, (3) number of chambers in the initial whorl, (4) rate of increase in cross-sectional chamber area, (5) total number of chambers in the test, and (6) chamber-by-chamber measurements of pore density, pore diameter, and shell porosity.

Comparisons of developmental morphologies were made for five species that inhabited the Austral Realm during the Late Cretaceous. These include Maastrichtian specimens of *H. sliteri, A. australis*, and *A. mateola* and Santonian specimens of *Archaeoglobigerina bosquensis* Pessagno and *Archaeoglobigerina cretacea* (d'Orbigny). Topotypes of *H. holmdelensis, H. monmouthensis* (both of Maastrichtian age), *Costellagerina pilula* Belford (Santonian age), and *Rugoglobigerina rugosa* Plummer (Maastrichtian age) were also analyzed.

Results indicate that there is a great deal of size and shape variability of test interior morphocharacters among the species populations, and no single character can be used to unequivocally discriminate between the different taxa. This variability was probably caused by differences in the ambient physicochemical environment from the initial formation of each prolocular chamber throughout the subsequent growth histories of individual specimens. Nevertheless, comparison of population means and standard deviations can have important taxonomic value for discriminating between some homeomorphic taxa and inferring ancestor-descendant relationships. This was demonstrated by contrasting the initial and penultimate whorl morphologies of *Costellagerina pilula* with *A. australis* and *R. rugosa*. Although *A. australis* had previously been identified as *Rugoglobigerina pilula* (= *C. pilula*), serial dissection revealed that the latter species has a greater number of chambers in the initial and penultimate whorls and a much more gradual rate of chamber size increase than *A. australis*. These features similarly distinguish *C. pilula* from the *R. rugosa* topotypes, with the additional observation that the chamber morphology of *R. rugosa* is reniform throughout ontogeny, whereas *C. pilula* chambers are more spherical.

Serial dissection of *A. australis, A. mateola*, and *A. bosquensis* revealed nearly identical developmental morphologies, demonstrating their close phylogenetic relationship. Differences in coiling pattern and surface ornamentation only become apparent in the final whorl chambers of adult specimens. Exceptions to this include two specimens of *A. mateola* which have distinctly enlarged proloculi compared to the other archaeoglobigerinids. Based on the observed similarities and biostratigraphic study of southern high-latitude sites, it is concluded that *A. australis* descended directly from *A. bosquensis* sometime during the Campanian and *A. mateola* descended from *A. australis* during earliest Maastrichtian time.

Because *A. cretacea* has previously been assigned to *Archaeoglobigerina*, specimens were analyzed in this study to evaluate similarity in growth morphology to *A. australis, A. bosquensis*, and *A. mateola*. Plots of proloculus and initial whorl diameters and observations of ontogenetic changes in chamber shape and ornamentation reveal that the latter species are distinctly different from *A. cretacea*, and therefore may not be congeneric. However, without comparative data from the type species of *Archaeoglobigerina, A. blowi*, any revision to the taxonomy and phylogeny of this group would be based more on conjecture than morphologic criteria.

Another important problem that has not been resolved in this study is the taxonomic status of high latitude forms that have faint meridional alignment of costellae and umbilical cover plates, as occurs in *Rugoglobigerina*, but ontogenetic morphologies that are identical to *A. australis*. Are these forms convergent from an ancestral *A. australis* stock, independently evolving the rugoglobigerinid features on adult chambers, or convergent from an ancestral rugoglobigerinid species, retaining its ancestral adult features but developing a juvenile morphology similar to *A. australis*? A more detailed study of these intermediate morphotypes is needed to resolve this question.

Ontogenetic changes in pore diameter, pore density, and porosity were measured for all studied species. This approach was used (1) to characterize the intraspecific variability of these parameters, (2) determine their value for discriminating between species groups, and (3) depict changes that occur in these parameters with increasing ontogeny. Results indicate that pore diameters are less variable and generally show a more conservative increase with increasing chamber number than pore density. Contrary to studies of modern planktonic foraminifera, pore diameter and pore density are positively correlated in nearly all species studied, and correlation coefficients for most species are 0.89 or higher. Pore distributions are similar in the early ontogeny of all species, with pores absent from the proloculus, absent or rare in the initial whorl, and initially concentrated near the spiral suture. The chamber number at which pores first appear or become evenly dispersed is quite variable within and between species. Most specimens show even pore distributions by the beginning of the penultimate whorl in adult specimens. Exceptions to this include *A. cretacea* and topotypes of *H. holmdelensis* and *H. monmouthensis*, which have a poreless peripheral margin throughout ontogeny.

All specimens of *H. holmdelensis, H. monmouthensis*, and *H. sliteri* have a microperforate wall texture throughout ontogeny, with pore diameters less than 1 μm, pore densities of

13 pores/625 μm^2, and porosities generally less than 1% and rarely up to 1.5%. Similar values for pore diameters and pore density were obtained for *A. australis, A. mateola,* and *C. pilula.* Porosities of these species generally range below 3%. *Archaeoglobigerina bosquensis* and *A. cretacea* both have up to 5%–9% porosity, and specimens of *R. rugosa* achieve up to 23% porosity. Pore measurements of these taxa from different paleoclimatic settings are needed to evaluate the influence of temperature or other envronmental factors on pore diameter, pore density, and porosity.

The shell pore analyses are also useful for characterizing transition from one developmental stage to another within individual specimens. In most cases, abrupt changes in the pore characters coincide with morphological changes. Interestingly, the changes in pore characters of *H. sliteri* and *C. pilula* are very uniform during growth, as is the rate of chamber size increase, such that juvenile, neanic, and adult growth stages all intergrade. These growth stages are easier to discern in the other species. The juvenile stage is characterized by a moderately slow and uniform increase in chamber size and shell porosity, an extraumbilical, nearly peripheral, position of the aperture, and smooth wall surface. Following the juvenile chambers are several chambers that increase rapidly in size and porosity. These are included in the neanic stage, and are also characterized by a more nearly umbilical positioning of the aperture, increase in surface ornament density and coarseness, and increase in height of the spiral axis. A faint expression of the ornamental pattern that characterize adult chambers (e.g., meridional costellae in *Rugoglobigerina* and *Costellagerina*) appears in the last one or two chambers of the neanic stage. Onset of the adult stage is typically characterized by attainment of maximum shell porosity, a diminishing rate of chamber size increase, occurrence of umbilical cover plates in some forms, maximum coarsening of surface ornament and, in *A. cretacea,* appearance of two weakly developed keels on the the axial periphery. Transitions from one growth stage to another may reflect change in metabolic activity and differences in food sources during the growth of individual specimens.

Serial dissection of *A. australis* enabled identification of pre-adult morphologies within the shells of adult specimens, and recognition of these same forms as isolated specimens that either died prematurely or grew under non-optimum environmental conditions. Because these neanic morphotypes have extraumbilical apertures, adherence to a conventional taxonomic scheme would suggest that these forms belong in the genus *Hedbergella* or *Globotruncanella.* This approach was used by previous authors studying the southern high latitude assemblages (Sliter, 1977; Krasheninnikov and Basov, 1983; Huber, 1988a). Perhaps the most important consequence of this study is the consolidation of a broad range of intergrading morphologies into *A. australis.* This is an significant step toward revision of taxonomic concepts among Late Cretaceous planktonic foraminiferal assemblages of the circum-Antarctic region.

Literature Cited

Adelseck, C.G., Jr., and W.H. Berger

1975. On the Dissolution of Planktonic Foraminifera and Associated Microfossils During Settling and on the Sea Floor. *In* W.V. Sliter, A.W.H. Bé, and W.H. Berger, Dissolution of Deep-sea Carbonates. *Cushman Foundation for Foraminiferal Research, Special Publication,* 13:70–81.

Anderson, O.R., and W.W. Faber, Jr.

1984. An Estimation of Calcium Carbonate Deposition Rate in a Planktonic Foraminiferal *Globigerinoides sacculifer* Using ^{45}Ca as a Tracer: A Recommended Procedure for Improved Accuracy. *Journal of Foraminiferal Research,* 14:303–308.

Arnold, A.J.

1982. Techniques for Biometric Analysis of Foraminifera. *Proceedings of the Third North American Paleontological Convention,* 1:13–15.

Banner, F.T.

1982. A Classification and Introduction to the Globigerinacea. *In* F.T. Banner and A.R. Lord, *Aspects of Micropaleontology (papers presented to Professor Tom Barnard),* pages 142–239. London: Allen and Unwin.

Banner, F.T., and W.H. Blow

1959. The Classification and Stratigraphical Distribution of the Globigerinaceae. *Palaeontology,* 2:1–27.

1960. Some Primary Types of Species Belonging to the Superfamily Globigerinaceae. *Contributions from the Cushman Foundation for Foraminiferal Research,* 11:1–41.

1967. The Origin, Evolution, and Taxonomy of the Foraminiferal Genus *Pulleniatina* (Cushman, 1927). *Micropaleontology,* 13:133–162.

Bé, A.W.H.

1968. Shell Porosity of Recent Planktonic Foraminifera as a Climatic Index. *Science,* 161:881–884.

Bé, A.W.H., J.K.B. Bishop, M.S. Sverdlove, and W.D. Gardner

1985. Standing Stock, Vertical Distribution, and Flux of Planktonic Foraminifera in the Panama Basin. *Marine Micropaleontology,* 9:307–333.

Bé, A.W.H., D.A Caron, and O.R. Anderson

1981. Effects of Feeding Frequency on Life Processes of the Planktonic Foraminiferal *Globigerinoides sacculifer* in Laboratory Culture. *Journal of the Marine Biological Association of the United Kingdom,* 61:257–277.

Bé, A.W.H., S.M. Harrison, W.E. Frerichs, and M.E. Heiman

1976. Variability in Test Porosity of *Orbulina universa* d'Orbigny at Two Indian Ocean Localities. *In* Y. Takayanagi and T. Saito, editors, *Progress in Micropalaeontology, Special Publication,* pages 1–9. New York: Micropaleontology Press, The American Museum of Natural History.

Bé, A.W.H., S.M. Harrison, and L. Lott

1973. *Orbulina universa* d'Orbigny in the Indian Ocean. *Micropaleontology,* 19(2):150–192.

Bé, A.W.H., C. Hemleben, O.R. Anderson, and M. Spindler

1979. Chamber Formation in Planktonic Foraminifera. *Micropaleontology,* 25(3):1–6.

Belford, D.J.

1960. Upper Cretaceous Foraminifera from the Toolonga Calcilutite and Gingin Chalk, Western Australia. *Bureau of Mineral Resources, Geology and Geophysics, Australia, Bulletin,* 57:1–198.

1983. Note on Costellate Planktonic Foraminifera, and the Generic Designation of Late Cretaceous Forms from Western Australia. *In* Palaeontological Papers 1983, *Bureau of Mineral Resources, Australia, Bulletin,* 217:1–9.

Berger, W.H.

1968. Planktonic Foraminifera: Selective Solution and Paleoclimatic Interpretation. *Deep-Sea Research,* 15:31–43.

1969. Planktonic Foraminifera: Basic Morphology and Ecologic Implications. *Journal of Paleontology,* 43:1369–1383.

1971a. Planktonic Foraminifera: Sediment Production in an Oceanic Front. *Journal of Foraminiferal Research,* 1:95–118.

1971b. Sedimentation of Planktonic Foraminifera. *Marine Geology,* 11: 325–358.

Berggren, W.A.

1962. Some Planktonic Foraminifer from the Maestrichtian and Type Danian Stages of Southern Scandinavia. *Stockholm Contributions in Geology,* 9:1–106.

Bijma, J., J. Erez, and C. Hemleben

1990. Lunar and Semi-lunar Reproductive Cycles in Some Spinose Planktonic Foraminifers. *Journal of Foraminiferal Research,* 20:117–127.

Bijma, J., W.W. Faber, Jr., and C. Hemleben

1990. Temperature and Salinity Limits for Growth and Survival of Some Planktonic Foraminifers in Laboratory Cultures. *Journal of Foraminiferal Research,* 20:95–116.

Blow, W.H.

1979. *The Cainozoic Globigerinida,* 3 volumes, 1413 pages. Leiden: E.J. Brill.

Bolli, H.M., A.R. Loeblich, Jr. and H. Tappan

1957. Planktonic Foraminiferal Families Hantkeninidae, Orbulinidae, Globorotaliidae, and Globotruncanidae. *United States National Museum Bulletin,* 215:3–50.

Brönnimann, P.

1952. Globigerinidae from the Upper Cretaceous (Cenomanian–Maestrichtian) of Trinidad, B. W. I. *Bulletin of American Paleontology,* 34(140):1–70.

Brönnimann, P., and N.K. Brown

1956. Taxonomy of the Globotruncanidae. *Eclogae Geologicae Helvetiae,* 48:503–562.

1958. *Hedbergella,* a New Name for a Cretaceous Planktonic Foraminiferal Genus. *Journal of the Washington Academy of Sciences,* 48:15–17.

Brummer, G.-J.A.

1988. Comparative Ontogeny of Modern Microperforate Planktonic Foraminifers. *In* G.-J.A. Brummer and D. Kroon, *Planktonic Foraminifers as Tracers of Ocean-climate History,* pages 77–129. Amsterdam: Free University.

Brummer, G.-J.A., C. Hemleben, and M. Spindler

1986. Planktonic Foraminiferal Ontogeny and New Perspectives for Micropaleontology. *Nature,* 319:50–52.

1987. Ontogeny of Extant Spinose Planktonic Foraminifera (Globigerinidae): A Concept Exemplified by *Globigerinoides sacculifer* (Brady) and *G. ruber* (d'Orbigny). *Marine Micropaleontology,* 12:357-381.

Caron, D.A., A.W.H. Bé, and O.R. Anderson

1981. Effects of Variations in Light Intensity on Life Processes of the Planktonic Foraminiferal *Globigerinoides sacculifer* in Laboratory Culture. *Journal of the Marine Biological Association of the United Kingdom,* 62:435–451.

Caron, M.

1985. Cretaceous Planktonic Foraminifera. *In* H.M. Bolli, J.B. Saunders, and K. Perch-Neilsen, editors, *Plankton Stratigraphy,* pages 17–86. Cambridge:Cambridge University Press.

Cifelli, R.
1961. *Globigerina incompta*, a New Species of Pelagic Foraminifera from the North Atlantic. *Contributions from the Cushman Foundation for Foraminiferal Research*, 12:83–86.
1973. Observations on *Globigerina pachyderma* (Ehrenberg) and *Globigerina incompta* Cifelli from the North Atlantic. *Contributions from the Cushman Foundation for Foraminiferal Research*, 3:157–166.

Frerichs, W.E., M.E. Heiman, L.E. Borgman, and A.W.H. Bé
1972. Latitudinal Variations in Planktonic Foraminiferal Test Porosity, Part 1: Optical Studies. *Journal of Foraminiferal Research*, 2(1):6–13.

Gandolfi, R.
1942. Ricerche micropaleontologiche e stratigraphfiche sulla Scaglia e sul flysch Cretacici dei Dintorni di Balerna (Canton Ticino). *Rivista Italiana Paleontologia*, 48:1–160.

Hanzlíková, E.
1972. Carpathian Upper Cretaceous Foraminiferida of Moravia (Turonian-Maestrichtian). *Rozpravy Ustredniho ústavu geologického*, 39: 1–160.

Hecht, A.D., E.V. Eslinger, and L.B. Garmon
1975. Experimental Studies on the Dissolution of Planktonic Foraminifera. *In* W.V. Sliter, A.W.H. Bé, and W.H. Berger, Dissolution of Deep-sea Carbonates. *Cushman Foundation for Foraminiferal Research, Special Publication*, 13:56–69.

Hecht, A.D., and S.M. Savin
1970. Oxygen-18 Studies of Recent Planktonic Foraminifera: Comparison of Phenotypes and of Test Parts. *Science*, 170:69–71.
1971. Oxygen-18 Studies of Recent Planktonic Foraminifera: Reply to Bé and Van Donk. *Science*, 173:167–169.
1972. Phenotypic Variation and Oxygen Isotope Ratios in Recent Planktonic Foraminifera. *Journal of Foraminiferal Research*, 2: 55–67.

Hemleben, C., and M. Spindler
1983. Recent Advances in Research on Living Planktonic Foraminifera. *Utrecht Micropaleontological Bulletin*, 30:141–170.

Hemleben, C., M. Spindler, and O.R. Anderson
1988. *Modern Planktonic Foraminifera*. 363 pages. New York:Springer Verlag.

Hemleben, C., M. Spindler, I. Breitinger, and W.G. Deuser
1985. Field and Laboratory Studies on the Ontogeny and Ecology of Some Globorotaliid Species from the Sargasso Sea Off Bermuda. *Journal of Foraminiferal Research*, 15:254–272.

Hemleben, C., M. Spindler, I. Breitinger, and R. Ott
1987. Morphological and Physiological Responses of *Globigerinoides sacculifer* (Brady) Under Varying Laboratory Conditions. *Marine Micropaleontology*, 12:305–324.

Huang, C.
1981. Observations on the Interior of Some Late Neogene Planktonic Foraminifera. *Journal of Foraminiferal Research*, 11:173–190.

Huber, B.T.
1987. Ontogenetic Morphometrics of Some Upper Cretaceous Foraminifera from the Southern High Latitudes. *Antarctic Journal of the United States*, 22(5):15–17.
1988a. Upper Campanian–Paleocene Foraminifera from the James Ross Island Region (Antarctic Peninsula). *In* R.M. Feldmann, and M.O. Woodburne, editors, Geology and Paleontology of Seymour Island, Antarctica. *Geological Society of America, Memoirs*, 169:163–252.
1988b. Campanian–Maastrichtian Foraminifera of the High Southern Latitudes: Ontogenetic Morphometrics, Biostratigraphy, and Biogeography. 329 pages. Doctoral dissertation, The Ohio State University, Columbus, Ohio.
1990. Maestrichtian Planktonic Foraminiferal Biostratigraphy of the Maud Rise (Weddell Sea, Antarctica): ODP Leg 113 Holes 689B and 690C. *In* P.F. Barker, J.P. Kennett, et al., *Proceedings of the Ocean Drilling Program, Scientific Results*, 113:489–513. College Station, Texas: Ocean Drilling Program.
1991a. Planktonic Foraminifer Biostratigraphy of Campanian–Maestrichtian Sediments from Sites 698 and 700, Southern South Atlantic. *In* P.F. Ciesielski, Y. Kristoffersen, et al., *Proceedings of the Ocean Drilling Program, Scientific Results*, 114:281–297. College Station, Texas: Ocean Drilling Program.
1991b. Maestrichtian Planktonic Foraminifer Biostratigraphy and the Cretaceous/Tertiary Boundary at ODP Hole 738C (Kerguelen Plateau, Southern Indian Ocean). *In* J.A. Barron, B.L. Larsen, et al., *Proceedings of the Ocean Drilling Program, Scientific Results*, 119:451–465. College Station, Texas: Ocean Drilling Program.
1992a. Paleobiogeography of Campanian–Maastrichtian Foraminifera in the Southern High Latitudes. *Palaeogeography, Palaeoclimatolology, Palaeoecology*, 92:325–360.
1992b. Upper Cretaceous Planktic Foraminiferal Biozonation for the Austral Realm. *Marine Micropaleontology*, 20:107–128.

International Commission on Zoological Nomenclature (ICZN)
1985. *International Code of Zoological Nomenclature*. Edition 3. Adopted by the 20th General Assembly of the International Union of Biological Sciences. 338 pages. Berkeley: University of California Press.

Keller, G.
1978. Morphologic Variation of *Neogloboquadrina pachyderma* (Ehrenberg) in Sediments of the Marginal and Central Pacific Ocean and Paleoclimatic Interpretation. *Journal of Foraminiferal Research*, 8:208–224.

Kennett, J.P.
1968. Latitudinal Variation in *Globigerina pachyderma* (Ehrenberg) in Surface Sediments of the Southwest Pacific Ocean. *Micropaleontology*, 14:305–318.
1970. Comparison of *Globigerina pachyderma* (Ehrenberg) in Arctic and Antarctic Areas. *Contributions from the Cushman Foundation for Foraminiferal Research*, 21:47–48.

Koutsoukos, E.A.M., P.N. Leary, and M.B. Hart
1989. *Favusella* Michael (1972): Evidence of Ecophenotypic Adaptation of a Planktonic Foraminifer to Shallow-water Carbonate Environments During the Mid-Cretaceous. *Journal of Foraminiferal Research*, 19:324–336.

Krasheninnikov, V.A., and I.A. Basov
1983. Stratigraphy of Cretaceous Sediments of the Falkland Plateau Based on Planktonic Foraminifera, Deep Sea Drilling Project, Leg 71. *In* W.J. Ludwig, V.A. Krasheninnikov, et al., *Initial Reports of the Deep Sea Drilling Project*, 71:789–820. Washington: U.S. Government Printing Office.

Li Qianyu, and S.S. Radford
1991. Evolution and Biogeography of Paleogene Microperforate Planktonic Foraminifera. *Palaeogeography, Palaeoclimatology, Palaeoecology*, 83:87–115.

Loeblich, A.R., and H. Tappan
1964. Sarcodina, Chiefly "Thecamoebians" and Foraminiferida. *In* Raymond C. Moore, editor, *Treatise on Invertebrate Paleontology*, Part C, Protista (2): 900 pages. Lawrence, Kansas: University of Kansas Press.
1988. *Foraminiferal Genera and Their Classification*, volumes I–II: 970 pages. New York: Van Nostrand Reinhold Co.

Longoria, J.F., and M.A. Gamper
1984. Subfamily Helvetiellinae, a New Group of Late Cretaceous (Maastrichtian) Planktonic Foraminifera. *Micropaleontology*, 30:171–179.

Malmgren, B. and J.P. Kennett
1972. Biometric Analysis of Phenotypic Variation: *Globigerina pachyderma* (Ehrenberg) in the South Pacific Ocean. *Micropaleontolology*, 18:241–248.

1976. Biometric Analysis of Phenotypic Variation in Recent *Globigerina bulloides* d'Orbigny in the Southern Indian Ocean. *Marine Micropaleontology*, 1:3–25.
1977. Biometric Differentiation between Recent *Globigerina bulloides* and *Globigerina falconensis* in the Southern Indian Ocean. *Journal of Foraminiferal Research*, 7:130–148.

Masters, B.A.
1977. Mesozoic Planktonic Foraminifera: A World-wide Review and Analysis. *In* A.T.S. Ramsay, editor, *Oceanic Micropaleontology*, volume 1: pages 301–731. London: Academic Press.

McNeil, D.H., and W.G.E. Caldwell
1981. Cretaceous Rocks and Their Foraminifera in the Manitoba Escarpment. *The Geological Association of Canada, Special Paper*, 21:1–439.

Olsson, R.K.
1960. Foraminifera of Latest Cretaceous and Earliest Tertiary Age in the New Jersey Coastal Plain. *Journal of Paleontology*, 34:1–58.
1964. Late Cretaceous Planktonic Foraminifera from New Jersey and Delaware. *Micropaleontology*, 10:157–188.
1971. Pliocene–Pleistocene Planktonic Foraminiferal Biostratigraphy of the Northeastern Pacific. *In* A. Farinacci, editor, *Proceedings of the II Planktonic Conference (Roma 1970)*, volume II:921–928. Rome:Edizioni Technoscienza.
1972. Growth Changes in the *Globorotalia fohsi* Lineage. *Ecologae Geologicae Helvetiae*, 65:165–184.
1974. Pleistocene Paleoceanography and *Globigerina pachyderma* (Ehrenberg) in Site 36, DSDP, Northeastern Pacific. *Journal of Foraminiferal Research*, 4:47–60.
1976. Wall Structure, Topography, and Crust of *Globigerina pachyderma* (Ehrenberg). *In* Y. Takayanagi and T. Saito, editors, *Progress in Micropaleontology, Special Publication*, pages 244–257. New York: Micropaleontological Press, The American Museum of Natural History.

Olsson, R.K., C. Hemleben, W.A. Berggren, and C. Liu
1992. Wall Texture Classification of Planktonic Foraminifera Genera in the Lower Danian. *Journal of Foraminiferal Research*, 22:195–213.

Orbigny, A.D. d'
1840. Mémoire sur les Foraminifères de la craie blanche du Bassin de Paris. *Société Géologique de France, Mémoire*, 4:1–51.

Parker, F.L.
1962. Planktonic Foraminiferal Species in Pacific Sediments. *Micropaleontology*, 8:219–254.

Pessagno, E.A., Jr.
1967. Upper Cretaceous Planktonic Foraminifera from Western Gulf Coastal Plain. *Palaeontographica Americana*, 5(37):245–445.

Petters, S.W., H.A. El-Nakhal, and R.K. Cifelli
1983. *Costellagerina*, a New Late Cretaceous Globigerine Foraminiferal Genus. *Journal of Foraminiferal Research*, 13:247–251.

Plummer, H.J.
1927. Foraminifera of the Midway Formation in Texas. *University of Texas, Bureau of Economic Geology, Bulletin*, 2644:1–206.

Quilty, P.G.
1992. Upper Cretaceous Planktonic Foraminifera and Biostratigraphy, ODP Leg 120, Southern Kerguelen Plateau. *In* R. Schlich, S.W. Wise, Jr., et al., *Proceedings of the Ocean Drilling Program, Scientific Results*, 120:371–392. College Station, Texas: Ocean Drilling Program.

Reynolds, L.A., and R.C. Thunell
1986. Seasonal Production and Morphologic Variation of *Neogloboquadrina pachyderma* (Ehrenberg) in the Northeast Pacific. *Micropaleontology*, 32:1–18.

Rhumbler, L.
1911. Die Foraminiferen (Thalamoporen) der plankton expedition, erster Teil: Die allgemeinen Organisationsverhältnisse der Foraminiferen. *Ergebrisse der Plankton-Expedition der Humboldt Stiftung*, 3:1–331.

Robaszynski, F., M. Caron, J.M. Gonzalez Donoso, A.A.H. Wonders, editors, and the European Working Group on Planktonic Foraminifera
1984. Atlas of Late Cretaceous Globotruncanids. *Revue de Micropaléontologie*, 26:145–305.

Sliter, W.V.
1977. Cretaceous Foraminifera from the Southwest Atlantic Ocean, Leg 36, Deep Sea Drilling Project. *In* P.F. Barker, I.W.D. Dalziel, et al., *Initial Reports of the Deep Sea Drilling Project*, 36:519–573. Washington: U.S. Government Printing Office.
1989. Biostratigraphic Zonation for Cretaceous Planktonic Foraminifers Examined in Thin Section. *Journal of Foraminiferal Research*, 19:1–19.

Smith, C.C., and E.A. Pessagno, Jr.
1973. Planktonic Foraminifera and Stratigraphy of the Corsicana Formation (Maestrichtian), North-Central Texas. *Cushman Foundation for Foraminiferal Research, Special Publication*, 12:1–68.

Steineck, P.L., and R.L. Fleisher
1978. Towards the Classical Evolutionary Reclassification of Cenozoic Globigerinacea (Foraminiferida). *Journal of Paleontology*, 52:618–635.

Sverdlove, M.S., and A.W.H. Bé
1985. Taxonomic and Ecological Significance of Embryonic and Juvenile Planktonic Foraminifera. *Journal of Foraminiferal Research*, 15:235–241.

Webb, P.N.
1973. Upper Cretaceous–Paleocene Foraminifera from Site 208 (Lord Howe Rise, Tasman Sea), DSDP, Leg 21. *In* R.E. Burns, J. Andrews, et al., *Initial Reports of the Deep Sea Drilling Project*, 21:541–573. Washington: U.S. Government Printing Office.

Weidich, K.F.
1987. Perforated Portici and Imperforated Tegilla on Upper Cretaceous Planktonic Foraminiferal Taxonomy. *Revue de Micropaleontologie*, 30:52–62.

Plates

PLATE 1

Upper Campanian–Maastrichtian planktonic foraminifera from southern, extra-tropical latitudes previously illustrated in Deep Sea Drilling Project reports. The taxonomic classification of these forms is revised in this study. (Scale bars represent 50 μm.)

FIGURES 1, 2.—*Hedbergella sliteri* Huber, previously identified as *Hedbergella monmouthensis* (Olsson) by Webb (1973, pl. 3: figs. 1, 2) from south Tasman Sea DSDP Site 208.

FIGURES 3–5.—*Hedbergella sliteri* Huber, previously identified as *Hedbergella holmdelensis* Olsson by Sliter (1977, pl. 2: figs. 1–4) from the Falkland Plateau DSDP Site 327.

FIGURES 6, 10, 11.—Micromorph of *Archaeoglobigerina australis* Huber, previously identified as *Hedbergella monmouthensis* (Olsson) by Sliter (1977, pl. 3: figs. 1–3) from Falkland Plateau DSDP Site 327.

FIGURES 7–9.—Intermediate form between *Archaeoglobigerina australis* Huber and *Rugoglobigerina rugosa* Plummer, previously identified as *Hedbergella monmouthensis* (Olsson) by Krasheninnikov and Basov (1983, pl. 7: figs. 5, 7, 8) from Falkland Plateau DSDP Site 511; note presence of faint meridional costellae in spiral view of antepenultimate chamber.

FIGURES 12–14.—*Archaeoglobigerina australis* Huber (gerontic form), previously identified as *Rugoglobigerina pilula* Belford by Sliter (1977, pl. 10: figs. 7–9) from Falkland Plateau DSDP Site 327.

FIGURES 15–17.—*Archaeoglobigerina australis* Huber (gerontic form), previously identified as *Rugoglobigerina pilula* by Krasheninnikov and Basov (1983, pl. 11: figs. 4–6) from Falkland Plateau DSDP Site 511.

FIGURES 18–20.—*Archaeoglobigerina australis* Huber (gerontic form), previously identified as *Rugoglobigerina pustulata* Brönnimann by Krasheninnikov and Basov (1983, pl. 10: figs. 10–12) from Falkland Plateau DSDP Site 511.

FIGURES 21, 22, 26, 27.—*Archaeoglobigerina australis* Huber (gerontic form), previously identified as *Rugoglobigerina rotundata* Brönnimann by Krasheninnikov and Basov (1983, pl. 11: figs. 7–11) from Falkland Plateau DSDP Site 511.

FIGURES 23–25.—*Rugoglobigerina pennyi* Brönnimann, previously identified as *Rugoglobigerina rotundata* Brönnimann by Sliter (1977, pl. 11: figs. 1–3) from Falkland Plateau DSDP Site 327. Note axially compressed final chamber and faint meridional costellae.

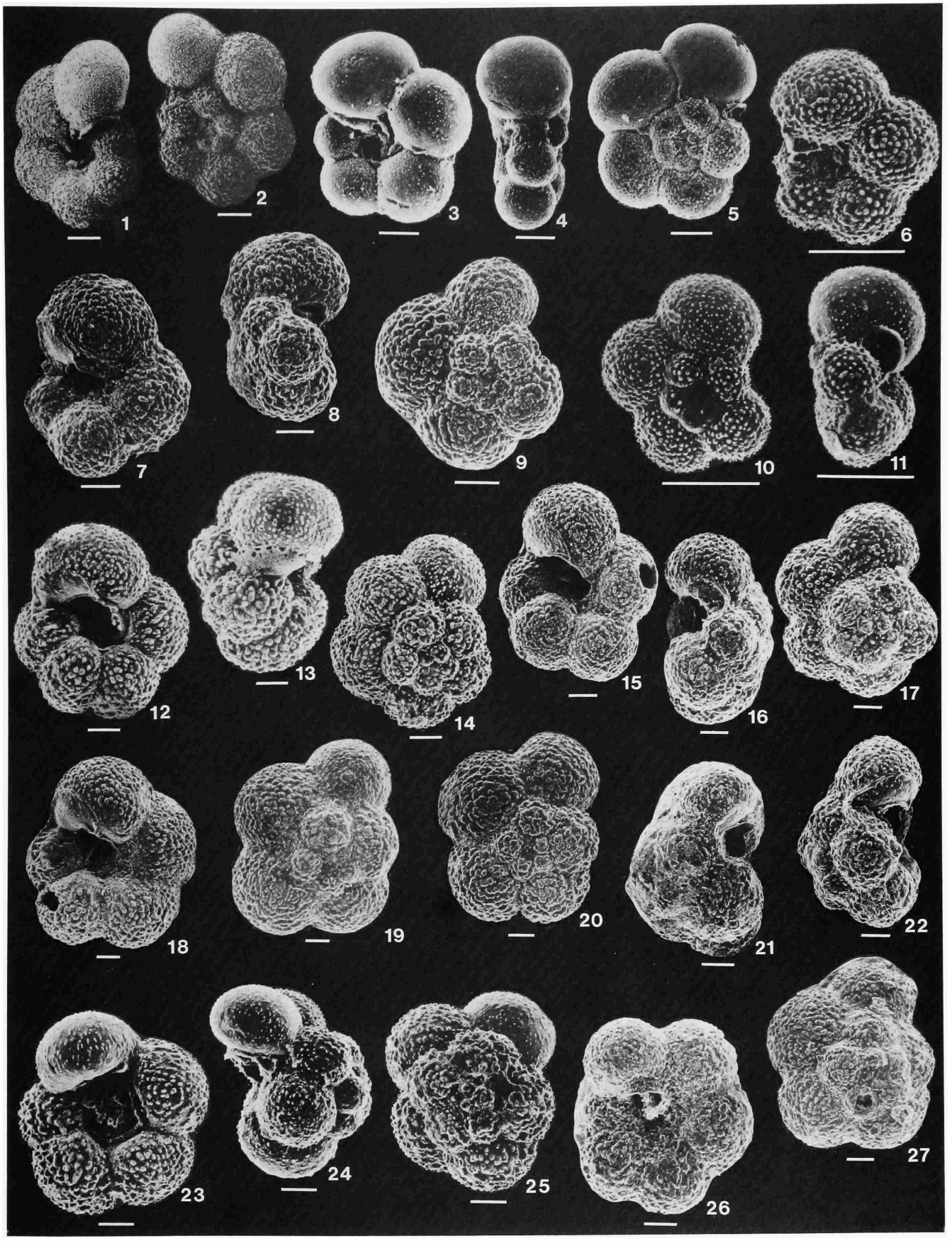
1
2
3
4
5
6
7
8
9
10
11
12
13
14
15
16
17
18
19
20
21
22
23
24
25
26
27

PLATE 2

External and internal views of topotype specimens of *Hedbergella holmdelensis* Olsson from the Navesink Formation and *Hedbergella monmouthensis* (Olsson) from the Red Bank Formation (New Jersey). Maximum test diameter in parentheses.

FIGURES 1–3, 6, 7.—*Hedbergella holmdelensis* Olsson (171 μm): 1, umbilical view; 2, edge view; note chamber compression in the direction of the equatorial plane; 3, spiral view; 6, outer whorl chambers dissected revealing penultimate whorl with aperture that is nearly equatorial in position; 7, complete dissection.

FIGURES 4, 5, 8.—*Hedbergella holmdelensis* Olsson (130 μm): 4, edge view; note chamber compression in the direction of the equatorial plane; 5, umbilical view; 8, complete dissection.

FIGURES 9–11, 14, 15.—*Hedbergella monmouthensis* (Olsson) (140 μm): 9, umbilical view; 10, edge view; 11, spiral view; 14, most outer whorl chambers dissected revealing penultimate whorl; 15, complete dissection.

FIGURES 12, 13, 16.—*Hedbergella monmouthensis* (Olsson) (154 μm): 12, edge view; 13, umbilical view; 16, complete dissection.

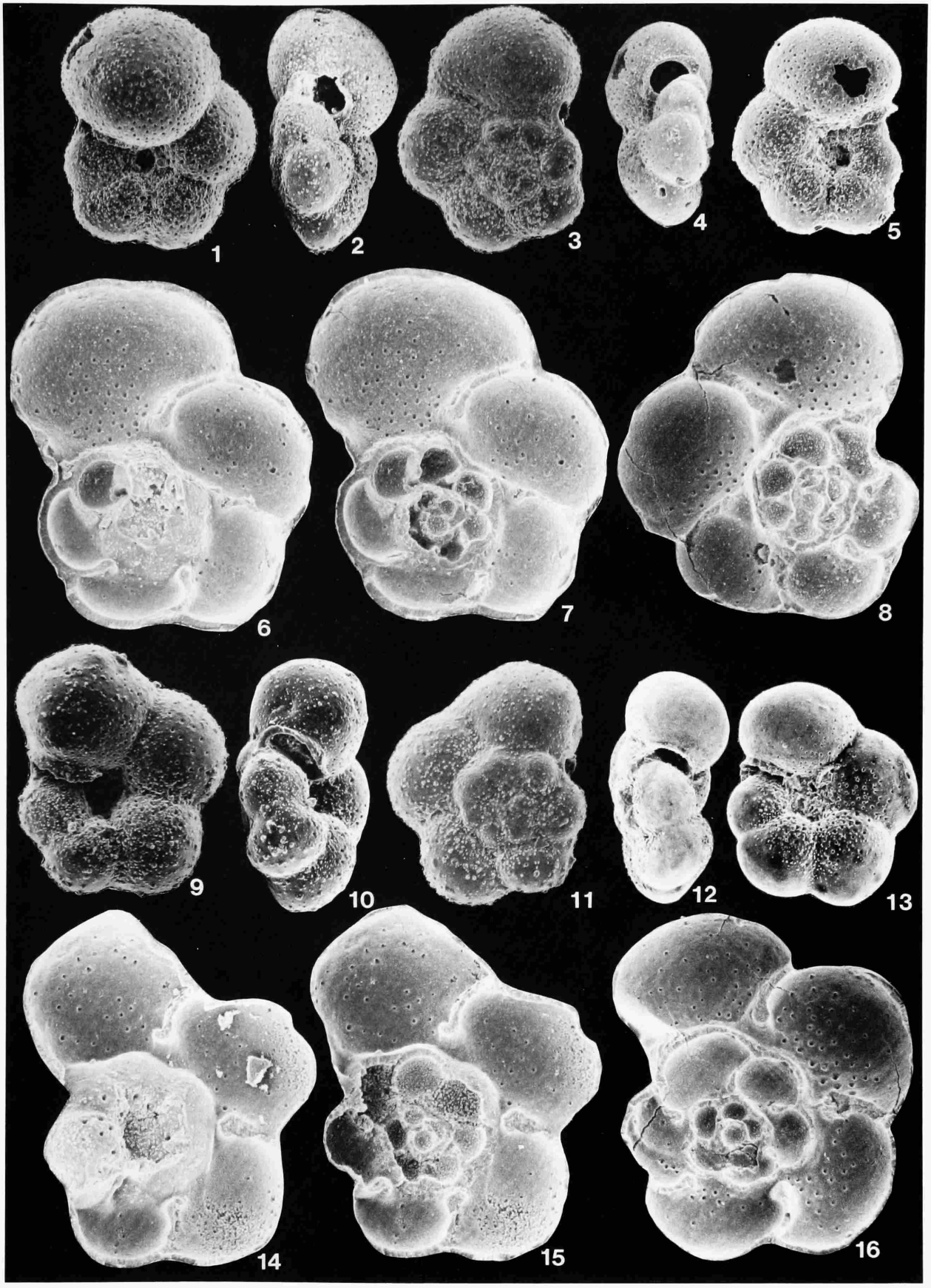
1
2
3
4
5
6
7
8
9
10
11
12
13
14
15
16

PLATE 3

Serial dissections and x-radiographs of *Hedbergella sliteri* Huber from the lower Maastrichtian DSDP Site 327 on Falkland Plateau. Maximum test diameter in parentheses.

FIGURES 1–4.—External views and x-radiograph of the same specimen (236 μm). Note that the complete ontogenetic series of chamber development is visible in the x-radiograph because of the low trochospire and wide umbilicus.

FIGURES 5–7.—Serial dissection of a single specimen (236 μm): 5, specimen with dissected outer whorl; 6, same specimen with all chambers dissected; 7, enlargement of the initial whorl. Note the pattern of pore distribution with increasing ontogeny.

FIGURES 8, 9.—Completely dissected specimen showing entire test and enlargement of the initial whorl (252 μm).

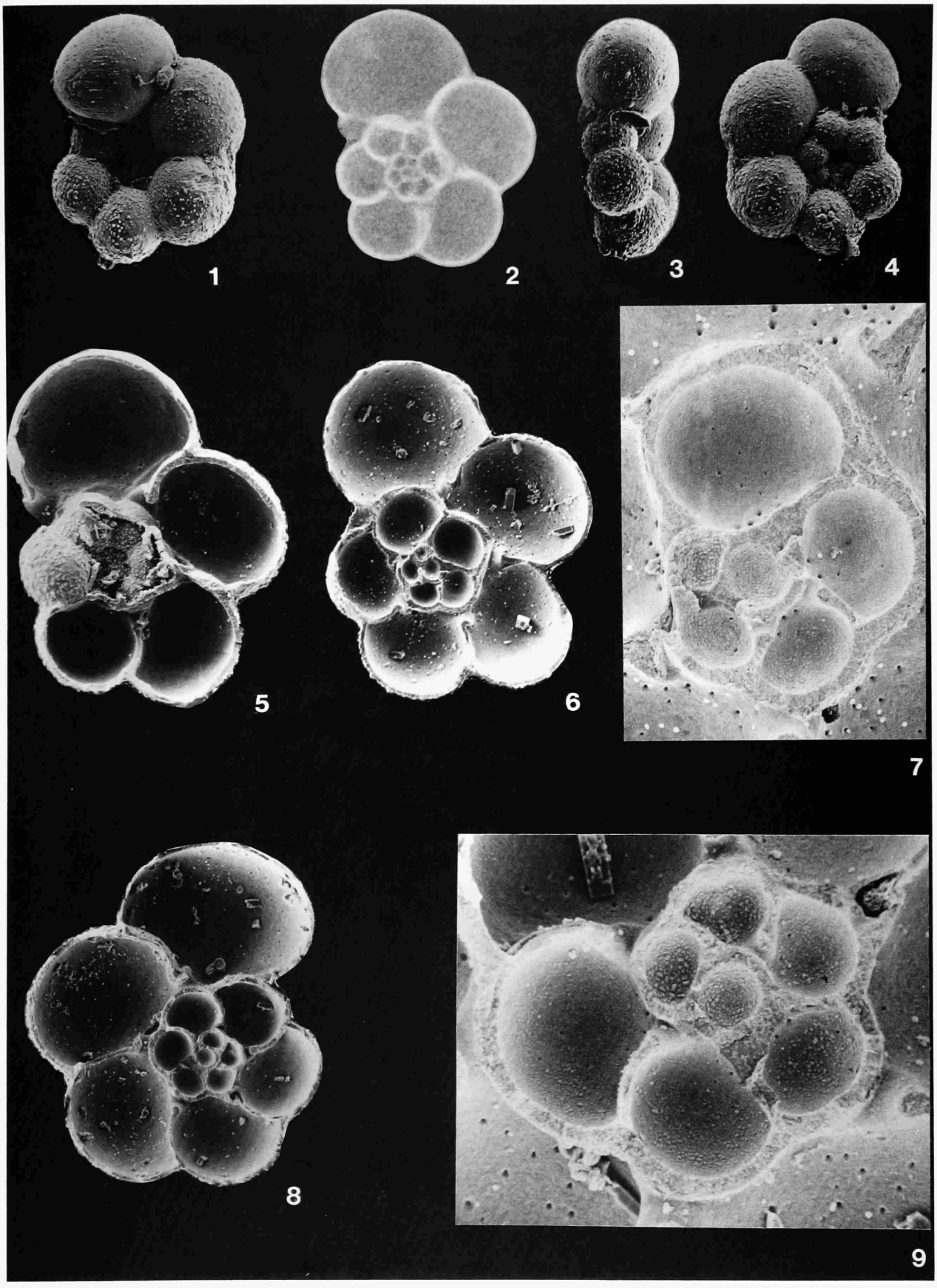
1
2
3
4
5
6
7
8
9

PLATE 4

Serial dissections and x-radiographs of topotype specimens of *Costellagerina pilula* (Belford), Toolonga Calcilutite, Pillarawa Hill, Western Australia. Morphologic similarity of the ontogenies revealed by serial dissection of the 4, 5, and 5.5 chambered morphotypes suggests that these are ecophenotypes of a single species. Maximum test diameter in parentheses.

FIGURES 1–4.—Four chambered morphotype designated as *Rugoglobigerina bulbosa* by Belford (1960) and subsequently recognized as *Costellagerina bulbosa* (Belford) by Petters et al. (1983) (216 μm): 1, x-radiograph; 2, external view; note meridional alignment of costellae; 3, dissected outer whorl revealing smoother-walled penultimate whorl; 4, complete dissection revealing initial whorl morphology. Note similarity of initial whorl in this morphotype to the initial whorls of the five-chambered morphotypes.

FIGURES 5–10.—External views, x-radiograph, and serial dissection of larger, 5.5 chambered morphotype (348 μm). Note that meridional costellae are faint or absent on chambers on umbilical side.

FIGURES 11–13.—External view, x-radiograph, and complete dissection of a five chambered morphotype (288 μm).

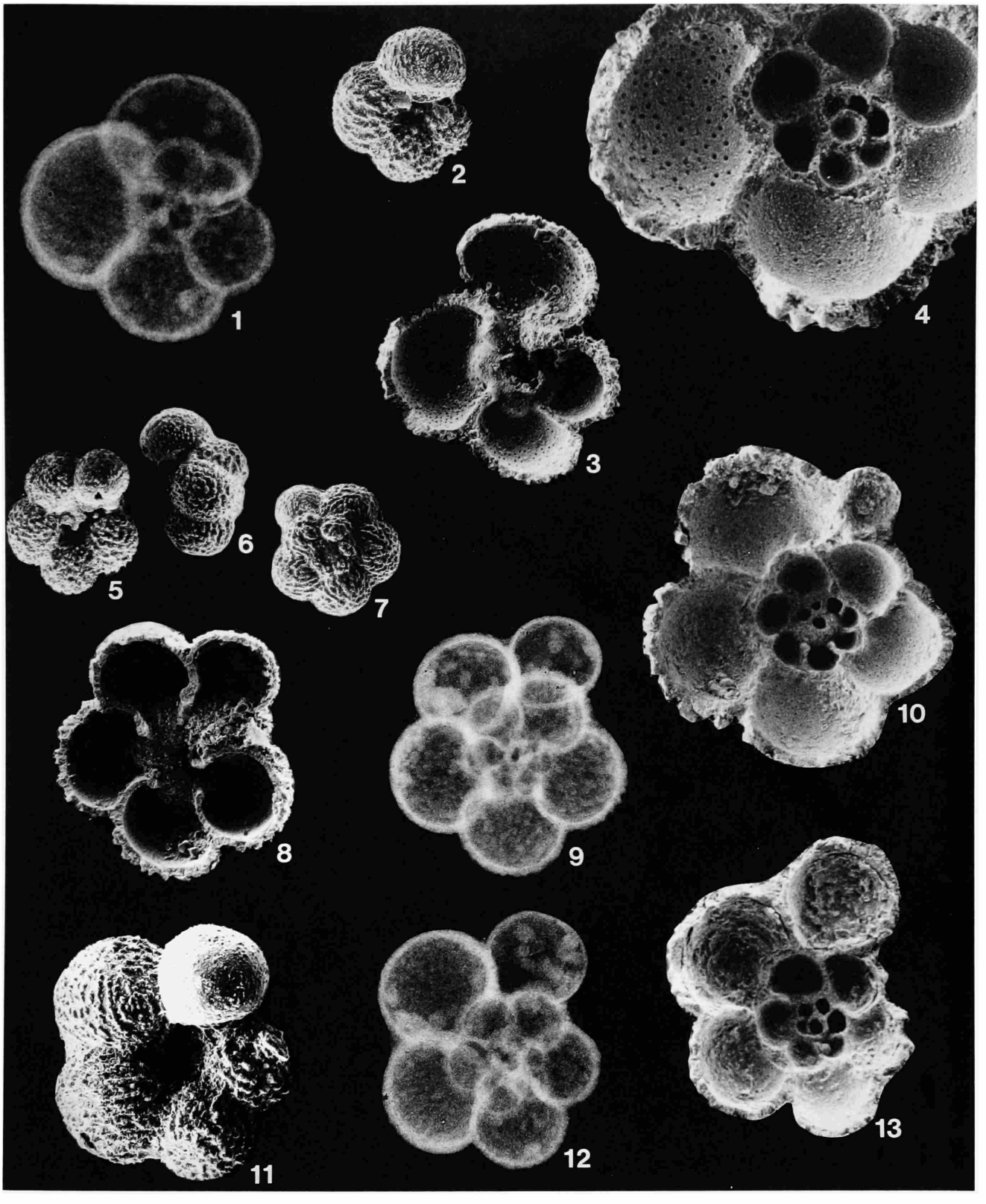
1
2
3
4
5
6
7
8
9
10
11
12
13

PLATE 5

Intermediate forms and adult morphotypes of *Archaeoglobigerina australis* Huber. Maximum test diameter in parentheses.

FIGURES 1–4.—Intermediate form between *Archaeoglobigerina australis* Huber and *Rugoglobigerina rugosa* (Plummer), (252 μm): 1, external view, showing faintly developed meridional costellae and a weak umbilical tegillum; 2, microradiograph; 3, dissection of outer whorl revealing penultimate whorl chambers with a relatively rapid chamber size increase, a finely pustulose surface texture, and an extraumbilical position of the aperture; 4, enlarged view of portical flap and delicate tegillum attached to final chamber. The presence of meridional costellae and a tegillum suggest affinity with *R. rugosa,* but the ontogenetic morphology more strongly resembles *A. australis.*

FIGURES 5–9.—External views and complete serial dissection of *Archaeoglobigerina australis* Huber from Falkland Plateau (316 μm). Note the presence of a broad porticus, but absence of a tegillum.

FIGURE 10.—Oblique view of a partially dissected adult specimen of *Archaeoglobigerina australis* Huber from Maud Rise (281 μm). Dissection reveals whorl of chambers formed in the neanic stage; note rapid rate of chamber size increase and subcircular aperture that is extraumbilical in position.

FIGURES 11–13.—External views and complete dissection of *Archaeoglobigerina australis* Huber from Maud Rise (230 μm).

FIGURE 14.—Complete dissection of *Archaeoglobigerina australis* Huber from Maud Rise (262 μm).

FIGURE 15.—Complete dissection of *Archaeoglobigerina australis* Huber from Maud Rise (253 μm).

FIGURES 16, 17.—Complete dissection of *Archaeoglobigerina australis* Huber specimen from Falkland Plateau (310 μm): 16, width of photo = 141 μm. 17, whole specimen.

FIGURES 18, 19.—External view and complete serial dissection of *Archaeoglobigerina australis* from Falkland Plateau (362 μm).

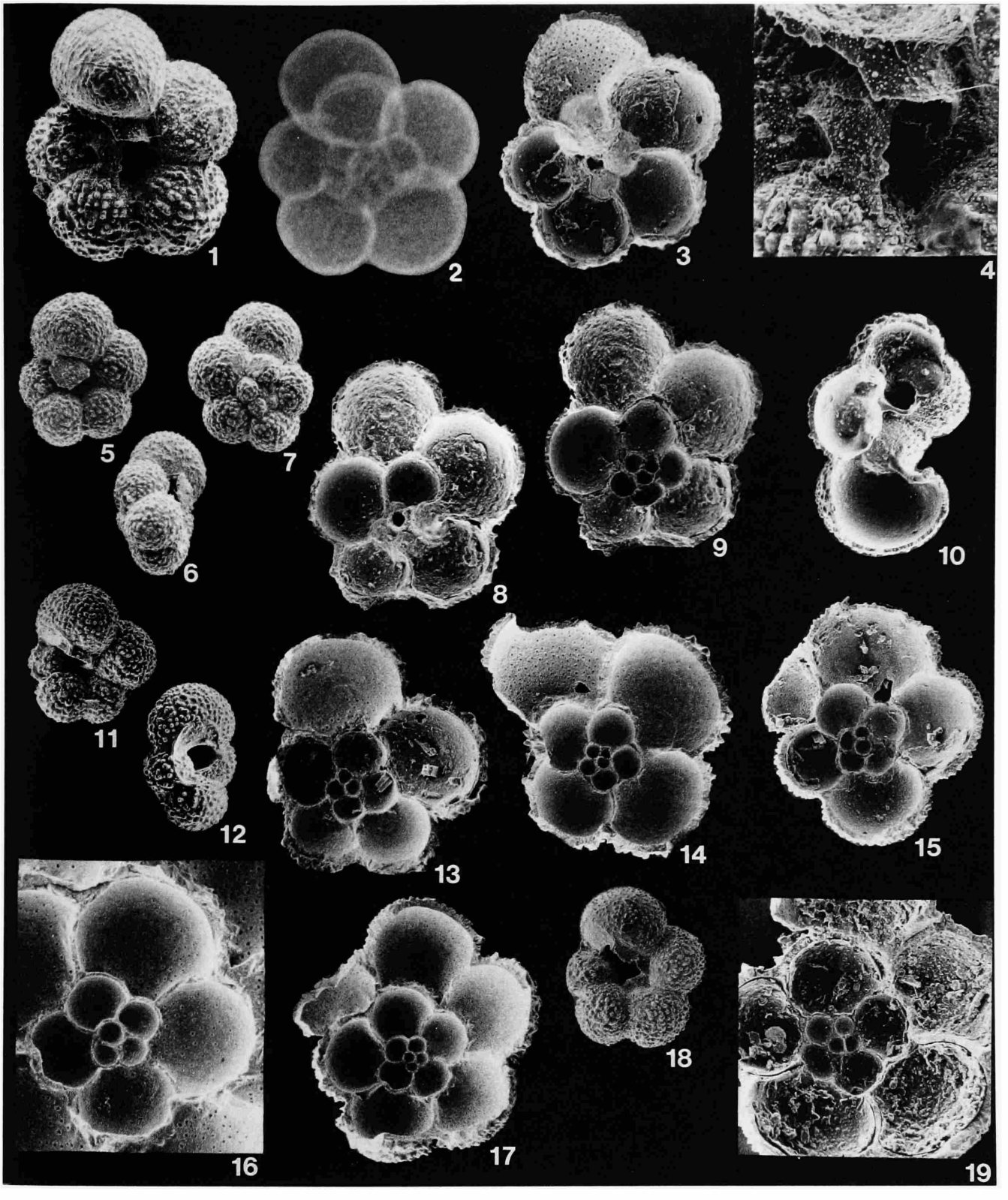
1
2
3
4
5
6
7
8
9
10
11
12
13
14
15
16
17
18
19

PLATE 6

Micromorphs of *Archaeoglobigerina australis* Huber from DSDP Site 511, Falkland Plateau. Maximum test diameter in parentheses.

FIGURES 1–6.—External views, x-radiograph, and serial dissections of a single specimen with a total of eight chambers (178 μm). Note the relatively rapid rate of chamber size increase, the extraumbilical position, and subcircular shape of the aperture, as can be observed in pre-adult chambers of gerontic individuals of *A. australis* (e.g., compare with Plate 5: Figure 10).

FIGURES 7, 8.—External view and complete dissection (170 μm).

FIGURES 9, 10.—Complete dissection and enlarged view of the initial whorl (181 μm).

FIGURES 11–14, 17, 18.—External view, x-radiograph, and serial dissection of a single kummerform specimen (265 μm).

FIGURES 15, 16.—External view and complete dissection of a kummerform specimen (170 μm).

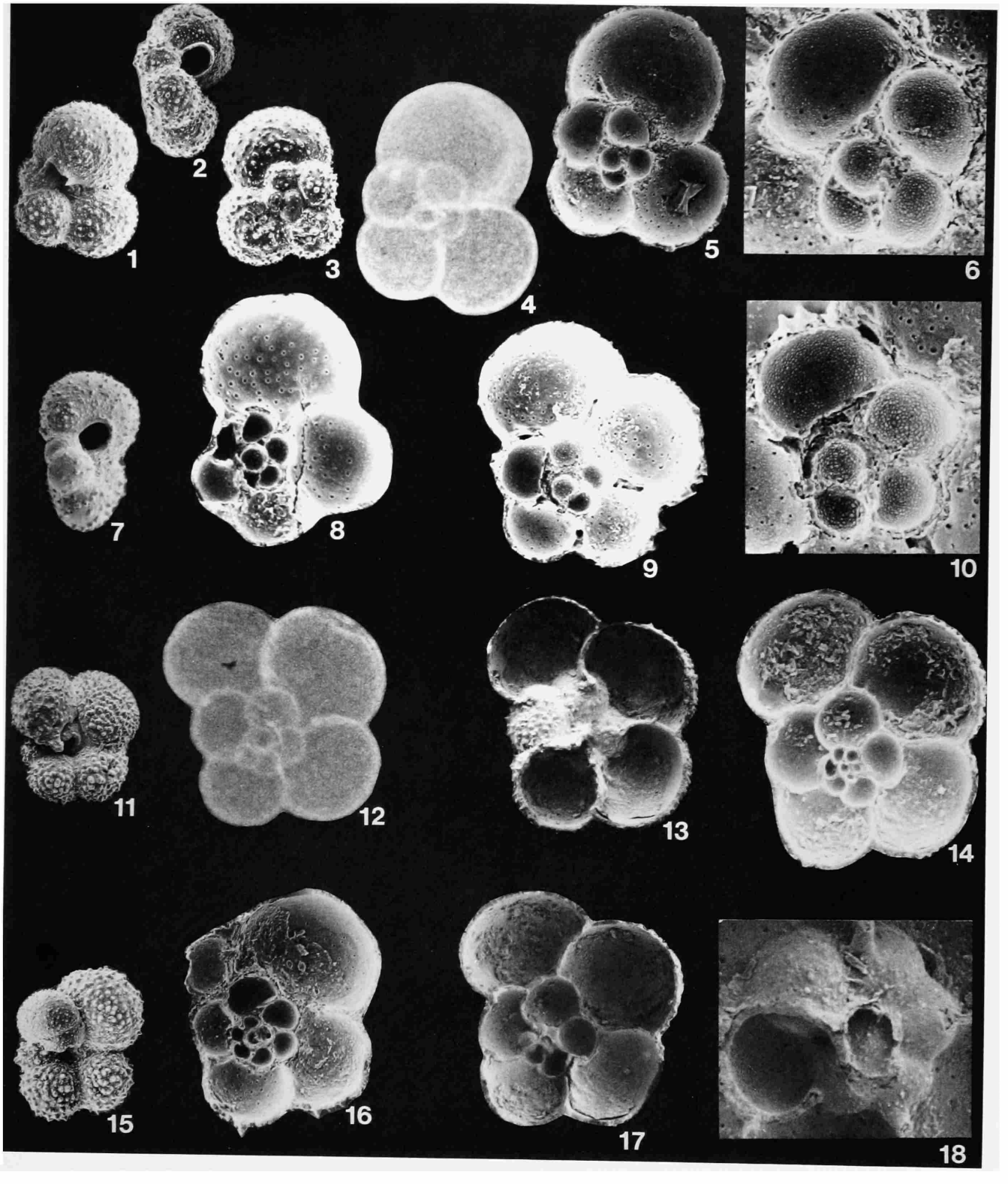
1
2
3
4
5
6
7
8
9
10
11
12
13
14
15
16
17
18

PLATE 7

Santonian specimens of *Archaeoglobigerina bosquensis* Pessagno from Falkland Plateau. Maximum test diameter in parentheses.

FIGURES 1–5.—Exterior views, micrograph, and serial dissection of a kummerform adult specimen (355 μm).

FIGURES 6, 7.—Exterior view and complete dissection of a neanic individual (273 μm).

FIGURES 8, 9.—Complete dissection of an adult specimen and enlargment of the initial whorl (288 μm).

FIGURE 10.—Complete dissection of an adult specimen (325 μm).

FIGURE 11.—Complete dissection of an adult specimen (313 μm).

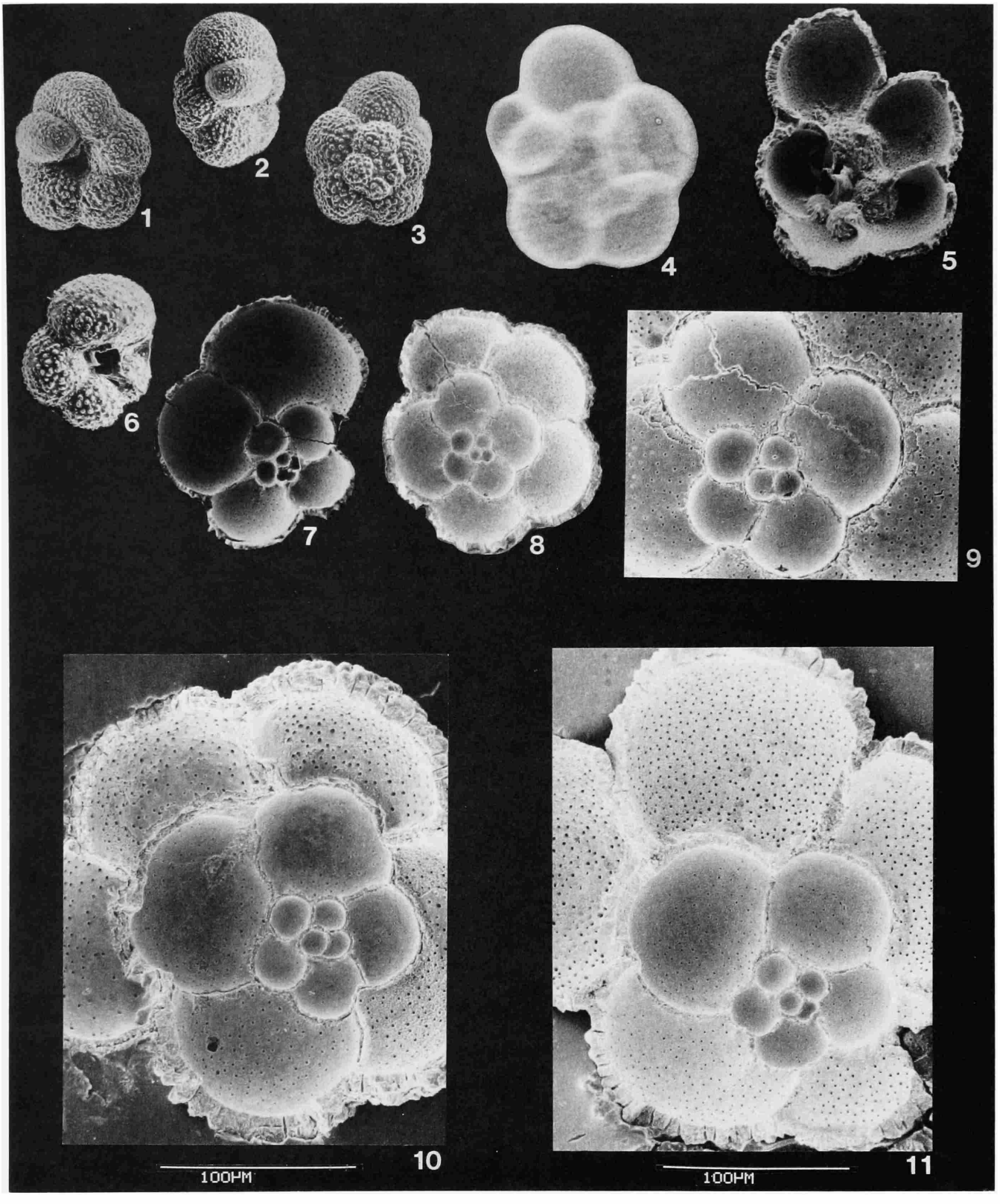
1
2
3
4
5
6
7
8
9
100μm
10
100μm
11

PLATE 8

Adult forms of *Archaeoglobigerina cretacea* (d'Orbigny) and intermediate forms between *Rugoglobigerina rugosa* (Plummer) and *Archaeoglobigerina australis* Huber. Maximum test diameter in parentheses.

FIGURES 1–8.—External views, microradiograph, and serial dissections of a single specimen of *Archaeoglobigerina cretacea* (d'Orbigny) from the Campanian of Falkland Plateau (424 μm). Note the reniform chamber morphology that appears in the initial whorl and continues throughout the ontogeny. Also note that pores are absent from the axial periphery throughout ontogeny.

FIGURES 9–15.—External views, microradiograph, and serial dissection of morphotype from Seymour Island that is intermediate between *Rugoglobigerina rugosa* (Plummer) and *Archaeoglobigerina australis* Huber (301 μm). Affinity to *R. rugosa* is indicated by the faint presence of meridional costellae on the penultimate chamber and a thin tegillum (Figures 9, 13). However, serial dissection reveal an ontogenetic morphology that more closely resembles *A. australis* than *R. rugosa* (e.g., compare Figure 15 on this plate with Plate 5: Figures 13–17, 19); the early chambers are spherical rather than reniform, and chamber size increase is more rapid in the initial whorl.

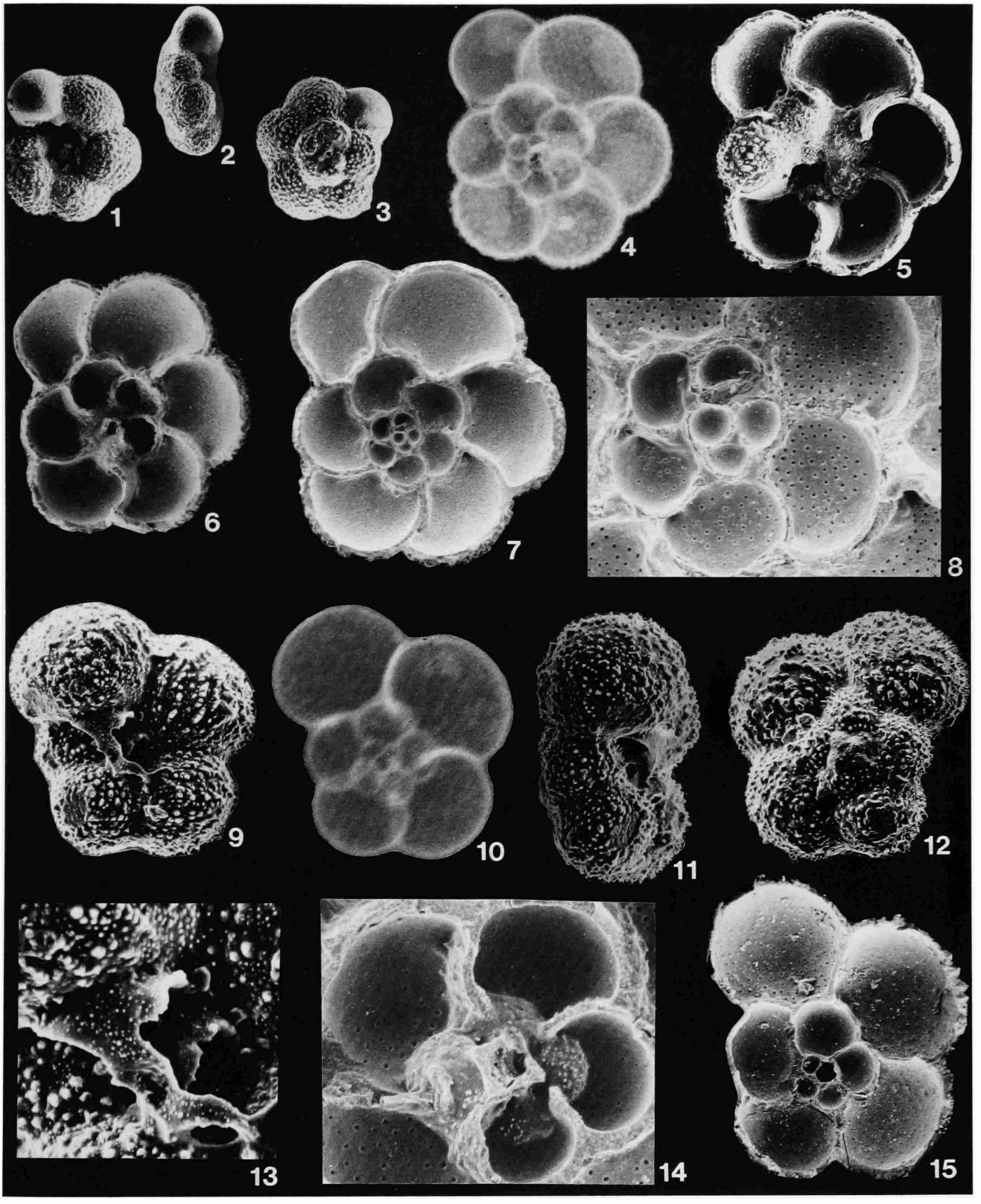
1
2
3
4
5
6
7
8
9
10
11
12
13
14
15

PLATE 9

External views and serial dissections of *Archaeoglobigerina mateola* from the upper Maastrichtian of Maud Rise. Maximum test diameter in parentheses.

FIGURES 1–4.—External views of specimen with an aberrant final chamber and view showing dissected ultimate whorl. Note the smoother surface of the penultimate whorl chambers (280 μm).

FIGURE 5.—Complete dissection showing initial whorl morphology (278 μm).

FIGURES 6, 7.—Serial dissection of a specimen with elongate pseudospines revealing penultimate whorl chamber and initial whorl mophology (306 μm).

FIGURE 8.—Complete dissection of a specimen with a large (28 μm) prolocular chamber (310 μm).

FIGURES 9–12, 17.—External view and serial dissection of specimen with a 27 μm proloculus (253 μm).

FIGURES 13–16.—External views and serial dissection of specimen with a 12 μm proloculus (376 μm).

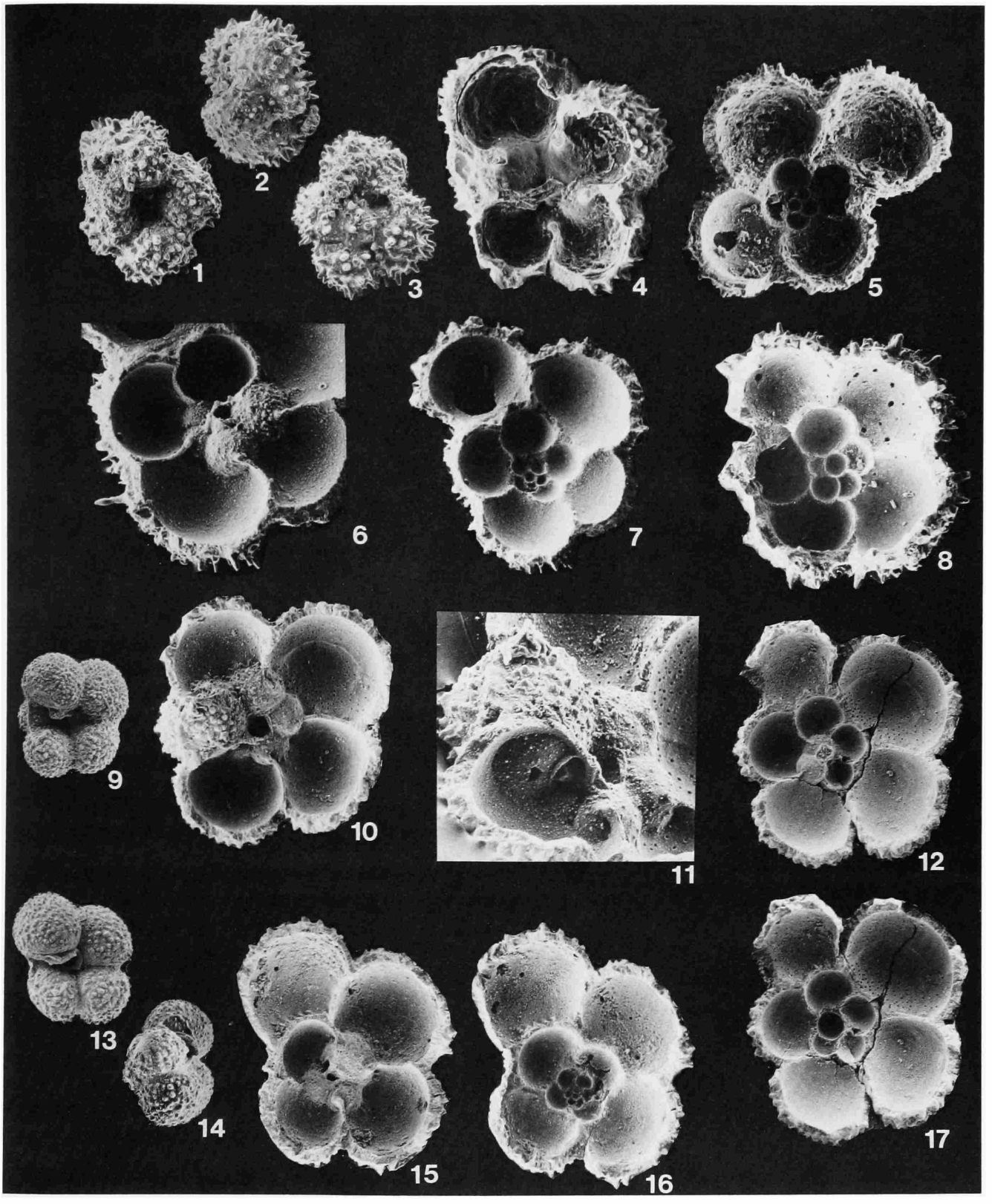
1
2
3
4
5
6
7
8
9
10
11
12
13
14
15
16
17

PLATE 10

Neanic and normal-sized adult forms of *Rugoglobigerina rugosa* (Plummer) from the upper Maastrichtian Kemp Clay (Texas) near the location from which this species was originally described. Maximum test diameter in parentheses.

FIGURES 1–6.—Exterior, microradiograph, and interior views of a neanic specimen (220 μm). The neanic morphology is characterized by the poor development of meridionally aligned costellae on the antepenultimate and earlier chamber surfaces and the continuing rapid rate of chamber size increase in the final whorl. The magnified view of the tegillum (Figure 6) shows that this structure is more delicate in neanic specimens than in fully mature individuals (e.g., compare with Figure 9 on this plate).

FIGURES 7, 8.—Complete serial dissection of a neanic specimen showing the whole specimen and an enlargement of the initial whorl (219 μm).

FIGURES 9–13.—Exterior, microradiograph, and complete dissection of an adult specimen (424 μm). Note that the the chambers in the final whorl show a heavy meridional specimens.

FIGURE 14.—Complete serial dissection of adult specimen (404 μm).

FIGURES 15, 16.—Complete serial dissection of adult specimen (290 μm). Note the somewhat reniform morphology of the initial whorl chambers (Figure 16). These initial whorl morphologies are identical in neanic specimens (see Figures 5, 7 on this plate).

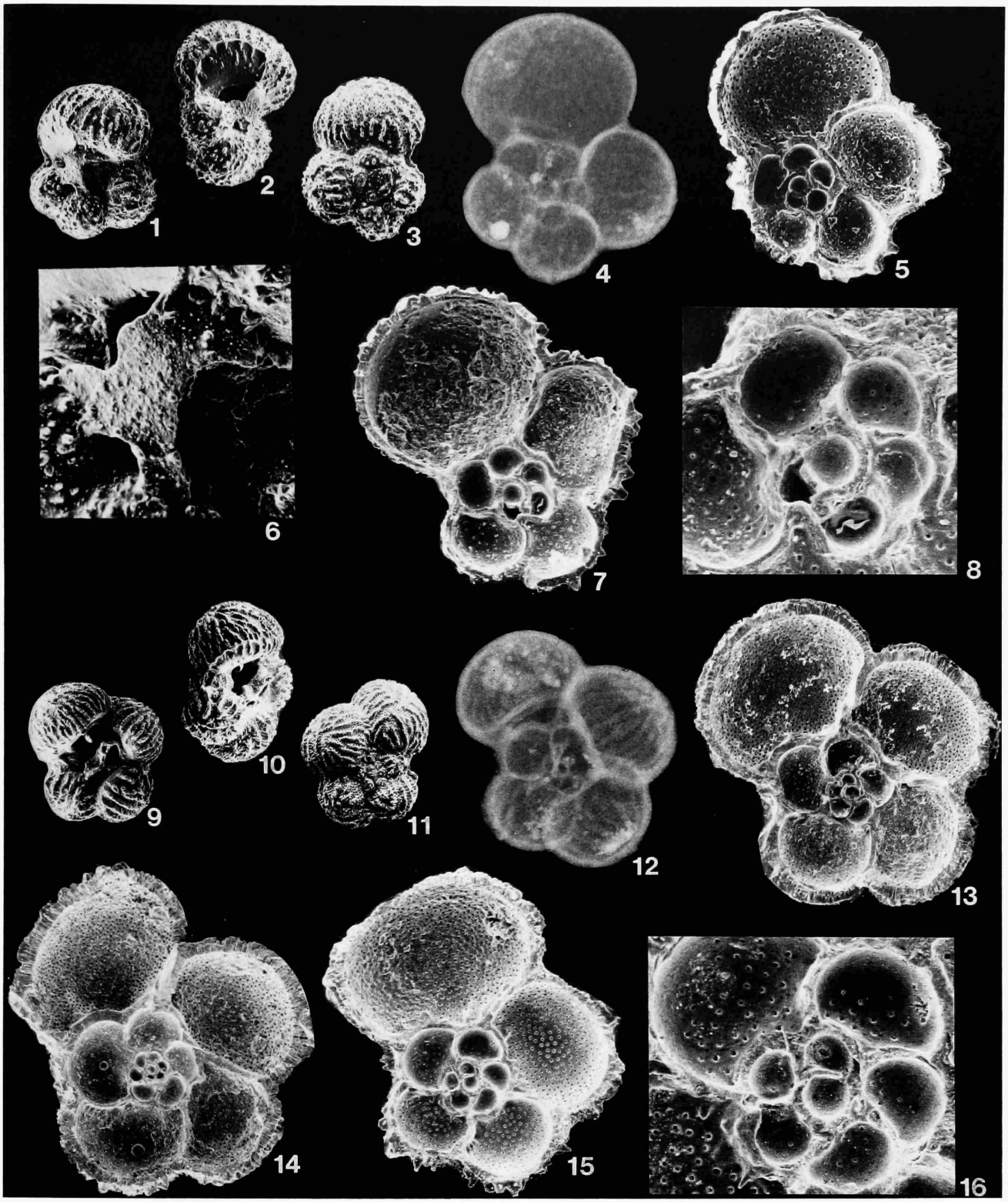
1
2
3
4
5
6
7
8
9
10
11
12
13
14
15
16